

**UNIVERSIDADE FEDERAL DE SANTA MARIA**  
**CENTRO DE CIÊNCIAS RURAIS**  
**PROGRAMA DE PÓS-GRADUAÇÃO EM CIÊNCIA DO SOLO**

**Cassiane Jraj de Melo Victoria Bariani**

**COMBINAÇÃO DE MODELOS DE BALANÇO HÍDRICO NO SOLO E  
SENSORIAMENTO REMOTO PARA O MONITORAMENTO DE  
ÁREAS IRRIGADAS**

Santa Maria, RS

2016

**Cassiane Jayj de Melo Victoria Bariani**

**COMBINAÇÃO DE MODELOS DE BALANÇO HÍDRICO NO SOLO E  
SENSORIAMENTO REMOTO PARA O MONITORAMENTO DE ÁREAS  
IRRIGADAS**

Tese apresentada ao Curso de Doutorado do Programa de Pós-Graduação em Ciência do Solo, Área de Concentração em Processos Físicos e Morfogenéticos do Solo, da Universidade Federal de Santa Maria (UFSM, RS), como requisito parcial para a obtenção do grau de **Doutor em Ciência do Solo**.

Orientador: Prof. Dr. Reimar Carlesso

Santa Maria, RS  
2016

Ficha catalográfica elaborada através do Programa de Geração Automática da Biblioteca Central da UFSM, com os dados fornecidos pelo(a) autor(a).

Jrayj de Melo Victoria Bariani, Cassiane  
COMBINAÇÃO DE MODELOS DE BALANÇO HÍDRICO NO SOLO E  
SENSORIAMENTO REMOTO PARA O MONITORAMENTO DE ÁREAS  
IRRIGADAS / Cassiane Jrayj de Melo Victoria Bariani.-  
2016.

143 p. ; 30cm

Orientador: Reimar Carlesso  
Tese (doutorado) - Universidade Federal de Santa  
Maria, Centro de Ciências Rurais, Programa de Pós-  
Graduação em Ciência do Solo, RS, 2016

1. Sistema de Informação Geográfica 2. SIMDualKc 3.  
NDVI 4. Pivô Central 5. Fenologia I. Carlesso, Reimar II.  
Titulo.

---

© 2016

Todos os direitos reservados a Cassiane Jrayj de Melo Victoria Bariani. A reprodução de partes ou do todo deste trabalho só poderá ser feita mediante a citação da fonte.

E-mail: cassiane.victoria@gmail.com

---

**Cassiane Jayj de Melo Victoria Bariani**

**COMBINAÇÃO DE MODELOS DE BALANÇO HÍDRICO NO SOLO E  
SENSORIAMENTO REMOTO PARA O MONITORAMENTO DE ÁREAS  
IRRIGADAS**

Tese apresentada ao Curso de Doutorado do Programa de Pós-Graduação em Ciência do Solo, Área de Concentração em Processos Físicos e Morfogenéticos do Solo, da Universidade Federal de Santa Maria (UFSM, RS), como requisito parcial para a obtenção do grau de **Doutor em Ciência do Solo**.

**Aprovado em 10 de maio de 2016:**

---

**Reimar Carlesso, PhD. (UFSM)**  
(Presidente/Orientador)

---

**Mirta Teresinha Petry, Dr<sup>a</sup>. (UFSM)**

---

**Fábio Marcelo Breunig, Dr. (INPE)**

---

**Eloir Missio, Dr. (UNIPAMPA)**

---

**Juliano Dalcin Martins, Dr. (IFRS)**

Santa Maria, RS  
2016

## DEDICATÓRIA

*Dedico este trabalho ao meu marido Nelson Mario Victoria Bariani, aos nossos filhos Joaquim Manuel, Lilian, Beatriz e Sofia, e aos meus pais Santoaires e Diamantina por me apoiarem incondicionalmente em todos os momentos da minha vida.*

## AGRADECIMENTOS

Primeiramente gostaria de agradecer à Natureza, por ter me direcionado a trilhar estes caminhos.

Agradeço a dois homens que se dedicaram a me auxiliar desde o dia em que os conheci e que nunca falharam comigo. Meu querido **pai** e meu **marido**.

Agradeço a minha amorosa **mãe** que me autorizou a fazer as minhas próprias escolhas, me deixando livre para decidir as estradas por onde seguir.

Agradeço aos meus filhos, **Beatriz, Lilian, Joaquim Manuel** e **Sofia** por não me deixarem entristecer com as pedras e espinhos do caminho.

Também quero agradecer aos colegas que me acompanharam ao longo deste trabalho, em especial: **Viviane Ávila, Gabriel Awe** e **Diogo Kersten**.

Faço um agradecimento especial ao meu orientador de tese, o professor **Reimar Carlesso**, pelo convite, paciência e coragem para desenvolver abordagens interdisciplinares no campo das ciências agrárias, a partir do seu vasto conhecimento na área de irrigação.

Também agradeço a professora **Mirta Petry** pelos ajustes, comentários e revisões dos artigos.

Agradeço ainda o professor **Luis Santos Pereira** pelo seu claro direcionamento e transformação do trabalho em algo possivelmente aplicável na agricultura.

Agradeço a professora **Isabel Poças** pelos debates científicos e correções técnicas dos artigos que contribuíram para a elevação do nível do trabalho final.

Agradeço ainda a **UFSM** por ter me possibilitado a oportunidade de ter cursado uma pós-graduação gratuita e de qualidade.

Sinto-me grata por estar dando uma pequena contribuição à ciência brasileira. Por fim agradeço a **CAPES** e ao **Governo Federal** pela política de apoio à graduação e pós-graduação no Brasil, seja por meio da criação de novas universidades e programas como pelo financiamento das bolsas, as quais foram importantes para conseguir chegar ao título de doutora.

"Havia um importante trabalho há ser feito, e *todo mundo* tinha certeza que *alguém* o faria. *Qualquer um* poderia tê-lo feito, mas *ninguém* fez. *Alguém* se zangou porque era um trabalho de *todo mundo*. *Todo mundo* pensou que *qualquer um* poderia fazê-lo, mas *ninguém* imaginou que *todo mundo* deixasse de fazê-lo. No final *todo mundo* culpou *alguém* porque *ninguém* fez o que *qualquer um* poderia ter feito".

(Autor desconhecido)

## RESUMO

### COMBINAÇÃO DE MODELOS DE BALANÇO HÍDRICO NO SOLO E SENSORIAMENTO REMOTO PARA O MONITORAMENTO DE ÁREAS IRRIGADAS

AUTORA: Cassiane Jayj de Melo Victoria Bariani  
ORIENTADOR: Reimar Carlesso

Este trabalho aplicou técnicas de sensoriamento remoto (SR) e sistema de informação geográfica (SIG) para o apoio ao monitoramento de áreas irrigadas por pivô central com ênfase principalmente na estimativa do coeficiente de cultura basal ( $K_{cb}$ ). O uso de informações de sensores de moderada resolução espacial (TM/Landsat) tem avançado muito nas últimas décadas implementados em modelos de balanço de energia à superfície do solo como o SEBAL e o METRIC, ou assimiladas e correlacionadas com modelos de balanço de água no solo como SIMDualKc. Complementados com dados meteorológicos, podem prover estimativas de coeficientes de cultura ( $K_c$ ) e a evapotranspiração (ET) mais condizentes com as condições locais, de uma forma espacializada, visto que as imagens de satélite possuem informações específicas em cada pixel. Essas informações podem apoiar o manejo da irrigação e serem agrupadas e organizadas em SIG para uma visualização eficiente da atividade agrícola, de forma a retratar a realidade de áreas cultivadas. O cruzamento das informações permite um entendimento das características da vegetação, do solo, da precipitação e da demanda de água pelas culturas. O banco geográfico desenvolvido no SIG foi capaz de identificar: (i) a distribuição espacial das chuvas; (ii) culturas e estádios fenológicos, por meio do índice de vegetação por diferença normalizada (NDVI); (iii) uso dos solos; e (iv) áreas de risco a erosão e aptidão agrícola. O NDVI mostrou-se uma boa ferramenta para a identificação dos estádios fenológicos das culturas do milho e soja na região Sul do Brasil, pois sua sensibilidade foi de 0,02, permitindo, também, determinar os principais estádios de desenvolvimento das culturas e apoiar o calendário de irrigações. Os resultados dos estádios de desenvolvimento para milho e soja foram respectivamente: [0,0-0,4] e [0,0-0,3] inicial; [0,4-0,75] e [0,3-0,85] desenvolvimento rápido; [0,75-0,1] e [0,85-1,0] desenvolvimento intermediário; [0,75-0,3] e [0,85-0,3] estágio final. O erro médio relativo (ARE) ficou em torno de 7%. As curvas de NDVI também mostraram uma espécie de impressão digital das espécies de culturas locais e práticas de manejo agrícola. Os resultados globais da calibração local dos  $K_{cb}$  a partir do SR correlacionados e assimilados com dados do modelo SIMDualKc mostraram um bom ajuste para condições de ausência de estresse hídrico. Em condições de possível ocorrência de estresse, o  $K_{cb}$  real assimilado,  $K_{cb\ act\ NDVI}$  pode ser calculado pelo produto do  $K_{cb\ pot\ NDVI}$  com o coeficiente de estresse ( $K_s$ ) fornecido pelo SIMDualKc, e assim prover um melhor ajuste com a realidade da cultura. O erro médio relativo ARE < 30% foi achado entre a curva média representativa da região e as curvas dos pivôs individuais. Considerando os resultados obtidos, a estimativa de  $K_{cb}$  por meio de NDVI pode representar uma ferramenta útil para a determinação das necessidades hídricas das culturas da soja e milho, irrigadas por pivô central no Sul do Brasil, visando apoiar o planejamento e gerenciamento da irrigação. Esta metodologia é adequada como base a ser adaptada para o monitoramento por meio de veículos aéreos não tripulados (VANT) equipados com sensores NDVI, onde as informações como fenologia,  $K_c$  e ET, poderão ser estimadas, ajustadas, calibradas e assimiladas em tempo real por modelos de balanço de água no solo e/ou modelos de balanço de energia na superfície.

**Palavras-chave:** Coeficiente de cultura. Evapotranspiração. Fenologia. Sistema de informação geográfica.



## ABSTRACT

### COMBINATION OF SOIL WATER BALANCE MODELING AND REMOTE SENSING FOR IRRIGATED AREAS MONITORING

AUTHOR: Cassiane Jayj de Melo Victoria Bariani  
ADVISER: Reimar Carlesso

This work uses remote sensing (RS) and geographic information system (GIS) techniques for the support of irrigation management and crop monitoring of center pivot irrigated areas with particular emphasis on the estimation of the basal crop coefficient ( $K_{cb}$ ). Besides the traditional meteorological approach, it can be seen that the use of information from moderate spatial resolution sensors (TM/Landsat) is coming forward, especially in the last two decades. The remote sensing information, implemented in energy balance models of the soil surface as SEBAL or METRIC, or assimilated and correlated with soil water balance models as SIMDualKc can provide estimations of crop coefficient ( $K_{cb}$ ) and evapotranspiration (ET) which are closer to local conditions, due to pixel level spatial information. The organization of information related to irrigation management in GIS environment provides the means for efficient visualization of the agricultural cycle dynamics in several levels. Cross-linked information allows the understanding of vegetation and soil characteristics, together with rainfall and irrigation effects and the crop water demand. The GIS database created in this work helped to identify: (i) rainfall spatial distribution; (ii) crops and phenological stages, by the normalized difference vegetation index (NDVI); (iii) land use; e (iv) erosion risk and agricultural potential. The NDVI showed a sensitivity of 0.02 units for the identification of phenological stages and crop cycle features for central pivot irrigated soybean and maize in the typical conditions of southern Brazil. The resulting FAO56-like crop growth stages for maize and soybean were, respectively: [0.0-0.4] and [0.0-0.3] for the initial period; [0.4-0.75] and [0.3-0.85] for the rapid growth period; [0.75-0.1] and [0.85-1.0] for mid-season period; [0.75-0.3] and [0.85-0.3] for late season period. The average relative error (ARE) was around 7%. The curves also showed a kind of “fingerprint” of the crop type and management practices in the region that could be associated with the phenological stages in the growing season, as a good tool for agricultural monitoring. The assimilation of NDVI data to  $K_{cb}$  was made through the correlation equation between the  $K_{cb}$  output of a FAO56-like soil water balance model (SIMDualKc) and the obtained a  $K_{cb\ NDVI}$  assimilated function. The actual irrigation coefficient  $K_{cb\ act\ NDVI}$  was obtained through the product of the assimilated  $K_{cb\ pot\ NDVI}$  with the stress coefficient ( $K_s$ ) output of the SIMDualKc model. The average relative error (ARE) between the assimilated general  $K_{cb\ NDVI}$  curve and the individual pivot curves was lower than 30% for both potential and actual  $K_{cb}$ . The results showed that the assimilation of NDVI for the calculation of  $K_{cb}$  with the methodology proposed can potentially benefit the irrigation management with a better adjustment of the values to the actual condition of the crop during the growing season. This can be a useful tool for the determination of the water demand of soybean and maize in irrigated fields in Brazil. The methodology may also be adequate as a base to be adapted for unmanned air vehicles based monitoring with NDVI sensors.

**Palavras-chave:** Crop coefficient. Evapotranspiration. Phenology. Geographic information System.

## LISTA DE TABELAS

### INTRODUÇÃO

Tabela 1. Vantagens e desvantagens do cálculo da ET via sensoriamento remoto.	17
Tabela 2. Vantagens e desvantagens do cálculo da ET via FAO 56	17

### ARTIGO II

Table 1. Examples of potential spatial analysis in the geo-relational database of irrigation.	67
Table 2. Comparison of land use classes analyzed between the years 1991, 2001 and 2011.	71
Table 3. Evapotranspiration of corn in the seven analyzed pivots on the date of January 26, 2005.	73

### ARTIGO III

Table 1. Information of the path and date (for row 80) of the Landsat5/TM images analyzed.	99
Table 2. Exemplification of the output of Tukey's HSD tests for the identification of significative differences between pivots' average NDVI.	101
Table 3. NDVI intervals for development periods determined for soybean and maize.	105
Table 4. Statistical indicators for the comparison of the average curve with the individual pivots' curve.	105
Table 5. Validation of the phenology calibration.	105

### ARTIGO IV

Table 1. Comparison of $K_{cb\ pot\ NDVI}$ with $K_{cb\ pot\ SIMDual}$ and $K_{cb\ act}$ derived from NDVI ( $K_{cb\ act\ NDVI}$ ), with $K_{cb}$ obtained from $SIMDualKc$ ( $K_{cb\ SIMDual}$ ) for the soybean crop cycle and maize in twenty eight pivots analyzed.	120
Table 2. Statistical parameters for the comparison between the potential and actual crop coefficients calculated by NDVI and $SIMDualKc$ .	122

## LISTA DE FIGURAS

### ARTIGO II

Figure 1. Location of the study area. The rectangle shows there sults of super imposed images of orbits 222 and 223, path 80 from Landsat 5/TM satellite.	56
Figure 2. Table of non-spatial data from SPRING software.	61
Figure 3. Geo-relational database from SPRING software.	62
Figure 4. Attributes checking – Precipitation = 0 (zero).	63
Figure 5. Results of geo-relational database check.	64
Figure 6. Land slope map showing the identified center pivot irrigation locations (red circles).	68
Figure 7. Soil use map for the years 1991, 2001 and 2011.	69
Figure 8. Map of the spatial distribution of NDVI values and their growth stages for pivot No. 13 using the satellite image obtained on 13th January 2005.	72
Figure 9. Erosion risk map for the pivot No. 13 for the image obtained on November 13, 2005.	74

### ARTIGO III

Figure 1. Location and number of the centered pivots in Cruz Alta, Rio Grande do Sul, Brazil. The Landsat paths 222 and 223 row 80 overlap in the region.	99
Figure 2. Thematic maps resulting from the NDVI values during the crop cycle.	100
Figure 3. NDVI profile for maize and soybean along the crop cycle (Days After Sowing, DAS).	102
Figure 4. Relation between NDVI, Phenology, Height and Days After Sowing for Soybean and maize.	103
Figure 5. The first derivative analysis helps in the definition of the stages of the crop cycle.	104

### ARTIGO IV

Figure 1. Location of the study area. The rectangle is in the overlapped region of the paths 222/80 and 223/80 of the Landsat 5 satellite imagery.	111
Figure 2. Linear relationships between the NDVI and $K_{cb\ SIMDual}$ for soybean and maize crop cycles.	119
Figure 3. Seasonal variation of the daily basal crop coefficients obtained from SIMDualKc model for both potential ( $K_{cb\ pot\ SIMDual}$ ) and actual ( $K_{cb\ act\ SIMDual}$ ) conditions and those obtained from the NDVI ( $K_{cb\ pot\ NDVI}$ ) as well as the precipitation and irrigation during the soybean crop cycle (November to May).	126
Figure 4. Seasonal variation of daily basal crop coefficients obtained from SIMDualKc model for both potential ( $K_{cb\ pot\ SIMDual}$ ) and actual ( $K_{cb\ act\ SIMDual}$ ) conditions and those obtained from the NDVI ( $K_{cb\ pot\ NDVI}$ ) as well as the precipitation and irrigation during the maize crop cycle (September to February).	127

## SUMÁRIO

INTRODUÇÃO GERAL.....	15
<b>ARTIGO I - SENSORIAMENTO REMOTO PARA ESTIMATIVA DA EVAPOTRANSPIRAÇÃO E COEFICIENTES DE CULTURA EM ÁREAS IRRIGADAS .....</b>	<b>23</b>
RESUMO.....	23
ABSTRACT.....	23
INTRODUCTION.....	23
DEVELOPMENT.....	26
<i>Remote Sensing (RS)</i> .....	26
<i>Remote Sensing of Vegetation</i> .....	26
<i>Vegetation Indices</i> .....	27
<i>Landsat</i> .....	28
<i>Evapotranspiration</i> .....	30
<i>Reference evapotranspiration (<math>ET_o</math>)</i> .....	30
<i>Crop evapotranspiration (<math>ET_c</math>)</i> .....	31
<i>Crop evapotranspiration under no standard conditions (<math>ET_{adj}</math>)</i> .....	31
<i>Direct methods to measure evapotranspiration</i> .....	31
<i>Methods based on meteorological data - <math>ET_o</math></i> .....	32
<i>Methods for calculating crop evapotranspiration - <math>ET_c</math></i> .....	33
<i>Methods for calculating the actual evapotranspiration - <math>ET_{c act}</math></i> .....	34
<i>Estimation of <math>ET_{c act}</math> by assimilation of remote sensing data</i> .....	35
<i>Remote sensing for estimating plant water stress</i> .....	35
<i>Models for estimating the energy balance</i> .....	37
<i>Crop coefficients calculated from soil water balance models assimilated to     vegetation indexes</i> .....	39
FINAL CONSIDERATIONS.....	44
REFERENCES.....	45
<b>ARTIGO II - SISTEMA DE INFORMAÇÃO GEOGRÁFICA PARA APOIO AO MANEJO DA IRRIGAÇÃO .....</b>	<b>53</b>
INTRODUCTION.....	53
METHODOLOGY.....	55
<i>Study sites</i> .....	55
<i>Remote sensing data and products</i> .....	56
<i>Creation of related database</i> .....	57
<i>Processing of images</i> .....	57
<i>Crop and meteorological data</i> .....	59
<i>Association of tables with objects</i> .....	59
RESULTS AND DISCUSSION.....	59
CONCLUSIONS.....	75
REFERENCES.....	75

<b>ARTIGO III - SENSORIAMENTO REMOTO PARA MONITORAMENTO DE MILHO E SOJA IRRIGADOS POR PIVÔ-CENTRAL NO RIO GRANDE DO SUL.....</b>	<b>79</b>
INTRODUCTION .....	79
MATERIALS AND METHODS .....	80
<i>Study area</i> .....	80
<i>Remote sensing data and products</i> .....	81
<i>Field monitoring system information</i> .....	82
<i>Phenology</i> .....	83
<i>Sensitivity of the NDVI to phenological stage identification: Tukey difference</i> .....	83
<i>Validation of the average curve and phenology model</i> .....	84
RESULTS AND DISCUSSION .....	85
<i>Geographic data base and image processing</i> .....	85
<i>Statistical processing of NDVI pixel's values</i> .....	85
<i>ANOVA and Tukey Honestly Significant Difference Test</i> .....	86
<i>NDVI vs DAS curves</i> .....	87
<i>Profile and sub-division of the curves</i> .....	87
<i>Phenology and NDVI</i> .....	88
<i>FAO56 Irrigation management stages</i> .....	89
<i>Validation of the phenology general calibration curve</i> .....	91
<i>GIS Thematic Maps for Crop Stage Monitoring</i> .....	92
CONCLUSIONS .....	94
REFERENCES .....	95

<b>ARTIGO IV - ASSIMILAÇÃO DO NDVI PARA A ESTIMATIVA DE COEFICIENTES DE CULTURA BASAIS PARA SOJA E MILHO IRRIGADOS POR PIVÔS CENTRAIS NO SUL DO BRASIL .....</b>	<b>107</b>
ABSTRACT.....	107
INTRODUCTION.....	107
MATERIALS AND METHODS .....	110
<i>Study area</i> .....	110
FIELD MONITORING .....	111
CROP IDENTIFICATION IN GIS AND GEOGRAPHIC DATABASE .....	112
SIMDUALKC .....	112
PRODUCTS AND REMOTE SENSING DATA .....	115
STATISTICAL ANALYSIS .....	115
RESULTS AND DISCUSSION.....	118
<i>Basal crop coefficient (<math>K_{cb}</math>) derived from NDVI</i> .....	118
CONCLUSIONS.....	128

<b>DISCUSSÃO GERAL.....</b>	<b>132</b>
<b>CONCLUSÃO GERAL .....</b>	<b>136</b>
<b>REFERÊNCIAS BIBLIOGRÁFICAS GERAIS .....</b>	<b>139</b>

## INTRODUÇÃO GERAL

Atualmente, a agricultura é responsável pela retirada de 70% de toda a água doce mundial, embora seja o setor que oferece as melhores oportunidades para tirar proveito da eficiência hídrica, melhorando a produtividade e reduzindo a pobreza (UNESCO & WWAP, 2015). Por esse motivo faz-se necessário implementar políticas públicas que objetivem o uso inteligente dos recursos hídricos, principalmente quando se refere à agricultura. Porém, ainda existem dificuldades em se conciliar desenvolvimento econômico com preservação ambiental. Desta forma, o suprimento de água de boa qualidade pode estar sendo comprometido para as gerações futuras.

O rápido crescimento da agricultura irrigada, como vem acontecendo no Planalto Médio do estado do Rio Grande do Sul, coloca uma nova demanda sobre os recursos hídricos e traz à tona esta problemática da implementação de políticas de outorga e gestão do uso da água. Porém, são necessárias estimativas precisas do consumo e reservas de água para gerenciar eficazmente o manejo da cultura, requerendo das autoridades públicas, universidades e dos pesquisadores, o desenvolvimento de ferramentas capazes de avaliar o volume de água utilizado na agricultura irrigada. No entanto, esta é uma tarefa complexa e as informações necessárias geralmente não estão disponíveis em nível de parcela agrícola, nem em áreas irrigadas (DROOGERS et al., 2010), sendo utilizadas aproximações de larga escala calculadas com base nas estimativas de alguma estação meteorológica próxima e coeficientes de cultura padrões.

Neste sentido, o mapeamento da evapotranspiração (ET) e coeficientes de cultura ( $K_c$ ) mediante o uso de imagens de sensores orbitais para apoiar o manejo da irrigação e estimar o consumo de água pelas culturas vêm sendo uma prática comum (BASTIAANSSEN 2009; ALLEN et al., 2005; FOLHES, 2007; ANDERSON et al., 2012b). A estimativa da água por meio do sensoriamento remoto tem a vantagem de ser aplicável a extensas áreas sem a necessidade de coleta de dados a campo (FAO, 2012).

A abordagem desenvolvida pela Bastiaanssen (2009) centra-se no consumo de água de quatro diferentes tipos de uso do solo: áreas protegidas, pastos, de sequeiro e agricultura irrigada. A abordagem faz uma distinção entre as partes benéficas e não benéficas da evaporação, transpiração e interceptação da água, expressa em produtividade por unidade de terra e a produtividade por unidade de água consumida. Uma vez que a abordagem baseia-se na informação de sensoriamento remoto, ela tem a vantagem de que um estudo pode ser

implementado em um curto espaço de tempo e que a fonte de informação é imparcial e não depende de dados de campo que podem ou não já terem sido recolhidos (FAO, 2012).

A avaliação do volume de água consumido por uma cultura, ou seja, evapotranspirado parece ser um critério viável (HUFFAKER et al., 1998) para um bom planejamento de projetos de irrigação e o acompanhamento do uso e consumo da água. No entanto, a ET varia no tempo e no espaço dependendo da cultura agrícola, do manejo empregado, das características físicas e químicas do solo e das condições meteorológicas (ALLEN et al., 1998). Neste contexto as imagens permitem capturar essas condições específicas e ajustar os níveis de irrigação.

Dentre as vantagens de se utilizar o sensoriamento remoto (SR) para obter a ET, em detrimento a outras perspectivas - como a clássica abordagem FAO56 (ALLEN et al., 1998), é que sua estimativa pode ser obtida sem necessidade de definir o tipo de cultura agrícola e o teor de água no solo (SCHERER-WARREN & RODRIGUES, 2013). Nas Tabelas 1 e 2 estão resumidas algumas vantagens e desvantagens do método para a estimativa da ET via sensoriamento remoto e via FAO56 respectivamente.

O boletim FAO56 não forneceu meios específicos para estimar ET por meio de imagens de satélite. No entanto, desde que foi publicado, houve um progresso substancial alcançado no cálculo da ET por SR, que agora fornece uma base confiável para a determinação da ET por meio do balanço de energia à superfície e para explorar índices de vegetação que podem ser relacionados com o  $K_c$  ( $K_{c IV}$ ). Vários artigos de revisão de base teórica foram desenvolvidos (GLENN et al., 2007; IRMAK et al., 2012), além de artigos sobre a aplicabilidade da ET derivada do SR para manejo da irrigação e aconselhamento aos agricultores (CALERA et al., 2005; D'URSO et al., 2010; TEIXEIRA, 2010; PÔÇAS et al., 2015).

Concomitante com o desenvolvimento das abordagens FAO24 e FAO56 para a estimativa da evapotranspiração, o lançamento do primeiro satélite Landsat na década de 70, propiciou o desenvolvimento de técnicas e métodos que se utilizam do sensoriamento remoto (HEILMAN et al., 1977; BASTIAANSSEN, 1995; FASSNACHT et al., 1997; ALLEN et al., 2007c). O desenvolvimento desses métodos para a estimativa da evapotranspiração vem crescendo paulatinamente e permitindo aplicações eficientes na agricultura (BASTIAANSSEN et al., 1998a; ALLEN et al., 2001; ALLEN et al., 2005; PADILHA et al., 2011). As abordagens atuais para a estimativa da evapotranspiração utilizam-se de sensores orbitais com imagens na faixa do termal (BASTIAANSSEN, 1995; ALLEN et al., 2007a; ANDERSON et al., 2012a), ou metodologias que combinam o coeficiente de cultura basal



derivados de índices de vegetação com balanço hídrico do solo (PADILHA et al., 2011; MATEOS et al., 2013; GONZÁLEZ-DUGO et al., 2013).

KANAMASU et al., (1977) fizeram uma das primeiras tentativas para estimar a ET, por meio do sensor MSS do satélite Landsat, que ainda não possuía uma banda termal. Posteriormente, no final da década de 1980, o sensor TM ganha importância devido a banda termal adicionada aos satélites 4 e 5 da mesma série (MORAN et al., 1989), mas foi somente na década de 1990 que se iniciaram os trabalhos relacionando os índices de vegetação com a evapotranspiração por meio da estimativa do balanço de energia na superfície (BASTIAANSEN, 1995; BASTIAANSEN et al., 1998a; BASTIAANSEN et al., 1998b; SZILAGYI et al., 1998; PEREIRA et al., 1999).

Tabela 1. Vantagens e desvantagens do cálculo da ET via sensoriamento remoto.

<b>ET via SENSORIAMENTO REMOTO</b>	
<b>VANTAGENS</b>	<b>DESVANTAGENS</b>
ET em nível de parcelas do tamanho do pixel da imagem (900m <sup>2</sup> para TM/L5)	Dados reais da ET somente no momento da passagem do satélite
Calcula a distribuição espacial da ET dentro da parcela agrícola ou região	Necessidades de técnicos treinados para o complexo processamento das informações
Não utiliza o coeficiente da cultura (K <sub>c</sub> ) pré determinados na literatura	Baixa resolução temporal e incerteza na disponibilidade das imagens
Permite avaliar o K <sub>c</sub> em nível de pixel	Não permite ou prejudica o cálculo da ET em dias nublados ou com nuvens
Obtém diretamente a ET <sub>c</sub>	
Uma única estação meteorológica pode calibrar uma cena de 185Km <sup>2</sup>	Necessidade de dados meteorológicos de boa exatidão, acurados e representativos
Não necessita informações da cultura como: época de semeadura e estágio fenológico	Necessidade de manutenção da cultura de grama ou alfafa a uma altura de 12cm e 50cm respectivamente dentro de um raio de 100m da estação meteorológica
Não necessita de informações de umidade do solo	
Não necessita reconhecimento da cultura a campo ou classificação da imagem para o cálculo da ET	Necessidade de realizar ajustes nos dados meteorológicos, segundo FAO 56 ou ASCE-EWRI (2005) ou ALLEN <i>et al.</i> (2007b), para estações não padronizadas
Dados utilizados podem ser de domínio público: imagens de satélite e dados meteorológicos.	
Utilização de dados de reflectância próprios de cada pixel para o cálculo da ET	Necessita software de processamento comercial ou programação local

Tabela 2. Vantagens e desvantagens do cálculo da ET via FAO 56

<b>ET via FAO 56</b>	
<b>VANTAGENS</b>	<b>DESVANTAGENS</b>
ET calculada por um procedimento reconhecidamente robusto e confiável	Dependem de dados de estações meteorológicas próximas cerca de 8Km
Metodologia padronizada internacionalmente	Utilização de coeficientes de cultura ( $K_c$ ) pré estabelecidos e não necessariamente correspondentes à realidade da região sob estudo
Cálculos que demandam recursos computacionais simples	
Software de processamento livre	
Possibilidade de cálculo da ET independente da condição climática (mesmo em dias nublados ou com nuvens)	Necessidade informações sobre a cultura: estágio fenológico e época de semeadura
Permite montar um sistema de monitoramento contínuo para cálculos de taxa de irrigação	Necessidade informações sobre umidade do solo
ET calculada com medições em intervalos de tempo horários	Necessidade de monitoramento periódico a campo

Abordagens recentes foram desenvolvidas para estimar ET a partir de dados exclusivamente de sensoriamento remoto. BOIS et al. (2008) utilizaram dados de radiação solar do satélite HelioClim-1. Mais recentemente, DE BRUIN et al. (2010, 2012) propuseram uma equação radiação-temperatura com base na equação Makkink para estimar a ET diária usando dados de radiação de um satélite geostacionário (LANDSAT). Uma melhoria foi conseguida utilizando os dados de temperatura por satélite em adição à radiação (CRUZ-BLANCO et al., 2014). Atualmente, resultados disponíveis para a Andaluzia, Sul da Espanha, e Portugal, que adotaram fatores de ajuste calibrados localmente para a radiação e temperatura são bastante promissores (PEREIRA et al., 2015).

As abordagens para a estimativa da ET que se utilizam exclusivamente de dados de sensoriamento remoto ou aquelas computadas por modelos matemáticos a partir do balanço de energia na superfície são complexas e pouco operacionais, ficando estas técnicas limitadas à pesquisa. Já a abordagem FAO56 é comumente aceita para objetivos operacionais e de pesquisa (PEREIRA et al., 2015).

Nos últimos anos, outra abordagem envolvendo as abordagens FAO56 e sensoriamento remoto vem sendo explorada: ela é baseada na abordagem FAO56 para calcular ET, onde o  $K_c$  pode ser relacionado com índices vegetação ( $K_{c IV}$ ) provindos da reflectância de superfície medida em faixas específicas do espectro eletromagnético, especialmente bandas do vermelho e infravermelho, obtidas por sensoriamento remoto. Desta

forma, a evapotranspiração de referência ( $ET_0$ ) é multiplicada pelo  $K_c$  obtido por SR e assim se obtém a  $ET_c$ . Esta abordagem,  $K_{c\ IV}$ , tem sido usada por HUNSAKER et al. (2005); ER-RAKI et al. (2013); MATEOS et al. (2013); PÔÇAS et al. (2015).

A abordagem  $K_{c\ IV}$  é mais simples do que a abordagem baseada no balanço energético, uma vez que precisa de menos medidas e é baseada em princípios elementares. No entanto, ela é considerada pouco sensível a fenômenos de curto prazo, como por exemplo a redução da ET devido ao fechamento dos estômatos causado por déficit hídrico no solo ou déficit de vapor de água, um efeito que é detectado pelos métodos de balanço de energia. Portanto, o pressuposto subjacente ao método  $K_{c\ IV}$  é que efeitos de curto prazo como o fechamento dos estômatos tem um pequeno efeito sobre a redução da evapotranspiração em comparação com o tamanho da cultura. Esta parece ser uma suposição razoável para as culturas irrigadas por pivô central. Por outro lado, o efeito mais importante do estresse hídrico em culturas é a redução do crescimento, que é tido em conta pelo método  $K_{c\ IV}$  (MATEOS et al., 2013).

Os campos agrícolas irrigados por pivô central possuem características que favorecem a aplicação de métodos como  $K_{c\ IV}$ , pois o crescimento uniforme das culturas dentro de uma área bem definida, como o pivô central, favorecem as definições de  $K_c$  e possibilitam o ajuste e a calibração dos valores obtidos pelos índices de vegetação com estádios de desenvolvimento da cultura a campo e ao longo de seu ciclo. Neste sentido os índices de vegetação tornam-se ferramentas promissoras para auxiliar no apoio ao manejo, gerenciamento e monitoramento da irrigação por aspersão.

Um aspecto diferencial da utilização da abordagem  $K_{c\ IV}$  é a facilidade para obter a variação espacial do  $K_c$  ou  $K_{cb}$  nas áreas agrícolas. Esta quarta abordagem é considerada promissora devido ao fato das imagens de satélite poderem ser integradas a modelos matemáticos tornando-se possível a estimativa de  $K_c$  e ET no tempo e no espaço, em uma distribuição geográfica em forma de matriz. O que não acontecia no passado quando a estimativa de ET e  $K_c$  eram determinadas de forma homogênea em uma única área.

Outra vantagem é sua sensibilidade ao crescimento da vegetação que pode proporcionar a identificação de fenômenos anormais, como infestações por pragas e doenças, déficit hídrico e ocorrência de geadas (HUNSAKER et al. 2005; YANG et al., 2005; REISIG & GODFRE, 2006; KARNIELI et al., 2010). Além de fornecer uma descrição campo-a-campo da variação de  $K_c$  ou  $K_{cb}$ , devido às variações de datas de plantio, espaçamento entre plantas e cultivares (PEREIRA et al., 2015). A avaliação das vantagens e desvantagens dos coeficientes de cultura à base de IV foi apresentada por ALLEN et al. (2011).

Estudos que se utilizam da abordagem  $K_c$  IV têm apresentado bons resultados evidenciando a potencialidade desta ferramenta (MATEOS et al., 2013; PÔÇAS et al., 2015). Esses estudos estimaram valores de  $K_c$  e  $K_{cb}$  por meio de equações onde é utilizado um coeficiente de densidade ( $K_d$ ) proposto por ALLEN & PEREIRA (2009), cujo cálculo utiliza coeficientes gerais tabelados para várias culturas e a fração de cobertura do solo ( $f_c$ ) calculada por índices de vegetação. Eles obtiveram boa aproximação com relação à metodologia tradicional FAO56. No entanto, sugeriram que esta aplicação não permite estimar o  $K_{cb}$  para períodos em que ocorre déficit hídrico no solo ou déficit de vapor de água, onde um coeficiente de estresse hídrico do solo ( $K_s$ ) deve ser calculado e multiplicado ao  $K_{cb}$ .

O estudo de PÔÇAS et al. (2015) propôs a utilização de  $K_s$  e  $K_e$  derivados de um modelo de balanço de água no solo, o modelo SIMDualKc, junto com dados de  $K_{cb}$  advindos de equações gerais que usam os índices de vegetação como parâmetro de ajuste. Essa metodologia diminuiu a influência dos índices de vegetação no cálculo de  $K_c$ , e deu maior peso à influência do modelo SIMDualKc nos resultados do  $K_c$  VI. No entanto, os autores colocam que esta abordagem recupera informações úteis a partir de imagens de satélite com o objetivo de aconselhamento ao manejo da irrigação para o agricultor.

Várias relações entre  $K_c$  e índices de vegetação tem sido estabelecidas. No entanto, não há acordo sobre a natureza e a generalidade dessas relações (GONZÁLEZ-DUGO & MATEOS, 2008). Alguns estudos como os de GONZALEZ-PIQUERA et al. (2003); DUCHEMIN et al. (2006); ER-RAKI et al. (2010); PÔÇAS et al. (2015) têm mostrado que essas relações são lineares, mas outros não têm encontrado relações de linearidade, a exemplo de HUNSAKER et al. (2003,2005); ER-RAKI et al. (2007); GONZÁLEZ et al. (2008). Portanto, o estabelecimento de uma relação única entre coeficiente de culturas e índices de vegetação é um tópico de pesquisa em andamento. A FAO recomenda que o  $K_c$  deva ser calibrado localmente, para assim se obter estimativas de ET mais próximas à realidade de solo, clima e cultura estabelecida na região sob estudo (ALLEN et al., 1998).

Por outro lado, para o manejo da irrigação, também é desejável o uso de estimativas da ET com alta frequência temporal. A alta frequência temporal é necessária para se capturar a dinâmica da ET ao longo do tempo, já que essa sofre alteração em função da condição atmosférica e quantidade de água precipitada ou aplicada por irrigação sobre o solo (SCHERER-WARREN & RODRIGUES, 2013).

A resolução espacial e temporal da atual geração de satélites com sensores necessários para a estimativa da ET são restritas (KALMAN et al., 2008), pois apresentam limitações em aplicações em escala local, como manejo agrícola, por exemplo. Atualmente estão disponíveis

sensores de baixa resolução espacial e alta resolução temporal (MODIS, AVHRR) ou sensores de média resolução espacial e baixa resolução temporal (TM, ETM, Aster).

Os sensores de baixa resolução espacial apresentam erros na obtenção da ET, pois a agregação da ET em diferentes escalas espaciais não é linear (SU et al., 1999; HONG, 2009). Para os sensores de média resolução espacial as limitações são em função da intermitência de eventos de precipitação e irrigação no período de aquisição de duas imagens de média resolução espacial ( $\geq 16$  dias), no qual o padrão espaço-temporal da precipitação/irrigação altera a evapotranspiração em intervalo bastante inferior a 16 dias (JHORAR et al., 2002).

Para se tentar diminuir as limitações inerentes a tecnologia disponível, esta pesquisa trabalha em uma região onde ocorre a sobreposição de duas órbitas (222 e 223) no mesmo ponto de passagem (80) do sensor TM a bordo do satélite Landsat 5. Desta forma é possível otimizar a resolução espacial de 16 para 8 dias, possibilitando a obtenção de boas imagens com maior frequência de tempo. Dito de outra forma, depois de imagear a área em uma órbita o satélite irá imagear a órbita subsequente após oito dias; como a área de estudo está sobreposta, se consegue diminuir a resolução espacial de 16 para 8 dias. Porém, isso não significa que será possível a obtenção de imagens a cada 8 dias, e sim, que a probabilidade de se obter boas imagens com melhor frequência temporal é aumentada.

Pelo exposto, a ênfase desta pesquisa está centrada no monitoramento e mapeamento de variáveis importantes para o manejo da irrigação em 30 pivôs centrais, por meio da assimilação de dados de sensoriamento remoto em modelos de balanço de água no solo, organizando as informações em SIG. Variáveis como a fenologia, ET,  $K_c$  e  $K_{cb}$  de culturas como milho e soja cultivadas no Brasil, podem ser estimadas e mapeadas com o apoio de técnicas de sensoriamento remoto associadas a informações de campo, visando apoiar o manejo da irrigação.

Os objetivos do trabalho foram:

- 1) Propor uma estrutura baseada em bancos de dados geográficos dentro de um SIG que seja adequada para o gerenciamento da irrigação por pivô central.
- 2) Analisar a sensibilidade do NDVI para a descrição do ciclo das culturas de soja e de milho irrigados com pivô central e para a detecção de estádios fenológicos no Sul do Brasil.
- 3) Determinar os intervalos de valores de NDVI correspondentes aos períodos de desenvolvimento descritos pelo boletim FAO56 (inicial, crescimento rápido, intermediário e final).

- 4) Desenvolver um procedimento de assimilação dos dados de NDVI com os dados provenientes do procedimento da FAO56 implementado em um modelo de balanço de água no solo, o SIMDualKc.
- 5) Determinar a curva geral de valores do coeficiente de cultura basal atual para o ciclo da soja e o milho no Sul do Brasil, e compará-la com curvas específicas individuais de cada pivô para determinar o grau de ajuste esperado.
- 6) Determinar os intervalos de valores de  $K_{cb}$  atuais assimilado ao NDVI para os períodos inicial, crescimento rápido, intermediário e final.

Para se atingir este objetivo utilizou-se do sensoriamento remoto de dados espectrais provenientes do sensor TM, abordo do satélite Landsat 5, na sobreposição do ponto 80 nas órbitas 222 e 223, compreendendo imagens entre 2003 a 2011. Dados meteorológicos (temperatura, umidade relativa, velocidade dos ventos) provenientes da estação meteorológica do INMET de Cruz Alta, Rio Grande do Sul, também foram utilizados, além de informações a campo (cultura, época de semeadura, estágio fenológico, altura da planta, solo e irrigações) adquiridas por meio do monitoramento e gerenciamento da irrigação (Sistema Irriga<sup>®</sup>).

Há evidências que a utilização de uma grande diversidade de parcelas agrícolas, com diferentes especificidades e cobrindo todo o ciclo cultural, confere uma boa robustez aos resultados. O monitoramento agrícola organizado em sistema de informação geográfica com assimilação de informações satelitais em modelos de balanço de água no solo pode ser considerado ferramenta útil para determinação das necessidades hídricas das culturas de milho e soja no Sul do Brasil, visando apoiar o planejamento e gerenciamento da irrigação. Também pode servir de avaliação e adequação do manejo da irrigação para empresas que prestam este serviço na região.

## ARTIGO I - SENSORIAMENTO REMOTO PARA ESTIMATIVA DA EVAPOTRANSPIRAÇÃO E COEFICIENTES DE CULTURA EM ÁREAS IRRIGADAS

### Remote sensing for estimating evapotranspiration and crop coefficients in irrigated areas: a review

#### RESUMO

A avaliação de variáveis agrícolas e ambientais associada ao gerenciamento de culturas irrigadas por meio de sensores remotos é uma tendência em expansão. A atual disponibilidade de imagens de satélite e o iminente futuro de disponibilidade de imagens de veículos não tripulados colocam uma grande relevância às metodologias que permitem o uso destas informações no gerenciamento da produção agrícola. A tendência também vem ao encontro das necessidades da agricultura de precisão, fornecendo informações com melhor resolução espacial e temporal. Neste contexto, cobram relevância especial às estimativas com caráter operacional de variáveis tais como a evapotranspiração ou os coeficientes de cultura, que definem o consumo de água. Os enfoques mais promissores neste sentido são os baseados no balanço de energia na superfície do solo, e os que combinam correlações entre os coeficientes de cultura e índices de vegetação com modelos de balanço de água no solo. Uma vantagem destes enfoques comparados com a metodologia tradicional, que usa medições de estações meteorológicas, é a maior resolução espacial, apresentada em forma de matriz de parcelas quadradas menores, com informações específicas sobre estas. O objetivo deste trabalho é revisar criticamente as metodologias encontradas na literatura com vistas a sua aplicação em sistemas de irrigação por pivô central no sul do Brasil.

**Palavras-chave:** Coeficiente de cultura, NDVI, balanço de energia na superfície, balanço de água no solo, Landsat.

#### ABSTRACT

The evaluation of agricultural and environmental variables related to irrigate crop management through remote sensors is an expanding tendency. The present availability of satellite images and the near future of unmanned air vehicles images availability emphasize the importance of the methodologies that allow the use of this information for agriculture management. This tendency also matches the needs of precision agriculture, providing information with better spatial or temporal resolution. In this context, operational procedures for the estimative of variables such as evapotranspiration or crop coefficient, that define the water consumption, become especially relevant. The approaches that appear as more promissory are the ones that use the energy balance in soil surface, and the ones that combine the use of correlations between crop coefficients and vegetation indices with water balance models. An advantage of this kind of approach in comparison with the traditional methodology based on meteorological stations is a higher spatial resolution that appears in the format of a matrix of square plots, with plot-specific information. The objective of this work is to critically revise the so related methodologies found in the scientific literature, aiming at its application in central-pivot irrigated systems in South Brazil.

**Keywords:** NDVI, soil surface energy balance, soil water balance, Landsat.

#### Introduction

Evapotranspiration (ET) is a process by which water is lost from the soil surface and crop canopy to the atmosphere (Allen et al. 1998). It is a concept that defines the crop water requirement. This is a complex process and takes into account several factors of the region

where the crop is grown, such as climate, cropping intensity, environment, water availability, soil fertility, cultivation methods and irrigation practices. Since agriculture requires a high volume of water for the production and sustainability is a key factor, and there are many methods for estimating the crop water requirement because of the different environmental situations, however, the procedures used for the direct evaluation of crop water use in the field are difficult and awkward. The methodologies depend principally on the spatial scale and relief, for instance the direct methods such as lysimeters that measure the water balance of an area, roughly of a few square meters, are not suitable for rough terrain as a result of precision loss of irrigation depth required due to surface runoff and subsurface flow. Most methodologies were already verified, and used with variable success, as they are applied in agronomical and environmental conditions for which they were not conceived (Doorenbos and Pruitt 1977).

The monitoring of irrigated agriculture aiming the optimization of the natural resources without affecting crop production is a long-standing concern of scientists and technicians of arid regions, and is become increasingly important in subtropical regions with the expansion of agriculture which is putting pressure on soil and water resources. Since the 1970s, studies to estimate evapotranspiration have been developed, with various equations and empirical models being tested in several regions of the planet (Davies and Allen 1973; Allen et al. 1983; Allen et al. 1984; Allen and Asce 1986a, 1986b, 1986c; Allen et al. 1991; Scaloppi and Allen, 1993; Allen et al. 1996; Allen et al. 1998). However, after launching the FAO bulletin 56 (Allen et al. 1998), there has been standardization of evapotranspiration concepts, with conceptual review of theoretical and practical works and new trends in applying calculation procedures and relate them to other methods (Pereira et al. 1999; Sarwar and Bastiaanssen 2001; Boegh et al. 2002; Allen et al. 2005b; Silva et al. 2012). Nevertheless, irrigated fields monitoring in subtropical regions using remote sensing data of orbital or aerial platforms is very recent, even as a research topic (Ferreira 2008; Folhes et al. 2009).

Concurrently with the development of empirical methods for estimating crop evapotranspiration, the launch of the first Landsat satellite in the 70's led to the development of technical and semi-empirical methods that use information obtained through remote sensing, such as satellite images corresponding to different windows of the electromagnetic spectrum (Heilman et al. 1977; Bastiaanssen 1995; Fassnacht et al. 1997; Allen et al. 2007b). Since then, the development of these methods to estimate crop evapotranspiration permits its efficient application in agriculture (Bastiaanssen et al. 1998a; Allen et al. 2001, 2005a; Padilha et al. 2011). The current semi-empirical models to estimate evapotranspiration are



using orbital sensors that detect visible light and image them in the thermal range (Bastiaanssen 1995; Allen et al. 2007b; Anderson et al. 2012a), or methodologies that combine the crop coefficient ( $K_c$ ) or crop basal coefficient ( $K_{cb}$ ), derived from vegetation indices (VI), with soil water balance (Padilha et al. 2011; Mateos et al. 2013; González-Dugo et al. 2013).

Kanamasu et al. (1977) made one of the first registered estimations of ET with orbital data, using the Landsat 1 MSS sensor that had no thermal band. Later, at the end of the 1980s the TM sensor gained importance due to thermal band added to the satellites 4 and 5 (Moran et al. 1989), but it was only in the 1990s that studies began relating vegetation index with evapotranspiration by estimating the energy balance at the soil surface (Bastiaanssen 1995; Bastiaanssen et al. 1998a, 1998b; Szilagyi et al. 1998; Pereira et al. 1999).

On the other hand, conventional methods for estimating crop water requirements are not practicable under certain conditions, since they were developed for different regions in terms of specific agronomic, climatic and topographic conditions. For areas with irregular relief such as mountains and valleys, for example, it is difficult to estimate or measure crop evapotranspiration by conventional methods because of the complex hydrological process taking place. The quantification of the components of the water balance becomes complex, due to the under-surface flow of soil water, the runoff, and the presence of deep percolation.

For homogeneous regions, the integration of remote sensing and climatic variables has been widely used to estimate evapotranspiration and crops coefficients for both plot and regional scales (Allen et al. 2007b; Allen et al. 2011b; Anderson et al. 2012b; Mateos et al. 2013; Pôças et al. 2015). The semi-empirical models used enable updated spatial information at the time of passage of the satellite, besides a reliable estimate, thus facilitating the irrigation management of those areas. Considering the available satellite information, the more frequently used platforms are MODIS, Landsat, NOAA, GOES, ASTER, among others, which have thermal bands in addition to the visible and other infrared bands. This availability made possible the improvement of energy balance approaches, and also the water balance, vegetation index and crop coefficient combination approaches, which became increasingly relevant.

Therefore, the objective of this study was to carry out a literature review on estimating ET and  $K_c$  through the use of remote sensing including a revision of the key concepts both from remote sensing and evapotranspiration, and also the methodological aspects of the historical research.

In summary, alternative methodologies for the evaluation of evapotranspiration and crop coefficients were analyzed, which are based in the use of multi-spectral orbital sensors data and vegetation indices. The main advantages, disadvantages and limitations are discussed, with regard to its application in irrigated areas in South Brazil.

### **Development**

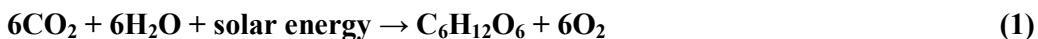
This literature review presents the basic concepts of the estimation of actual evapotranspiration ( $ET_{c \text{ act}}$ ) using remote sensing techniques, as well as traditional methodologies for measurements and estimations. A discussion of the advantages, disadvantages and limitations of each methodology is presented. A web search was performed and about 100 articles related to estimating evapotranspiration using remote sensing data from 1970s to the present were used. Also, information on remote sensing concepts and the technical characteristics of the satellites and sensors were obtained from NASA and INPE sites as well as reference books such as Jensen (2011). The basic concepts for the determination of evapotranspiration and the crop coefficients were based on Doorenbos and Pruitt (1977) e Allen et al. (1998).

### ***Remote Sensing (RS)***

The acquisition of information registers concerning the ultraviolet regions, visible, infrared and electromagnetic microwave spectrum, without contact, through the use of instruments such as cameras, scanners, lasers, linear devices and/or matrix located on platforms such as aircraft or satellites and analysis of the information acquired through visual or digital image processing, is called remote sensing (Jensen 2011).

### ***Remote Sensing of Vegetation***

In the early twentieth century, scientists found that oxygen for photosynthesis came from water. In fact, the solar energy that enters the plant breaks the water into oxygen and hydrogen. The well known photosynthetic process is described by the equation:



Photosynthesis is an energy storage process by the plant that occurs in leaves and other green parts of the plants in the presence of light. Light energy is stored in a single sugar molecule (glucose) that is produced from carbon dioxide ( $\text{CO}_2$ ) existing in the air, and water

(H<sub>2</sub>O) absorbed by the plant, mainly by the root system. When the carbon dioxide and water are combined, sugar molecule (C<sub>6</sub>H<sub>12</sub>O<sub>6</sub>) is formed in the chloroplast and oxygen gas (O<sub>2</sub>) is released as a by-product to the atmosphere. According to Jensen (2011), plants adapt their internal and external structures for photosynthesis, this structure and its interaction with electromagnetic energy have a direct impact on how the leaf and plant canopies appears spectrally when recorded using remote sensing instruments.

The energy flux relation when the light radiation interacts with the leaf is expressed as:

$$i\lambda = \rho\lambda + \alpha\lambda + \tau\lambda, \quad (2)$$

where:  $\rho\lambda$  is the spectral reflectance of hemispheric leaf;  $\alpha\lambda$  is the spectral absorbance of hemispheric leaf and;  $\tau\lambda$  is the spectral transmittance of the hemispheric leaf.

As reflectance is the most important property measured by remote sensors, then it becomes clearer if the energy flux relation is rearranged as:  $\rho\lambda = i\lambda - (\alpha\lambda + \tau\lambda)$ . Previous works of Gates et al. (1965) and Gausmann et al. (1969), and others have shown that pigment content, humidity and leaf morphology affect leaf reflectance and transmittance. In other words, the reflectance has specific information on the status and composition of the vegetation.

With the intuition of evaluating the growth stage, composition and state of plant canopies using remote sensing orbital information, scientists combined the capability of near infrared and red bands in the so called vegetation indexes, which are combinations of the bands in order to enhance the understanding of the changes due to plant development.

### ***Vegetation Indices***

Since the 1960s, scientists have been drawing and modeling various biophysical vegetation parameters using remote sensing data. Much of this effort has involved the use of vegetation indices, which are dimensionless radiometric measurements that indicate the relative abundance and activity of vegetation, including leaf area index (LAI), percentage of vegetal cover, chlorophyll content, green biomass, and photosynthetic active radiation (PAR).

There are many vegetation indices. The NDVI (Normalized Difference Vegetation Index), for example, is an index developed by Rouse et al. (1974):

$$NDVI = \frac{\rho_{nir} - \rho_{red}}{\rho_{nir} + \rho_{red}} \quad (3)$$

The NDVI is important index because: (i) seasonal and inter-annual changes in the development and activity of vegetation can be monitored and; (ii) the reduction ratio from many forms of multiplicative noise (solar lighting differences, cloud shadows, atmospheric attenuation, topographical variations) present in multiple bands of images of multiple dates (Jensen 2011).

On the other hand, the disadvantages of NDVI: (i) being an index based on ratio, it is not linear and can be influenced by noisy additive effects such as atmospheric path radiance; (ii) the NDVI is highly correlated with LAI; however, this relationship may not be as strong during periods of maximum LAI, apparently due to saturation of NDVI when the LAI is very high and; (iii) the NDVI is very sensitive to variations in the substrate under the canopy (e.g. soils that are visible under the canopy). The NDVI values are particularly high with darker substrates (Huete et al. 2002; Wang et al. 2005).

Despite these limitations, the NDVI has been widely adopted and applied to data obtained from the Landsat satellite MSS and TM sensors, mainly due to its relationship with biophysical parameters of plants, particularly the vegetation dynamics and phenology (Pettorelli et al. 2005; Xião et al. 2006; Tao et al. 2008), the LAI, the roughness height to turbulent transfers, emissivity and albedo (Bastiaanssen et al. 1998b; Allen et al. 2007a), as well as their relationship with processes such as evapotranspiration (Nagler et al. 2005; Zhang et al. 2009), agricultural productivity (Salazar et al. 2008) and the fraction of photosynthetic active radiation absorbed by plant canopy (Glen et al. 2008).

### ***Landsat***

The Landsat series is one of the mostly used satellites for many studies aimed to estimating evapotranspiration and crop coefficients, partly because of the widely available information or because the renowned researcher in the field. Richard Allen, who developed METRIC model, is also a member of the Landsat Science Team, thus contributing to the adaptation of satellite applications to irrigation management.

The first Landsat satellite, called the Earth Resources Technology Satellite (ERTS-1), was launched on July 23, 1972 by the USA. After launching, the program was renamed to Landsat. The Landsat 1 was closed in January 6, 1978 (Mather 1987). After this, the Landsat 2, which was launched on January 22, 1975 and closed on February 2, 1982 was followed by

Landsat 3, launched on 5 March 1978 and closed on March 31, 1983. The Landsat 1-3 had on board a multispectral scanning system, known as multispectral scanner subsystem (MSS). The Landsat 4 was the first one of a new generation of Landsat satellites. This satellite was launched on July 16, 1982, at an altitude of 705 km, in nearly circular orbit and synchronous sun, with a temporal resolution of 16 days, better than Landsat 1-3 that had a temporal resolution of 18 days.

The Landsat 4 was equipped with two sensors, the multispectral scanner subsystem (MSS) and Thematic Mapper (TM). The TM has a spectral coverage of from 0.45 to 12.5  $\mu\text{m}$ , that is, from visible to thermal infrared with a spatial resolution of 30 m, except for the hot band, which has a spatial resolution of 120 m. The Landsat 4 went to malfunctioning, failed to record image, although it was not disabled. So, Landsat 5 had to be released earlier than expected, precisely on 1 March 1984. The Landsat 5, imaged for nearly 30 years, despite the projected life span of five years, thus functioned for about 5 times longer than expected. However, in December 2011, it stopped imaging.

Some features of Landsat 5 that made it the satellite with the greatest history of durability include: (i) seven bands with intervals 0.45 to 2.35  $\mu\text{m}$ ; (ii) spatial resolution of 30 meters, except band 6 with a spatial resolution of 120 meters; (iii) radiometric resolution of 8 bits, or 256 levels of gray; (iv) imaging range of 185 km; (v) orbit almost polar (sun synchronous); (vi) nominal altitude of 705 km; (vii) inclination and period of 98.2° and 99 minutes, respectively; (viii) equatorial crossing at 9h45min (local solar time) and;(ix) repetition of cycle or spatial resolution of 16 days (Mather 1987).

On October 5, 1993, NASA launched the Landsat 6, but the satellite was lost shortly after launch and never came into operation phase. On April 15, 1999 Landsat 7 was launched. The satellite uses the Enhanced Thematic Mapper Plus (ETM+) to replace the TM sensor, used in the Landsat 4 and 5. The ETM+ is a radiometer of 8-band multispectral scanning, which provides high-resolution images of the Earth's surface. The Landsat 7 was very active until May 31, 2003, and while on the SLC-OFF mode after that date, the quality of images was distorted.

The current version of the Landsat series is Landsat 8, which has a spatial resolution of 16 days, with compensation of 8 days with the Landsat 7. Images are available within 24 hours after imaging and can be freely downloaded from Earth Explorer website or Landsat Look Viewer. Landsat 8 carries two instruments, the Operational Land Imager (OLI) sensor, which has finest bands, with three additional new bands namely: deep blue band for coastal

studies; shortwave infrared band; and a quality assessment band. The other is infrared (TIRS) sensor, which is a thermal sensor that provides two thermal bands. Compared to other 7 Landsat series, the evolution of the technical characteristics of Landsat 8 are: (i) sensors that provide a better signal to noise (SNR) relation; (ii) 12 bits, this translates into 4,096 potential gray levels in an image, compared with the only 256 gray levels of 8 bits of previous instruments; (iii) the SNR allow a better characterization of land cover status and condition of vegetation and; (iv) the products are delivered as 16 bit images (on a scale of 55,000 gray levels). However, Landsat 8 has a large file size, about 1 GB when compressed.

### ***Evapotranspiration***

The evapotranspiration (ET) is a combination of two processes, evaporation and transpiration. On one hand, water is lost from the surface of the soil, lakes, rivers and oceans by evaporation, and on the other hand it is lost by transpiration from vegetation. Evaporation and transpiration occur simultaneously and there is no easy way to distinguish between the two processes. In addition to the availability of water on the soil surface, evaporation from a soil is mainly determined by the fraction of solar radiation reaching the earth's surface. This fraction decreases over the period of growth as the crop grows and the shadow of the crop canopy which increasingly grows on the soil area. When the crop is small, water is predominantly lost by evaporation from the soil, but when the crop is well developed and completely covers the ground, transpiration becomes the main process (Allen et al. 1998).

### ***Reference evapotranspiration ( $ET_0$ )***

Several concepts have been formulated for reference evapotranspiration ( $ET_0$ ) over the last decades. However, due to the nature and development of crop, and management practices, the concept of  $ET_0$  generated ambiguous definitions. For this reason, FAO has set a standard for obtaining the reference evapotranspiration ( $ET_0$ ). For Allen et al. (1998),  $ET_0$  is the evapotranspiration rate of a reference surface, alfalfa or grass, about 0.12 meters high, active growing, and completely covering the ground, with a surface resistance ( $R_s$ ) of  $70 \text{ ms}^{-1}$  and albedo ( $\alpha$ ) of 0.23 and without water restrictions, corresponding to maximum evaporation possible. The author also advised against the use of other concepts such as potential evapotranspiration that may causes ambiguities in the definition. The  $ET_0$  is a function of meteorological variables, being mainly affected by solar radiation, temperature, relative humidity and wind speed.

The purpose of  $ET_o$  is to serve as standard to compare the evapotranspiration results in different periods of the year or at other localities. In addition, the evapotranspiration of other crops may be related. Thus, helps to avoid the need to define a separate ET level for each type of plant and each period of growth (Allen et al. 1998).

Factors related to both the plant and soil does not affect reference evapotranspiration as a result of no water restriction, thus only the interference of meteorological parameters causes the variability of  $ET_o$ . Allen et al. (1998) recommended, as the standard, the FAO Penman-Monteith method for calculating  $ET_o$ .

### ***Crop evapotranspiration ( $ET_c$ )***

The crop evapotranspiration is based on the reference evapotranspiration being multiplied by only one factor, the crop growth coefficient, that is,  $ET_c = ET_o * K_c$ . The  $ET_c$  calculated thus refers to the evapotranspiration of a disease free crop growing in a large field (one or several hectares) under optimal soil conditions, including sufficient nutrient and water availability to reach full potential production. Local conditions and agricultural practices, including the types of plants and the selection of varieties, can interfere considerably in  $ET_c$  and therefore require certain corrections (Doorenbos and Pruitt 1977). So  $ET_c$  is dependent on prevailing weather conditions, expressed by  $ET_o$ , the type of crop (more or less drought resistance) and leaf area. As the leaf area of standard crop is constant and that of the real crops varies, the  $K_c$  value also varies.

### ***Crop evapotranspiration under no standard conditions ( $ET_{adj}$ )***

The real or actual evapotranspiration ( $ET_{adj}$ ) can be defined by the amount of water transpired from vegetation under real atmospheric conditions, soil moisture status and crop physiology, i.e., with or without water restriction, absence or presence of disease and so on. According to Pereira et al. (1997), the amount of water transpired depends mainly on plant water supply, the evaporating power of the air and energy availability, with the latter factor predominates over the other, so that, the amount of water consumed by a given crop varying with the size of the area covered by the plant, atmospheric demand and growing seasons.

### ***Direct methods to measure evapotranspiration***

Methods such as lysimeters and soil moisture monitoring are direct methods for obtaining crop evapotranspiration. The lysimeter tank is inserted into the soil and grown to a crop of interest. This tank is usually built and coupled to a precision balance, so that the weight variation of the system corresponds to the actual evapotranspiration accumulated

within certain time interval. Soil moisture monitoring method determines the amount of soil water variation (evapotranspired) between two successive periods for a range of irrigation, and for various soil layers under study (Nicácio 2008). However, besides being costly, the direct methods of measuring evapotranspiration are often badly distributed in space and time. Field campaigns are generally required, mainly due to the complexity and cost of equipment related to measurements for the energy balance and microclimatological methods, as well as eddy covariance and scintillometry.

### ***Methods based on meteorological data - $ET_o$***

Various algorithms and approaches, physical and mathematical models, are now available to estimating evapotranspiration based on climatic variables collected from weather stations. Although these methods work with the same group of variables, however, the complexity of the soil-plant-atmosphere dynamic processes has led to multiple versions of models, calculations and approximations. In this context, it becomes necessary to consider the suggestion of a standard procedure as given by FAO, which resulted in the drafting of some procedures considered as reference, which were first adequately documented in the FAO 24 and in FAO56 bulletins (Doorenbos and Pruitt 1977; Allen et al. 1998).

Equations used for the determination of reference evapotranspiration are divided into four main groups: (i) radiation method using empirical equations involving solar radiation or radiation; (ii) the temperature method, involving widespread equations as Thornthwaite and Blaney-Criddle; (iii) the method of pan evaporation, for instance the USA class A pan and; (iv) the method combining the aerodynamic and radiation balance, which involves the Penman's equation Penman (1948) and its modifications (Jensen et al. 1990). However, these four groups are not the only ones, there are several other equations with their parameterization conditioned by other statistical relationships.

These methodologies are often characterized by estimation errors, occurring for both small and large time scale (Pereira et al. 1997). Researchers such as Burman and Pochop, (1994) showed that the algorithms that use solar radiation instead of temperature have fairly minor errors in estimating evapotranspiration. On the contrary, Pereira et al. (2002) also said that the use of empirical equations, which utilize solar radiation, is not necessary for time scale of more than two weeks. They concluded that equations that use air temperature give satisfactory results. Moreover, the Penman (1948), model, which arise from the combination of aerodynamic and radiation balance has a more rigorous physical basis.



Consistent  $ET_o$  values for different climates and regions can be found in the guidelines for computing evapotranspiration, FAO-56 bulletin (Allen et al. 1998). Because this update standardizes the procedures for calculating the evapotranspiration reference and without any ambiguity in its calculation, thus, the combined FAO-Pennan-Monteith equation is considered standard for  $ET_o$  estimates. The FAO-PM model assumes that the crop has height of 0.12 m, with an aerodynamic resistance of the surface of  $70 \text{ s.m}^{-1}$  and albedo of 0.23. These characteristics should be for large areas with grass of uniform height, actively growing, completely covering the soil surface and without water stress.

#### ***Methods for calculating crop evapotranspiration - $ET_c$***

The  $ET_c$  is calculated under standard conditions, where the crops are considered to be cultivated under optimal conditions, with excellent soil water availability, and perfect agricultural management. As the land cover, properties of the crop canopies and aerodynamic resistance are different from the ones of grass the calculation conditions for  $ET_c$  are different from the ones corresponding to  $ET_o$ . The effects of the distinctive characteristics of the crop with regard to grass are integrated in the  $K_c$  coefficient. Once  $ET_o$  is obtained, the crop evapotranspiration can be obtained by considering  $K_c$ . The values of the crop coefficient are dependent of the type of crop, the growing stage and the local climatic conditions. The  $ET_c$  can be obtained through the following equation:

$$\mathbf{ET_c = ET_o \times K_c} \quad \mathbf{(04)}$$

Differences in the evaporation and transpiration between ideal crops and a reference surface of grass can be integrated in a single  $K_c$  or separated into two coefficients: the basal crop coefficient ( $K_{cb}$ ) and a soil evaporation coefficient ( $K_e$ ), that is  $K_c = K_{cb} + K_e$ .

The  $ET_c$  of a crop surface can be directly measured by mass transfer methods or by the energy balance at the soil surface. It can also be derived from water balance studies or by measurement with lysimeters.

$ET_c$  can also be derived from meteorological data obtained in the crop field by Penman-Monteith equation, after adjustment of albedo and the surface aerodynamic resistance with the crop growing characteristics along the agricultural cycle. Nevertheless, those parameters, albedo and resistance, are difficult to be determined accurately, as they continuously change during the vegetative cycle, or due to climate conditions or soil wetness.

The canopy resistance will also be strongly influenced by soil water availability and increased if the crop is subject to water stress (Allen et al. 1998).

### ***Methods for calculating the actual evapotranspiration - $ET_{c\ act}$***

The mass balance method may be used to obtain  $ET_{c\ act}$ . The mass balance method determines the inputs and outputs of water flow in the crop root zone (Allen et al. 1998). However, some studies have observed an overestimation of  $ET_{c\ act}$  (Dias and Kan 1999).

As seen above, the energy balance is the measurement of energy available at the surface for air heating (heat sensitive) and soil (heat in the soil) and the evapotranspiration processes (latent heat).

A complicating factor in determining evapotranspiration by this method is the high cost involved in measurements, which most often happens in a manner limited in time and space, making it impossible to obtain evapotranspiration at regional scale. Estimating evapotranspiration through energy balance has become more frequent with the use of remote sensing as a source of information for the calculation of energy flows.

Through precise measurements of temperature gradients and relative humidity, one can calculate the Bowen ratio which is another way of obtaining ET values via components of energy balance (especially H and  $\lambda ET$ ). It is also important to mention the eddy correlation method for estimating the real ET. But this method requires precise measurements and high frequency of air temperature, wind speed, and vapor pressure. However, these two methods to estimate the real ET are limited, especially due to poor monitoring of the variables required and the local character of these measurements or estimates (Nicácio 2008).

Often ET study on time scale is monthly and the most common source of data for calculation is the weather station. But the poor distribution of meteorological stations and the scarcity of data are limiting factors for ET estimation. Therefore, a potential tool for determining surface and actual evapotranspiration flows is the use of data from remote sensing. Most of the time, the difficulty of obtaining the  $ET_{c\ act}$  is given by the lack of data needed to implement some of the methods; another important factor to be considered is the spatial distribution of  $ET_{c\ adj}$ . In general, the various methods of obtaining  $ET_{c\ act}$  permit its estimation at local scale. However, the heterogeneity of the regions with different surfaces (type of soil and vegetation, for example) has quite different values for evaporation rates, which in general cannot be perceived by the most traditional ways of estimating  $ET_{c\ act}$ . On the contrary, the remote sensing allows the estimation of evapotranspiration on wide spatial scale depending on the biophysical characteristics found in each pixel (Nicácio 2008).

### ***Estimation of $ET_{c\ act}$ by assimilation of remote sensing data***

The surface characteristics, such as the albedo, surface temperature and properties of vegetation (NDVI and LAI) are important variables to estimate the radiation balance. Methodologies that use satellite information in the visible and thermal infrared have been proposed by Bastiaanssen et al. (1998a) and Allen et al. (2007c) to estimate the radiation balance at the surface, being implemented with high and moderate resolution sensors.

It should be noted that the main advantage of using remote sensing to estimate the radiation balance, energy and evapotranspiration, with then spatial trend obtained. This fact enables the perception of variability patterns within the estimated variable, and is especially critical when the region under review is heterogeneous. One can also mention that the methodologies that resort to remote sensing application does not replace other methods that take into consideration the various measurements required to be made in the field, i.e. the traditional methods for estimating energy and evapotranspiration flows, but as an alternative methodology and in a complementary nature (Nicácio 2008).

Other models such as the NDVI (Normalized Difference Vegetation Index), SAVI (Soil Adjusted Vegetation Index) and EVI (Enhanced Vegetation Index) related to ET and the surface temperature with some vegetation characteristics. In other words, through remote sensing, one can obtain quantitative information on the spatial and temporal changes of vegetation cover related to the evapotranspiration estimation.

During normal supply of nutrients and water conditions to crops, there is a highly negative correlation between the surface temperature and vegetation indexes, since the increase in the vegetative vigor and cooling effect caused by the ET is associated with decreasing temperature the surface (Namani and Running 1989). Some studies have related the difference between surface temperature and air temperature ( $T_s$  vs  $T_{air}$ ), vegetation indices and evapotranspiration. This relationship is based on the fact that, usually, at any point, the surface temperature is higher than the air temperature. This difference tends to decrease as the latent heat flux increases and hence reduces the surface temperature due to evaporative cooling which depends on the water content of the plant (Folhes 2007). Thus, we can associate the plant water stress to evapotranspiration.

### ***Remote sensing for estimating plant water stress***

The relationships among the methods, which evaluate the plant water stress using data from remote sensing, provide the theoretical basis for generating new models. As an example, we

can mention the water deficit index (WDI) prepared by Moran et al. (1994). The estimated water deficit condition was established by WDI through the relationship between the difference in the surface temperature and air temperature and the value of NDVI. When water stress affects the plant cell metabolism, there exists a higher value of  $T_s - T_a$  for the same value of NDVI. In large areas, the estimated actual evapotranspiration is difficult to be determined by conventional methods, but knowing the WDI value and the reference evapotranspiration, it is possible to estimate the actual evapotranspiration.

In general, the models may require information on: (1) atmospheric conditions (temperature and humidity, wind speed and solar radiation); (2) structure of vegetation (leaf area index, canopy cover, canopy height); (3) thermal and hydraulic properties of the soil; (4) physiological properties of vegetation (stomata conductance) and; (5) optical properties of soil and vegetation (reflectance, albedo) (Olioso et al. 1999).

Some factors may hinder the operational application of estimating energy flow methods to the surface by remote sensing, such as: (1) models based on empirical relationships have not been sufficiently tested; (2) complex physical models describe, in details, the processes involved in the turbulent exchange of properties between the surface and the atmosphere, but they need a lot of data for its startup and; (3) less complex physical models, involving few empirical relationships, require data that cannot be obtained by remote sensing and are not routinely measured (Paiva 2005).

Models developed based on the description of the mechanism of physical processes associated with the soil-plant-atmosphere system are advantageous compared to empirical based models. The physical-based models better reflect the reality of the energy transmission and evapotranspiration, but require a set of data that are not always available and are not easily monitored. An alternative to operationalize the estimates of the components of the energy balance and evapotranspiration are the semi-empirical models. In this context, we highlight the energy balance algorithm for land surface, known as SEBAL by Bastiaanssen (1995) and METRIC by Allen et al. (2007b). These models have been widely used in heterogeneous surfaces (Bastiaanssen et al. 1998b; Tasumi 2003; Mohamed et al. 2004; Pace 2004; Paiva 2005; Folhes 2007) in an attempt to describe the spatial variation of surface flux based on semi-empirical functions.

### ***Models for estimating the energy balance***

At the time of passage of the satellite, the algorithms developed based on semi-empirical models, such as the SEBAL and METRIC, perform estimation of radiation and energy fluxes through a set of equations present in each.

The SEBAL algorithm calculates the spatial variability of most of the hydrosedimentological parameters required for the calculation of ET, requiring only information on the atmospheric transmittance of short wavelength, the surface temperature and the height of the vegetation (Bastiaanssen et al. 1998a). The authors proposed the use of few relationships and empirical assumptions, which relate to issues of heat flux estimates in the soil, surface emissivity and the aerodynamic roughness parameters of heat transfer.

The METRIC on the other hand is an algorithm developed from SEBAL model. The main differences between them are some peculiarities related to the choice of wet pixel and the calculation of the temperature difference in this pixel.

The use of satellite information such as the length of shortwave and thermal bands are the basis for obtaining the energy balance at the soil surface, calculated by METRIC and SEBAL models for the estimation of actual evapotranspiration (Allen et al. 2007b). The latent heat flux is estimated as the residual of the energy balance, resulting from the subtraction of the soil heat flux (G) and the sensible heat flux (H) by the net radiation ( $R_n$ ) as:

$$\lambda E = R_n - G - H \quad (05)$$

Where: the latent heat flux ( $\lambda E$ ) is directly converted to evapotranspiration.

In the METRIC model the components of energy balance are estimated from the data obtained from: (i) short and long radiation wavelength, albedo and emissivity of the surface to estimate the net radiation ( $R_n$ ); (ii) surface temperature, albedo and NDVI for calculating the heat flow from the soil (G) and; (iii) surface temperature to estimate the temperature gradients between two heights above the surface (dT), estimated aerodynamic resistance and wind speed to estimate sensible heat flux (H) (Allen et al. 2007b).

The soil heat flux is given by the equation developed by Tasumi (2003) as:

$$G/R_n = 0.05 - 0.18e^{-0.521LAI} \quad (LAI \geq 0.5) \quad (06a)$$

$$G/R_n = 1.80(T_s - 273.16) / R_n + 0.084 \quad (LAI \geq 0.5) \quad (06b)$$

Where:  $R_n$  is the net radiation ( $W\ m^{-2}$ ), LAI is the leaf area index estimated from the vegetation index, SAVI (dimensionless) and  $T_s$  is the surface temperature ( $^{\circ}K$ ).

The sensible heat flux (H) is calculated from equation:

$$H = (\rho \cdot C_p \cdot dT) / r^{ah} \quad (07)$$

Where:  $\rho$  is the density of air ( $kg\ m^{-3}$ ),  $C_p$  is the specific heat of air ( $1004\ J\ kg^{-1}\ K^{-1}$ ),  $dT$  is the temperature difference between two heights and  $r^{ah}$  is the aerodynamic resistance to heat transport ( $m\ s^{-1}$ ).

The calculation of H, specifically, the determination of  $dT$  in the cold pixel is the main difference between the SEBAL and METRIC. Using the data of wind speed and radiometric surface temperature, it is possible to model the transfer of energy to the atmospheric layers. For hot pixel, the same assumptions are considered in both models. In METRIC, the cold pixel must be associated with a rapidly developing crop, and the  $dT$  value is not exactly zero, as in SEBAL, but is calculated on the basis of  $ET_o$  (Allen et al. 2007b), which decreases the probability of errors in selecting the pixel cold.

The use of CIMEC process (Calibration Using Inverse Modeling at Extreme Conditions) for the internal calibration of the sensible heat flux eliminates the problems caused by: (i) the soil surface temperature ( $T_s$ ), (ii) the atmospheric correction of the estimated reflectance, and (iii) soil heat flux (Allen et al. 2007b). As mentioned earlier, an important difference between these two models refers to anchor pixels or pixel reference, dry and wet, which defines the boundary conditions for the energy balance, i.e., extreme humidity and temperature in the study area. In METRIC, cold pixel represents the maximum evapotranspiration, and is set on an agricultural area completely covered by vegetation, while in SEBAL, it is determined from the temperature in a pixel on a water surface. The METRIC uses  $ET_o$  data (Allen et al. 2005a), defined by meteorological data for the calibration of the sensible heat flux, while the traditional SEBAL applications assume that the sensible heat flux in the cold state is close to zero, so that the evaporation in this state is equal to the available energy (Bastiaanssen et al. 2005). Hot pixel is selected in both models, as a dried, non-cultivated land, where it assumes a zero evapotranspiration (Bastiaanssen et al. 1998a; Bastiaanssen et al. 2005), or on a pixel with positive value in the case of recent rainfall event, taking into consideration the daily soil water balance (Allen et al. 2007a). In estimating the sensible heat flux, both models (METRIC and SEBAL) assume a linear relationship between temperature difference of two vertical heights near the surface ( $dT$ ) and the temperature of the soil surface ( $T_s$ ) between the two anchored pixels.

However, there are risks relating to an erroneous choice of these pixels, for example, taking as hot, a pixel containing some burns and as cold pixel, a pixel containing clouds (Marx et al. 2008). Thus, it is easy to see that there is, at this point, a subjective question which should be treated with care and rigor. Another caution is the complexity of the minimum spatial resolution of the image to be used (Nicácio 2008).

### **Crop coefficients calculated from soil water balance models assimilated to vegetation indexes**

There are also in the literature approaches for the estimation of the crop water need which use the soil water balance modeling. Among the currently more widely used models are the SIMDualKc and AquaCrop (Martins et al. 2013; Pereira et al. 2015b). These models use input variables generally obtained by a combination of field monitoring, laboratory analysis and climate variables measurement. These variables include soil, irrigation conditions and information regarding the implanted crop. This methodology is quite sensible to the estimative of the depth corresponding to the roots' zone, and depends critically on the soil physical data as well as rainfall and irrigation frequency, which encourages the search for approaches with improvements in the quality of the data used - notably in adapting to local conditions.

In recent years, a new version of this approach is being considered, where the crop coefficient can be related to vegetation indexes ( $K_c v_i$ ) calculated from surface reflectance obtained from the red and infrared bands of remote sensors, typically orbital. The evaporation coefficient,  $K_e$  can also be calculated using the so called thermal band or water balance models. Thus  $ET_o$  is multiplied by  $K_c = K_{cb} + K_e$  and so you get the  $ET_c$  in conditions of absence of water stress, which is considered a maximum or "potential" crop coefficient value. When there is no water deficit in the root zone and the soil surface is dry, it is fulfilled that  $K_c = K_{cb}$ . The water stress may be taken into account by the introduction of stress coefficient  $K_s$  that varies between 0 and 1, and by modifying the equation as follows:  $K_c = K_s \cdot K_{cb} + K_e$ . To assess  $K_s$  it is necessary to model the water balance of the soil in the root zone with data from the physical analysis of it. The  $K_c v_i$  approach has been used by several authors (e.g., Hunsaker et al. 2005; Campos et al. 2012; Er-Raki et al. 2013; Mateos et al. 2013; Pôças et al. 2015) with relative success.

The  $K_c v_i$  approach is simpler than the approach based on energy balance, as in METRIC and SEBAL models, since it needs fewer steps and is based on first principles. However, it is very sensitive to the immediate effects of water stress, such as reducing ET due

to stomata closure caused by water deficit in the soil or water vapor deficit in the atmosphere, an effect that is detected by the energy balance methods. Therefore, the assumption underlying the method is that  $K_{c\ VI}$  effects such as stomata closure has a small relative weight on reducing the evaporation rate in comparison to the total evapotranspiration. This seems a reasonable assumption for the crops irrigated by center pivot in a humid subtropical region. On the other hand, the most important effect of water stress in plants, which is reduced growth, is detected properly by the vegetation index method,  $K_{c\ VI}$  (Mateos et al. 2013).

Another significative advantage of using  $K_{c\ VI}$  approach is the ease for the obtainment of the spatial variation of  $K_c$  in agricultural areas. This approach is considered promising due to the fact that the satellite or aerial vehicle images can be easily integrated into geographical information systems and mathematical models, thus making it possible to estimate  $K_c$  and ET in time and space, in a geographical distribution in matrix form. In the past, ET and  $K_c$  were generally determined homogeneously in a single area.

It should also be noted that the connection between the  $K_{cb\ VI}$  and vegetation index introduces a sensitivity to actual growth of vegetation which can permit - at a temporal and spatial scale - the identification of phenomena such infestations by pests and diseases, drought and frost occurrence (Hunsaker et al. 2005; Yang et al. 2005; Reisig and Godfre, 2006; Karnieli et al. 2010). This kind of applications depends, for its practical use in management and monitoring of agricultural systems, in the availability of an adequate spatial and temporal resolution of the images used, which is not always achieved with free satellite platforms, but whose availability is in intense phase of expansion due to increasing farm use of unmanned aerial vehicles for this purpose.

Remote systems have the potential to provide a field-by-field description of the variation of  $K_c$  or  $K_{cb}$  due to differences in planting dates, plant spacing and cultivars and other management factors (Pereira et al. 2015a). For these reasons, the evaluation of the advantages and disadvantages of crop coefficients based in VI has been discussed widely in the literature (Allen et al. 2011a).

Studies using the  $K_{c\ VI}$  approach have shown good results leaving in evidence the potential of this tool (e.g., Campos et al. 2012; Mateos et al. 2013; Pôças et al. 2015).

On the one hand, there is the possibility of obtaining numerical correlations between  $K_c$  and VIs, using local conditions, and using the most accurate information available about the actual  $K_c$  values, based on data from measurements in lysimeters or Penman -Monteith (PM) or Eddy covariance or energy balance models (SEBAL, METRIC ), or models of water balance as SIMDualKc (Padilha et al. 2011; Paredes, et al. 2014; Pôças et al. 2015).



Furthermore, the information contained in the crop cycle VI curves can be assimilated in their other models in order to produce a best fit with reality. The time scale for modeling is frequently adjusted in days after sowing (DAS) or related to the beginning or end of one of the various growing stages. In this sense, the very process of getting the correlation function between the  $K_c$  data calculated by the model, the  $K_c$  (DAS) function, with the continuous curve of the NDVI (DAS) function over time, obtained by remote sensing, can be considered a procedure of data assimilation. In this process, the  $K_c$  values calculated by the model are additionally influenced by the VI, creating a  $K_c$  (VI, DAS) function, through a correlation equation.

As an illustration, Campos et al. (2012) used PM; Allen et al. (2005) used METRIC and lysimeters; Hunsaker et al. (2005) performed direct measurements of water content in the soil through Time Domain Reflectometry (TDR) and neutron scattering and calculated the ET as a residual of the water balance in the soil.

In all cases,  $K_c$  (DAS) function showed experimental profiles equivalent to the VI (DAS) function, which is indicative of the importance of the information contained in the VI for the adjustment of  $K_c$  under operational situations.

In this sense, Pôças et al. (2015) decided to model the  $K_c$  through another intermediate variable more closely related with vegetation indexes, as the soil cover fraction ( $f_c$ ). They used NDVI and SAVI to estimate  $f_c$  where a density coefficient ( $K_d$ ) proposed by Allen and Pereira (2009) is also used. This approach allows better adjustment in the case of cultures where the ground cover is not total, as in the case of orchard or olive trees and it achieved good results. Pôças et al. (2015) proposed the use of  $K_c$  and  $K_s$  derived from a soil water balance model, SIMDualKc, in combination with  $K_{c\ VI}$ .

In this context, several relationships between  $K_c$  and IV were established. However, there is no agreement on the nature and generality of these relationships (González-Dugo and Mateos 2008). Some studies (e.g., Gonzalez-Piquera et al. 2003; Duchemin et al. 2006; Er-Raki et al. 2010; Pôças et al. 2015) have shown that these relationships are linear, but others have not found linear relationships (e.g., Hunsaker et al. 2003; Hunsaker et al. 2005; Er-Raki et al. 2007, González-Dugo and Mateos 2008). Therefore, the establishment of a relationship between crop coefficient and vegetation indexes is a research topic in progress.

As crop development intervals and  $K_{cb}$  are provided by FAO tables for most crops, but in standard culture density conditions and optimal agronomic management practices, the publication strongly recommends local calibration of the steps of growth. Thus, if proven by

research, the  $K_{cb}$  curves used should be modified to better reflect the use of water by the culture under local conditions (Hunsaker et al. 2005).

### ***SIMDualKc***

The SIMDualKc is a software directed to irrigation planning and scheduling (Rosa et al. 2012), that uses the approach of dual crop coefficients for  $K_c$  (Allen et al. 1998; Allen et al. 2005b), focusing on the estimated  $ET_o$  and the water balance in the soil. Following the dual  $K_c$  approach,  $K_{cb}$  and  $K_e$  are considered separately (Pereira et al. 2015b), thus allowing a better assessment of irrigation management practices.

The SIMDualKc model has been successfully applied to estimate ET and Kc for a wide range of agricultural crops (Paredes et al. 2014; Pereira et al. 2015b; Pôças et al. 2015.).

The  $K_{cb}$  calculation in SIMDualKc is done by the following equation (Allen and Pereira 2009; Rosa et al. 2012), where the impacts on the density of the plants and/or the leaf area are taken into consideration by a density coefficient:

$$K_{cb} = K_{cmin} + K_d(K_{cbfull} - K_{cmin}) \quad (08)$$

Where  $K_d$  is the coefficient of density,  $K_{cb\ full}$  is the value when the plant reaches the peak of its growth, under soil cover conditions almost full (or LAI > 3),  $K_{c\ min}$  is the minimum, when the soil is uncovered, in the absence of vegetation. The minimum  $K_c$  value can vary for (0.0 to 0.15) depending on the crop or vegetation and the frequency of rainfall or irrigation.  $K_{cb}$  is corrected by the model for local climatic conditions when the minimum relative humidity ( $RH_{min}$ ) differs from 45% and/or when the average wind speed is different to  $2\ m\cdot s^{-1}$  (Allen et al. 1998; Allen and Pereira 2009; Rosa et al. 2012). The  $K_d$  is calculated with the equation number 09, as proposed by Allen and Pereira (2009) and represents the combined effects of soil fraction effectively covered by culture ( $f_{ceff}$ ) and plant height (h):

$$K_d = \min(1, M_L f_{ceff}, f_{ceff}^{\frac{1}{1+h}}) \quad (09)$$

$K_e$  is calculated by a daily water balance in the evaporable layer of soil that is characterized by its depth ( $Z_e$ , m), total evaporable water (TEW, mm) and the readily evaporable water (REW, mm). TEW is the maximum depth of water that can be evaporated from the evaporable layer of soil when completely wet, and REW is the depth of water that

can be evaporated without water restrictions (Allen et al. 1998; Allen et al. 2007a). The maximum soil evaporation ( $E_s$ ) occurs when the soil is wet by rain or irrigation and with minimum shadowing of the culture which occurs during the early development stages of the crop. Minimum  $E_s$  occurs when the culture fully shades the soil and the energy available for evaporation is minimal (Pereira et al. 2015a).

When the soil is wet  $K_e$  is maximum, but is limited by the available power on the soil surface and its value cannot exceed the difference  $K_{c\ max} - K_{cb}$ . As the soil dries, less water is available for evaporation and there is a decrease in  $E_s$  in proportion to the amount of water that remains in the soil surface layer. Thus,  $K_e$  is expressed by:

$$K_e = K_r(K_{cmax} - K_{cb}) \quad \text{for} \quad K_e \leq f_{ew}K_{cmax} \quad (10)$$

where  $K_r$  is the evaporation reduction coefficient ( $\leq 1,0$ ),  $K_{c\ max}$  is the maximum value of  $K_c$ , for example, when  $K_{cb} = K_c + K_e$  following a rain or irrigation event, and  $f_{ew}$  is the fraction of soil that is exposed to radiation and wetting by rain or irrigation, which depends on the fraction of soil covered by crop ( $f_c$ ).  $K_r$  is calculated using the approach of the drying cycle in 2-stages (Allen et al. 1998).

When there is occurrence of water deficit in the soil a stress coefficient ( $K_s$ ) is calculated by the model for the whole root zone.  $K_s$  is expressed as a linear function of the depletion in the root zone  $D_r$  (Allen et al. 1998; Allen et al. 2005.):

$$K_s = \frac{TAW - D_r}{TAW - RAW} = \frac{TAW - D_r}{(1-p)TAW} \quad \text{for} \quad D_r > RAW \quad (11a)$$

$$K_s = 1 \quad \text{para} \quad D_r \leq RAW \quad (11b)$$

where TAW and RAW are respectively the total available and readily available soil water (mm),  $D_r$  is the depletion in the root zone (mm), and  $p$  is the fraction depleted for no stress.  $K_{cb}$  is multiplied by  $K_s$  to account for the effects of water deficiency stress to obtain the actual coefficient  $K_{cb\ act}$ .

$$K_{cb\ act} = K_s K_{cb\ pot} \quad (12)$$

The detailed calculation of  $K_{cb}$ ,  $K_e$  and  $K_s$  in SIMDualKc is described in Rosa et al. (2012).

The calibration of SIMDualKc is focused in optimizing the culture parameters and  $K_{cb}$  and  $p$  for the various crop growth stages and also the soil evaporation parameters, deep percolation parameters and the flow curve, using trial and error procedures until small errors are found (Rosa et al. 2012). As input data for SIMDualKc modeling of irrigated areas, it is needed information regarding i) type of crop, as sowing time, crop cycle duration and lengths of development stages and harvest period; ii) soil hydraulic parameters, as permanent wilting point and field capacity at different depths, soil particle distribution; iii) irrigation, as irrigation depths (mm); and iv) weather data, such as rainfall,  $ET_o$ , minimum relative humidity and wind speed, as well as location and altitude of the weather station providing the data.

### **Final considerations**

Based on previous discussion, it can be seen that there are several methodologies to estimate evapotranspiration which differ in the input variables chosen for the measurement and consequently the estimation models, justified by the enormous variety of climatic conditions and data availability encountered in practice. Its importance is due primarily to the need for efficient support for water management and planning of areas with irrigated agriculture and for the real knowledge of crop water consumption. In addition to the universal existence of methodologies, advances in the estimation of ET are being recorded-especially in the last decades - the use of spectral information of thermal sensors of moderate spatial resolution, such as the TM/Landsat. This information implemented in semi-empirical-based models such as the SEBAL and METRIC can provide estimates of the soil surface to heat flow and the daily actual evapotranspiration more consistent with local conditions, and in a spatial form, as the satellite images have specific information for each pixel. One thing that do not happen with other empirically based methods, which use data from specific weather stations, is that information is used without modification for any defined scope, regardless of climatic and agronomic characteristics.

However, some considerations should be observed. Even using real data of the region as a matrix, such as satellite images, both SEBAL and METRIC models need local calibrations to adjust the various calculation procedures to local conditions. These settings are now well developed for arid regions where they were designed. But such has not been widely done in the tropics and subtropical regions, where the scarcity and competition for water is becoming a concern. Thus, the problem of use, calibration and adjustment of these models in subtropical regions could highly relevant as a subject of study.

Another aspect that may make it even more realistic and accurate model is the use of geographic information systems containing remote sensing and field data for analysis of variables of interest in an integrated manner as well as their correlations. For example, calculated actual ET data can be compared with water consumption data in irrigated areas or regions.

Therefore, the main advantage of using remote sensing to estimate evapotranspiration and crop coefficients is in view of the spatial trend. This fact enables the perception of variability patterns of the estimated variables in space, which is essentially critical when the region under review is heterogeneous. One can also mention that the methodologies employing remote sensing does not replace the other traditional methods that take into account measurements in the field, rather it should be considered as an alternative and complementary methodology.

The current trend is the monitoring of agricultural areas not only with orbital data, but through the use of unmanned aerial vehicles, the UAS, with adequate sensors with which the VI and the surface temperature can be estimated, adjusted, calibrated and assimilated to models, thus supporting the management of irrigation more closely to the reality of each crop.

## References

- Allen, Richard G., Asce, A M, Brockway, Charles E, Asce, M, Wright, James L.1983. "Weather Station Siting and Consumptive Use Estimates." **J. Water Resour. Plann. Manage** 109: 134-136.
- Allen, Richard G., Asce, Member, Gichuki, Francis N., Rosenzweig, Cynthia. 1991. "CO<sub>2</sub>-Induced Climatic Changes and Irrigation-Water Requirements." **Journal of Water Resources Planning and Management** 117: 157-178. doi.org/10.1061/(ASCE)0733-9496(1991)117:2(157).
- Allen, R. G., Pereira, L., Raes, D., Smith, M. 1998. "FAO Irrigation and drainage paper No. 56." In: *FAO Food and Agriculture Organization of the United Nations*.
- Allen, R. G., Bastiaanssen, W., Tasumi, M., Morse, A. 2001. Evapotranspiration on the watershed scale using the SEBAL model and Landsat images. **ASAE Meeting Presentation**. doi: 10.13031/2013.4047.
- Allen, R. G., Tasumi, M., Morse, M., Trezza, R. 2005a. "A Landsat-based energy balance and evapotranspiration model in Western US water rights regulation and planning." **Irrigation and Drainage Systems** 19: 251-268. doi: 10.1007/s10795-005-5187-z.
- Allen, R. G., Clemmens, A. J., Burt, C. M., Solomon, K., O'Kalloran, T. 2005b. "Prediction accuracy for project wide evapotranspiration using crop coefficients and reference

evapotranspiration.” **Journal of Irrigation and Drainage Engineering, American Society of Civil Engineers** 131: 24-36. doi.org/10.1061/(ASCE)0733-9437(2005)131:1(24).

Allen, R. G., Wright, J. L., Pruitt, W. O., Pereira, L. S., Jensen, M. E. Water requirements. 2007a. In: *Design and Operation of Farm Irrigation Systems*. Edited by Hoffman, G. J., Evans, R. G., Jensen, M. E., Martin, D. L., Elliot, R. L. ASABE: 208-288.

Allen, R. G., Tasumi, M., Morse, A., Trezza, R., Wright, J. L., Bastiaanssen, W., Kramber, W., Lorite, I., Robison, C. W. 2007b. “Satellite-based energy balance for mapping evapotranspiration with internalized calibration (METRIC)—Applications.” **Journal of Irrigation and Drainage Engineering** 133: 395-406. doi.org/10.1061/(ASCE)0733-9437(2007)133:4(395).

Allen, R. G., Tasumi, M., Trezza, R. 2007c. “Satellite-based energy balance for mapping evapotranspiration with internalized calibration (METRIC)—Model.” **Journal of irrigation and drainage engineering** 133: 380-394. doi.org/10.1061/(ASCE)0733-9437(2007)133:4(380).

Allen, R. G., Pereira, L. S., Howell, T. A., Jensen, M. E. 2011a. “Evapotranspiration information reporting: I. Factors governing measurement accuracy.” **Agricultural Water Management** 98: 899-920. doi:10.1016/j.agwat.2010.12.015.

Allen, R. G., Irmak, A., Trezza, R., Hendrickx, J. M., Bastiaanssen, W., Kjaersgaard, J. 2011b. “Satellite-based ET estimation in agriculture using SEBAL and METRIC.” **Hydrological Processes** 25: 4011-4027. doi: 10.1002/hyp.8408

Allen, Richard G., Asce, M. 1986a. “Penman for All Seasons.” **Journal of Irrigation and Drainage Engineering** 112: 348-368. doi.org/10.1061/(ASCE)0733-9437(1986)112:4(348)

Allen, Richard G., Pruitt, William O., Asce, Members. 1986b. “Rational Use of the FAO Blaney-Criddle Formula.” **Journal of Irrigation and Drainage Engineering** 112: . 139-155. doi: 10.1061/(ASCE)0733-9437(1986)112:4(348).

Allen, Richard G., Asce, M. 1986c. “Sprinler Irrigation Project Design with Production Functions.” **Journal of Irrigation and Drainage Engineering** 112: 305-321. doi/abs/10.1061/(ASCE)0733-9437(1986)112:4(305).

Allen, Richard G., Asce, M., Brockway, Charles E. 1984. “Concepts for Energy-Efficient Irrigation System Design.” **Journal of Irrigation and Drainage Engineering** 110: 99-106. doi.org/10.1061/(ASCE)0733-9437(1984)110:2(99).

Allen R. G., Pereira, L. S. 2009. “Estimating crop coefficients from fraction of ground cover and height.” **Irrigation Science** 28: 17-34. doi: 10.1007/s00271-009-0182-z.

Anderson, M. C.; Allen, R. G.; Morse, A.; Kustas, W. P. 2012a. “Use of Landsat thermal imagery in monitoring evapotranspiration and managing water resources.” 2012a. **Remote Sensing of Environment** 122: 50-65. doi:10.1016/j.rse.2011.08.025.

Anderson, Martha C., Kustas, William P., Alfieri, Joseph G., Gao, Feng, Hain, Christopher, Prueger, John H., Evett, Steven, Colaizzi, Paul, Howell, Terry, Chávez, José L. 2012b.

- “Mapping daily evapotranspiration at Landsat spatial scales during the BEAREX’08.” **Advances in Water Resources** 50: 162-177, 2012b. doi: 10.1016/j.advwatres.2012.06.005.
- Bastiaanssen, W. G. M. 1995. “Regionalization of surface flux densities and moisture indicators in composite terrain : a remote sensing approach under clear skies in Mediterranean climates.” Wageningen, Netherlands: *Ph.D. Thesis*, 273.
- Bastiaanssen, W., Menenti, M., Feddes, R., Holtslag, A. 1998a “A remote sensing surface energy balance algorithm for land (SEBAL). 1. Formulation.” **Journal of hydrology** 212: 198-212. doi:10.1016/S0022-1694(98)00253-4.
- Bastiaanssen, W. G. M., Pelgrum, H., Wabg, J. 1998b. “A remote sensing surface energy balance algorithm for land (SEBAL): 2. Validation.” **Journal of Hydrology**, 212: 213-229. doi:10.1016/S0022-1694(98)00254-6.
- Bastiaanssen, W., Noordaman, E., Pelgrum, H, Davids, G., Thoreson, B., Allen, R. 2005. “SEBAL model with remotely sensed data to improve water-resources management under actual field conditions.” **Journal of Irrigation and Drainage Engineering** 131: 85-93. doi: 10.1061/(ASCE)0733-9437(2005)131:1(85).
- Boegh, E., Soegaard, H., Thomsen, A. 2002. “Evaluating evapotranspiration rates and surface conditions using Landsat TM to estimate atmospheric resistance and surface resistance.” **Remote Sensing of Environment** 79: 329-343.
- Burman, R., Pochop, L. O. 1994. “Evaporation, evapotranspiration and climatic, data.” In: *Developments in Atmospheric Science*, Amsterdam: Elsevier.
- Campos, I., Boteta, L., Balbontín, C., Fabião, M., Maia, J., Calera, A. 2012. “Remote sensing based water balance to estimate evapotranspiration and irrigation water requirements. Case study: Grape vineyards.” **Options Méditerranéennes**, B 67: 85-94.
- Davies, J., Allen, R. 1973. “Equilibrium, potential and actual evaporation from cropped surfaces in southern Ontario.” **Journal of Applied Meteorology**, 12: 649-657. doi: 10.1175/1520-0450(1973)012<0649:EPAAEF>2.0.CO%3B2
- Dias, N. L. D., Kan, A. 1999. “A hydrometeorological model for basin-wide seasonal evapotranspiration.” **Water Resource Research** 35: 3409-3418. doi: 10.1029/1999WR900230.
- Doorenbos, J., Pruitt, W. O. 1977. “Guidelines for predicting crop-water requirements.” In: *FAO Irrigation and Drainage Paper No. 24*, translated by Gheyi, H. R., Metri, J. E. C., Damasceno, F. A. V., 1-156. second rev. Rome: FAO.
- Duchemin, B., Hadria, R., Erraki, S., Boulet, G., Maisongrande, P., Chehbouni, A., Escadafal, R., Ezzahar, J., Hoedjes, J. C. B., Kharrou, M. H. 2006. “Monitoring wheat phenology and irrigation in Central Morocco: On the use of relationships between evapotranspiration, crops coefficients, leaf area index and remotely-sensed vegetation indices.” **Agricultural Water Management** 79: 1-27. doi:10.1016/j.agwat.2005.02.013.
- Er-Raki, S., Chehbouni, A., Guemouria, N., Duchemin, B., Ezzahar, J., Hadria, R. 2007. “Combining FAO-56 model and ground-based remote sensing to estimate water

consumptions of wheat crops in a semi-arid region.” **Agricultural Water Management** 87: 41-54. doi:10.1016/j.agwat.2006.02.004.

Er-Raki, Salah, Chehbouni, Abdelghani, Duchemin, Benoit. 2010. “Combining Satellite Remote Sensing Data with the FAO-56 Dual Approach for Water Use Mapping In Irrigated Wheat Fields of a Semi-Arid Region.” **Remote Sensing** 2: 375-387. doi:10.3390/rs2010375.

Er-Raki, S., Rodriguez, J. C., Garatuza-Payan, J., Watts, C. J., Chehbouni, A. 2013. “Determination of crop evapotranspiration of table grapes in a semi-arid region of Northwest Mexico using multispectral vegetation index.” **Agricultural Water Management** 122: 12-19. doi:10.1016/j.agwat.2013.02.007.

Fassnacht, K. S., Gower, S. T., Mackenzie, M. D., Nordheim, E. V., Lillesand, T. M. 1997. “Estimating the leaf area index of north central Wisconsin forests using the Landsat Thematic Mapper.” **Remote Sensing of Environment**.61: 229-245. doi:10.1016/S0034-4257(97)00005-9.

Ferreira, Rafael da Costa. 2008. “Calibração do SEBAL/METRIC e Mapeamento do Saldo de Radiação com Imagens Landsat 5 – TM e Modelo de Elevação Digital.” Campina Grande, *Tese de Doutorado*, Universidade Federal de Campina Grande.

Folhes, M. T. 2007 “Modelagem da evapotranspiração para a gestão hídrica de perímetros irrigados com base em sensores remotos.” *Tese de D.Sc*, São José dos Campos.

Folhes, M. T., Rennó, C. D., Soares, J. V. 2009. “Remote sensing for irrigation water management in the semi-arid Northeast of Brazil.” **Agricultural Water Management** 96: 1398-1408. doi:10.1016/j.agwat.2009.04.021.

Gates, D. M., Keegan, J. J., Schleter, J. C., Weidener, V. R. 1965. “Spectral Properties of Plants.” *Applied Optics*, 11-20.

Gausmann, H. W., Allen, W. A., Cardenas, R. 1969. “Reflectance of Cotton Leaves and their Structure.” **Remote Sensing of Environment** 1: 10-22.doi:10.1016/S0034-4257(69)90055-8.

Glen, E. P., Huete, A. R., Negler, P. L., Nelson, S. G. 2008. “Relationship between remotely-sensed vegetation indices, canopy attributes and plant physiological processes: what vegetation indices can and cannot tell us about the landscape.” **Sensor** 8: 2136-2160. doi: 10.3390/s8042136.

González-Dugo, M. P., Mateos, L. 2008. “Spectral vegetation indices for benchmarking water productivity of irrigated cotton and sugarbeet crops.” **Agricultural Water Management** 95: 48-58.doi:10.1016/j.agwat.2007.09.001.

González-Dugo, M. P., Escuin, E., Cano, F., Cifuentes, V., Padilla, F. L. M., Tirado, J. L., Oyonarte, N., Fernández, P., Mateos, L. 2013. “Monitoring evapotranspiration of irrigated crops using crop coefficients derived from time series of satellite images. II. Application on basin scale.” **Agricultural Water Management** 125: 92-104. doi: org/10.1016/j.agwat.2013.03.024.



- Gonzalez-Piquera, J., Calera, A. Belmonte, Gilabert, M. A., Cuestas, A. García, De la Cruz, F. Tercero. 2003. "Estimation of crop coefficients by means of optimized vegetation indices for corn." *Proceedings of the SPIE Congress. Barcelona, Spain*: 110-118.
- Heilman, J., Kanemasu, E., Bagley, J., Rasmussen, V. 1977. "Evaluating soil moisture and yield of winter wheat in the Great Plains using Landsat data." **Remote Sensing of Environment** 6: 315-326. doi:10.1016/0034-4257(77)90051-7.
- Huete, A. R., Didan, K., Miura, T., Rodriguez, E. P., Gao, X, Ferreira, G. 2002. "Overview of the Radiometric and Biophysical Performance of the MODIS Vegetation Indices." **Remote Sensing of Environment** 83: 195-213. doi:10.1016/S0034-4257(02)00096-2.
- Hunsaker, D. J., Pinter, P. J., Barnes, E. M., Kimball, B. A. 2003. "Estimating cotton evapotranspiration crop coefficients with a multispectral vegetation index." **Irrigation Science** 22: 95-104. DOI: 10.1007/S00271-003-0074-6.
- Hunsaker, D., Pinter, P. J., Kimball, B. 2005. Wheat basal crop coefficients determined by normalized difference vegetation index. **Irrigation Science** 24: 1-14. doi: 10.1007/s00271-005-0001-0.
- Jackson, R. D., Reginato, R. J., Idso, S. B. 1977. "Wheat canopy temperature: a practical tool for evaluating water requirements." **Water Resources Research** 13: 651-656. doi:10.1029/WR013i003p00651.
- Jensen, M. E., Burman, R., Allen, R. G. 1990. "Evapotranspiration and irrigation water requirements." In: *American Society of Civil Engineers*. New York.
- Jensen, J. R. 2011. "Sensoriamento Remoto do Ambiente: uma perspectiva em recursos terrestres." *Parêntese* 2: 1-598.
- Kanamasu, E., Hellman, J., Bagley, J., Powers, W. 1977. "Using Landsat data to estimate evapotranspiration of winter wheat." **Environmental Management** 1: 515-520. doi: 10.1007/BF01866686.
- Karnieli, A., Agam, N., Pinker, R. T., Anderson, M., Anderson, M. L., Anderson, G. G., Anderson, N., Anderson, A. 2010. "Use of NDVI and land surface temperature for drought assessment: Merits and limitations." **Jornal of Climate** 23: 618-633. doi: 10.1175/2009JCLI2900.1.
- Martins, J. D., Rodrigues, C., Gonçalo, Paredes, P., Carlesso, R., Oliveira, Z., Knies, A., Petry, M., Pereira, L. S. 2013. "Dual crop coefficients for maize in southern Brazil: Model testing for sprinkler and drip irrigation and mulched soil." **Biosystems Engineering** 115: 291-310. doi:10.1016/j.biosystemseng.2013.03.016.
- Marx, A., Kunstmann, H., Schuttmeier, D. 2008. "Uncertainty analysis for satellite derived sensible heat fluxes and scintillometer measurements over savannah environment and comparison to mesoscale meteorological simulation results." **Agricultural and Forest Meteorology** 148: 656-667. doi:10.1016/j.agrformet.2007.11.009.
- Mateos, L., González-Dugo, M. P., Testi, L., Villalobos, F. J. 2013. "Monitoring evapotranspiration of irrigated crops using crop coefficients derived from time series of

- satellite images.I. Method.” **Agricultural Water Management** 125: 81-91. doi:10.1016/j.agwat.2012.11.005.
- Mather, P. M. 1987. “Computer processing of remotely sensed images: an introduction.” 1. ed. *John Wiley & Sons*, New York.
- Mohamed, Y. A., Bastiaanssen, W. G., Savenije, H. H. G. 2004. “Spatial variability of evaporation and moisture storage in the swamps of the upper Nile studied by remote sensing techniques.” **Journal of Hydrology**, 289: 145-164. doi:10.1016/j.jhydrol.2003.11.038.
- Moran, M. S., Clarke, T. R., Inoue, Y. 1994. “Estimating crop water deficit using the relation between surface-air temperature and spectral vegetation index.” **Remote Sensing Environment** 49: 246-263. doi:10.1016/0034-4257(94)90020-5.
- Moran, M. S., Jackson, R. D., Raymond, L. H., Gay, L. W., Slater, P. N. 1989. “Mapping surface energy balance components by combining Landsat Thematic Mapper and ground-based meteorological data.” **Remote Sensing of Environment** 30: 77-87. doi:10.1016/0034-4257(89)90049-7.
- Nagler, P. L., Cleverly, J., Glenn, E., Lampkin, D., Huete, A., Wan, Z. 2005. Predicting riparian evapotranspiration from MODIS vegetation indices and meteorological data. **Remote Sensing of Environment** 94: 17-30. doi:10.1016/j.rse.2004.08.009.
- Namani, R. R., Running, S. W. 1989. “Estimation of regional surface resistance to evapotranspiration from NDVI and Thermal-IR AVHRR data.” **Journal of Applied Meteorology** 28: 276-284. doi: 10.1175/1520-0450(1989)028.
- Nicácio, R. M. 2008. “Evapotranspiração Real e Umidade do Solo Usando Dados de Sensores Orbitais e a Metodologia SEBAL na Bacia do Rio São Francisco.” Rio de Janeiro, *Tese de Doutorado*: Universidade Federal do Rio de Janeiro.
- Oliosio, A., Chauki, H., Courault, D. 1999. “Estimation of evapotranspiration and photosynthesis by assimilation of remote sensing into SVAT models.” **Remote Sensing of Environment** 68: 341-356. doi:10.1016/S0034-4257(98)00121-7.
- Pace, F. T. D. 2004. “Estimativa do balanço de radiação à superfície terrestre utilizando imagens TM – Landsat 5 e modelo de elevação digital.” Campina Grande, *Tese de D.Sc.*: Universidade Federal de Campina Grande.
- Padilha, F. L. M., González-Dugo, M. P., Gavilán, P., Domínguez, J. 2011. "Integration of vegetation indices into a water balance model to estimate evapotranspiration of wheat and corn." **Hydrology Earth System Sciences** 15: 1213-1225. doi:10.5194/hess-15-1213-2011.
- Paiva, C. M. 2005. “Estimativa do balanço de energia e da temperatura da superfície via satélite NOAA-AVHRR.” Rio de Janeiro: *Tese de D.Sc.*: Universidade Federal do Rio de Janeiro.
- Paredes, P., Rodrigues, G. C., Alves, I., Pereira, L. S. 2014. “Partitioning evapotranspiration, yield prediction and economic returns of maize under various irrigation management strategies.” **Agricultural Water Management** 135: 27-39. doi:10.1016/j.agwat.2013.12.010.

- Penman, H. L. 1948. "Natural evaporation from open water, bare soil and grass." **Proc. Roy. Soc. A. Londen** 193: 120-143.
- Pereira, A. R., Angelocci, L. R., Sentelhas, P. 2002. "Agrometeorologia Fundamentos e Aplicações Práticas." Guaíba: *Editora Agropecuária*.
- Pereira, A. R., Vila Nova, N. A., Sedyama, G. C. 1997. "Agrometeorologia Fundamentos e Aplicações Práticas." Guaíba: *Editora Agropecuária*.
- Pereira, L. S., Perrier, A., Allen, R. G., Alves, I. 1999. "Evapotranspiration: concepts and future trends." **Journal of Irrigation and Drainage Engineering, American Society of Civil Engineers**: 45-51. doi.org/10.1061/(ASCE)0733-9437(1999)125:2(45).
- Pereira, Luis S., Allen, G. Richard, Smith, Martin, Raes, Dirk. 2015a. "Crop evapotranspiration estimation with FAO56: Past and future." **Agricultural Water Management** 147: 4-20. doi:10.1016/j.agwat.2014.07.031.
- Pereira, L. S., Paredes, P., Rodrigues, G. C., Neves, M. 2015b. "Modeling malt barley water use and evapotranspiration partitioning in two contrasting rainfall years. Assessing AquaCrop and SIMDualKc models." **Agricultural Water Management** 159: 239-254. doi:10.1016/j.agwat.2015.06.006.
- Pettorelli, N., Vik, J. O., Mysterud, A., Gaillard, J. M., Tucker, C. J., Stenseth, N. C. 2005. "Using the satellite-derived NDVI to assess ecological responses to environmental change." **Trends in Ecology and Evolution** 20: 503-210. doi:10.1016/j.tree.2005.05.011
- Pôças, Is., Paço, T. A., Paredes, P., Cunha, M., Pereira, L. S. 2015. "Estimation of Actual Crop Coefficients Using Remotely Sensed Vegetation Indices and Soil Water Balance Modelled Data." **Remote Sensing** 7(3): 1-29. doi:10.3390/rs70302373.
- Reisig, D., Godfre, L. 2006. "Remote sensing for detection of cotton aphid–(homoptera: aphididae) and spider mite–(acari: tetranychidae) infested cotton in the San Joaquin Valley." **Environmental Entomology Pest Management** 1 1635-1675. doi: http://dx.doi.org/10.1093/ee/35.6.1635 1635-1646.
- Rosa, R. D., Paredes, P., Rodrigues, G. C., Alves, I., Fernando, R. M., Pereira, L. S., Allen, R. G. 2012. "Implementing the dual crop coefficient approach in interactive software. 1. Background Comput." **Strat** 103: 1204-1213. doi:10.1016/j.agwat.2011.10.013.
- Salazar, L., Kogan, F., Roytaman, L. 2008. "Using vegetation health indices and partial least squares method for estimation of corn yield." **International Journal of Remote Sensing** 29: 175-189. Doi: 10.1080/01431160701271974.
- Sarwar, A., Bastiaanssen, W. 2001. "Long-term effects of irrigation water conservation on crop production and environment in semiarid areas." **Journal of irrigation and drainage engineering, American Society of Civil Engineers** 127: 331-338. doi.org/10.1061/(ASCE)0733-9437(2001)127:6(331).
- Scaloppi, E. J., Aleen, R. G. 1993. "Hydraulics of center-pivot laterals." **Journal of irrigation and drainage engineering** 119: 554-567. doi.org/10.1061/(ASCE)0733-9437(1993)119:3(554).

- Silva, B. D., Braga, A. C., Oliveira, L. D., Galvncio, J. D., Montenegro, S. 2012. “Evapotranspiração e estimativa da água consumida em perímetro irrigado do Semiárido brasileiro por sensoriamento remoto.” **Pesquisa Agropecuária Brasileira** 47: 1218-1226.
- Szilagyi, J., Rundquist, D., Gosselin, D., Parlange, M. 1998. “NDVI relationship to monthly evaporation.” **Geophysical Research Letters** 25: 1753-1756.
- Tao, F., Yokozawa, Z., Zhang, H., Yishigooka, Y. 2008. “Land surface phenology dynamics and climate variations in the North East China Transect (NECT), 1982-2000.” **International Journal of Remote Sensing** 29: 5461-5478. Doi: 10.1080/01431160801908103.
- Tasumi, M. 2003. “Progress in operational estimation of regional evapotranspiration using satellite imagery.” Moscow: *PhD dissertation*.
- Wang, Q., Adiku, S., Tenhunen, J., Granier, A. 2005. “On the Relationship of NDVI with Leaf Area Index in a Deciduous Forest Site.” **Remote Sensing of Environment** 94: 244-255. doi:10.1016/j.rse.2004.10.006.
- Xião, X., Hagen, S., Zhang, Q., Keller, M., III, B. M. 2006. “Detecting leaf phenology of seasonally moist tropical forests in South America with multi-temporal MODIS images.” **Remote Sensing of Environment** 103: 465-473. doi:10.1016/j.rse.2006.04.013.
- Yang, Z., Rao, M. N., Elliot, N. C., Kindler, S. D., Popham, T. W. 2005. “Using ground-based multispectral radiometry to detect stress in wheat caused by greenbug (Homoptera: Aphididae) infestation”. **Computers and Electronics in Agriculture** 47: 121-135. doi:10.1016/j.compag.2004.11.018.
- Zhang, J., Hu, Y., Xião, X., Chen, P., Han, S., Song, G., Yu, G. 2009. “Satellite-based of evapotranspiration of an old-growth temperate mixed forest.” **Agricultural and Forest Meteorology** 149: 976-984. doi:10.1016/j.agrformet.2008.12.002.

## ARTIGO II - SISTEMA DE INFORMAÇÃO GEOGRÁFICA PARA APOIO AO MANEJO DA IRRIGAÇÃO

### Geographic information system to support irrigation management strategies

Variables associated to irrigation related processes such as meteorology, phenology, evapotranspiration, crop coefficients, among others, create a complexity in irrigation managing that can hardly be administered by merely conceptual or empirical models. Currently, the advent of geotechnology incorporation in agriculture and its integration with weather information in Geographic Information System (GIS) environments make possible the support of more detailed irrigation management and planning. This work is an effort to organize a GIS with information from 30 pivots located in Cruz Alta, RS, Brazil, with the objective to support irrigation management. The GIS organization took place in two stages: 1<sup>st</sup> acquisition, georeferencing, image vectorization, snipping and calculation of vegetation indices related to 107 images from the Landsat 5/TM satellite in 222 and 223 orbits in point 80; 2<sup>nd</sup> create geo-related tables for each pivot containing field obtained information and weather station information for the region. Thus, a geographic database was created in a system capable of integrating field information with that obtained by remote sensing and for mapping the distribution of key crop variables, enabling better visualization of the dynamics of the phenomena in progress and enabling a more comprehensive technical background in decision making linked to the management and production planning in irrigated crops.

**Keywords:** Landsat; remote sensing; NDVI; evapotranspiration; crop coefficients.

### INTRODUCTION

Humanity is going through a turbulent time, as the consequences of climate change are already being felt and it is known that in the near future, there will be more competition for water by different sectors of the society (Vörösmarty et al. 2000). The water is increasingly scarce in relation to its demand, or otherwise called quantitative criticality. The intensification of irrigated agriculture associated with increased water scarcity is a current concern in many regions of the world, especially in southern Brazil, where the quantitative criticality has increased due to increased irrigated agriculture (ANA 2014). Recent studies have mapped the areas irrigated by center pivot in Brazil and detected 17,878 pivots covering an area of 1,179,176 hectares, of which 1,111 pivots are located in Rio Grande do Sul state with an irrigated area of 76,081 hectares (EMBRAPA and ANA 2013).

Irrigation plays an important role in food context, since the productivity of an approximate 1 ha irrigated is equivalent to 3 ha by rainfall (Brasil 2009). Worldwide, about 18% of cultivated areas are irrigated and accounted for about 44% of agricultural production on the planet. In Brazil, it is estimated that 16% of the total food production comes from irrigated areas and these are still expanding. World irrigated areas could increase by about 70% and of these, 13% will come from Brazil (Christofidis 2007).

Currently, the risks of failures caused by dry and drought spells are increasing due to climate change and the high costs of agricultural production in the country. However, with

irrigation, the farmer is sure of at least minimum guarantee of productivity even when there are periods of drought.

On the other hand, this management practice that gives productivity assurance "without climate risks" is also responsible for the consumption of 69% of freshwater on our planet. Although Brazil is considered privileged in terms of water resources, having about 13% of the world's fresh water, however the largest State, in terms of economic and population, São Paulo, is going through a critical time because of drought. About 8 million people had to adopt water rationing measures (ANA 2015; SABESP 2015). One of the Brazilian Laws on Water Resources states that in situation of water scarcity, priority should be accorded to human and livestock needs (Brasil 1997), but specified that the management of water resources should be proportioned to the multiples uses. Thus, it becomes necessary to search for alternative management, monitoring and support for irrigation with a view to optimizing water resources without prejudice to food production, as well as for urban supply.

An alternative for the optimization of water use, especially in humid subtropical regions, where rainfall occurs frequently, such as the area under study, is the use of supplementary irrigation. The irrigation should meet the demand of crops in a sustainable manner, and in regions where there are significant rainfall, these should be considered in the planning, management and processing of water (Pires et al. 2008). For this reason, there is a need to monitor and manage the irrigated areas in an integrated manner where both soil and crop characteristics can be evaluated together with climatic factors, such as wind speed, temperature and precipitation, and thus tailor the water use according to actual need of the crop.

The establishment of plans for the management, planning and water conservation, soil and vegetation has always been of interest in advanced societies. But until recently this was done only in documents and maps on paper; which makes difficult an analysis combining several maps and data. Since 1950, the simultaneous advent of computer technology and development had made it possible to store and represent information in computer environment (Câmara et al. 2001), such as Geographic Information System (GIS).

In this context, the need for localized information becomes important, because for each region, in the case of this study area, each center pivot irrigation area has its own characteristics that must be taken into consideration when it is time to irrigate. In addition to the morphological and phenological characteristics of crops and meteorological conditions of the region, pests, diseases, soil fertility and texture are other features inherent to each irrigated area, which can also influence the amount of water to be applied by irrigation. These

information can be organized and visualized using GIS tool where information (e.g., maps, images, data collected in the field, meteorological data) can be manipulated, integrated and processed, besides ensuring spatial visualization, this could be a support for irrigation management, especially in the context of economic and environmental sustainability.

Currently, there is a increase in irrigation by center pivot system, because of its several advantages over surface irrigation system, including labor saving, high yields (Bernardo et al. 2008), possibility of complete system automation, applicability to a wide range of crops such as: grains, vegetables, coffee, and forage grasses (Jacinto 2001). With this great progress, integrated monitoring and management of the irrigated areas by center pivot using remote sensing tools in GIS are more accurate, faster and less costly compared to total reliance on field observations. In addition, the integration of information emanating from satellite images with databases of each producer or manager will make it possible to redeem the history of each region in organized form, thus enabling more valuable information for proper planning of crop management and irrigation projects.

Therefore, the objective of this study was to elaborate and discuss the organization of geo-relational database with information from 30 center pivots located in Cruz Alta, RS, with a view to support irrigation management. Presented within the GIS is a history of the area under study, with information relating to: i) Relief: slope and hypsometry; ii) land use: crop type, planting time, growth stage; iii) climate: rainfall, wind speed, temperature, humidity and soil and evapotranspiration; iv) statistical analysis of NDVI values of pixels (picture elements) within each pivot, such as variance, standard deviation, coefficient of variation, skewness, kurtosis, minimum and maximum values, upper and lower quartile, and median. The composition of the database, processing of images, combination of information, computations and statistical analyzes, as well as generation of maps were performed and organized using SPRING software (Câmara et al. 1996). Thus, we present a system capable of integrating field information with those obtained by remote sensing and map the distribution of important crop variables, which will enable better visualization of the dynamics of phenomena in progress and a more comprehensive technical background in making decision related to the management of irrigated crops.

## **METHODOLOGY**

### ***Study sites***

The area of interest of this study is the municipality of Cruz Alta, located in the North western part of Rio Grande do Sul State, Brazil (Figure 1), between latitude 28°34'05" and 28°45'14"

S and longitude  $53^{\circ}14'22''$  and  $53^{\circ}30'33''$  W. The irrigation system in the region are mainly center pivot.

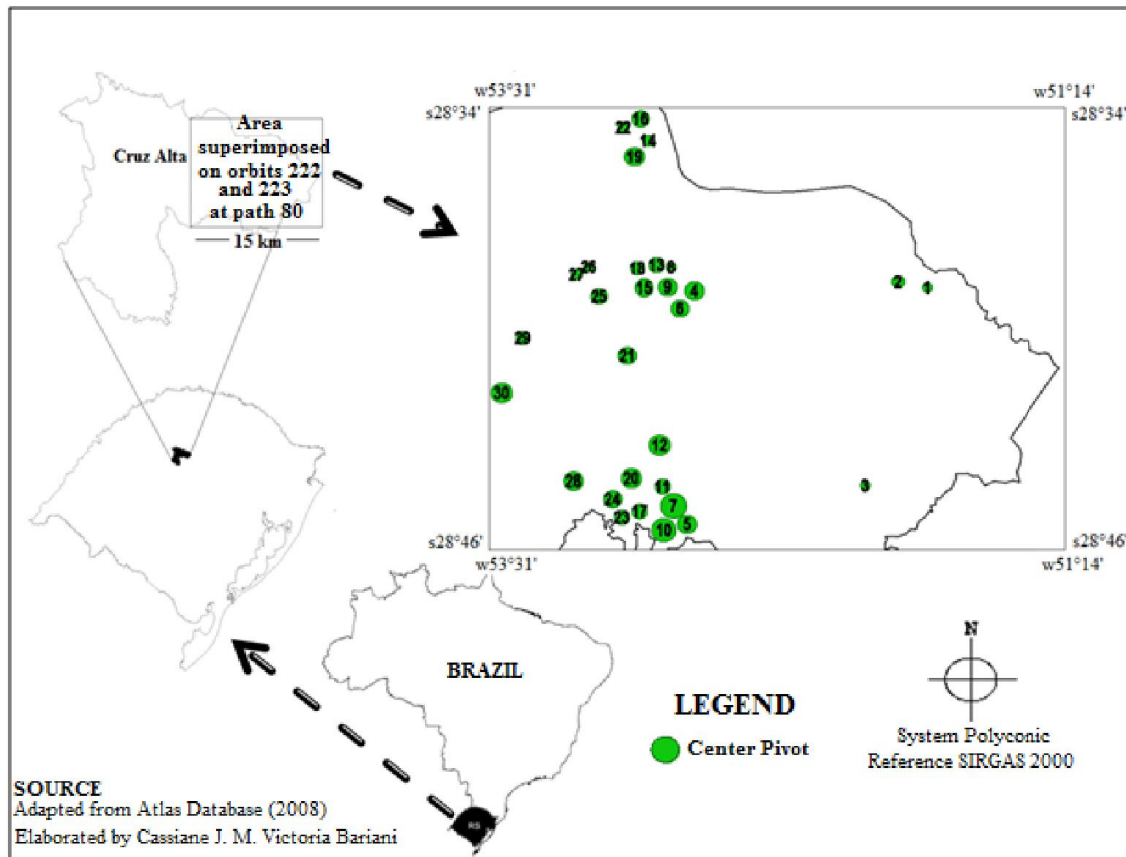


Figure 1. Location of the study area. The rectangle shows there sults of super imposed images of orbits 222 and 223, path 80 from Landsat 5/TM satellite.

### *Remote sensing data and products*

Images of the TM sensor (Thematic Mapper) aboard the Landsat 5 satellite, covering periods from January 2003 to December 2011, totaling 107 superimposed images from path/row 222/80 and 223/80, were used in this study. The reason for using two orbits is to improve the temporal resolution of the images, i.e. the frequency of satellite passage of the study area increased from 16 days to 8 days. As shown in Figure 1, the orbits have overlap of 15 km for the path 80 analyzed, thus ensuring better imagery and cover several months and in some months, we had more than one image which is good for agricultural monitoring.

The images, from LANDSAT 5, were obtained free of charge via the Internet at INPE <<http://www.dgi.inpe.br/CDSR/>>. Image search of the required path and row was made from all images available between 2003 and 2011 in the database of the site. The selected images were those that had clouds coverage ratio less than 10%. Digital processing of images including recording, vector editing and extraction were made using SPRING software ,



version 5.2.6 (Câmara et al. 1996) while georeferencing of images was done using Geocover Mosaic images (USGS 2004).

### ***Creation of related database***

SPRING software was designed as a geographic database projected to operate in conjunction with a manager database system (DBMS). The geographic database is the data repository of GIS, storing and retrieving geographical data in different geometry (images, vectors, grids) and descriptive information (non-spatial attributes) stored in tables. In SPRING, all the descriptive information about the geographic data are stored in relational DBMS tables associated with the system (Câmara et al. 1996).

The DBMS can also be called the model "geo-relational" where the spatial and descriptive components of the geographical object are stored separately. The conventional attributes are stored in a database (in tables) and the spatial data is handled by a dedicated system. The connection is made by identifiers (id) objects (Câmara et al. 2001). To retrieve an object, the two subsystems must be investigated and the response is a composition of results. Examples managers are: SQLite, Access, Oracle8i, MySQL, PostgreSQL and DBase. In the present study, we used the Access manager.

### ***Processing of images***

After correction of the native georeferencing of Landsat 5/TM images by registration procedure, using a composition of false color given as blue color to band 3, green color to band 4 and red color to band 5 (BGR345 composition), the center pivots were identified for visual interpretation. The limits of center pivots were drawn by vector editing in an information plan of thematic category.

With the pixel values obtained by digital processing of the images corresponding to bands 3 and 4 of Landsat 5/TM, and for each of the identified pivot, it was possible to calculate the normalized vegetation index (NDVI) in matrix format (image or grid) using spatial language for algebraic geoprocessing (LEGAL) available in SPRING, according to programming code adapted from (Neto et al. 2008).

To obtain the statistical parameters of mean, variance, standard deviation, skewness, kurtosis, coefficient of variation and median, the statistical tool for image polygon was used and a table with information for the 30 pivots analyzed for each of the 107 dates of imagery was obtained. This table was automatically included in the database.

For the preparation of soil use maps, we used the supervised classification by regions. Three Landsat 5 satellite images of orbit 223 and path 80 obtained on three different occasions, March 25, 1991, March 04, 2001 and March 16, 2011 were classified. The supervised classification by regions was made after Principal Component Analysis (PCA). For the principal component analysis, composite bands 5, 4, and 3 in RGB were used. Before the creation of samples for the supervised classification of images, the segmentation of the images is required, or in other words, the creation of regions. For the segmentation, the method "growth by regions" was used, where the value of 15 was assigned to similarity and 30 to the area of the pixel. The type of classification used was the "Bhattacharya" with 95% level of acceptance. After the image classification was created, the thematic map of the classified image was created, where the matrix image was transformed to thematic map vector. The classes created were bare soil, native vegetation, maize, soybean and water.

For the erosion risk map, the universal soil loss equation (USLE) was implemented in LEGAL subroutine in SPRING, following the programming code. The USLE estimates average annual soil loss by sheet erosion (Kinnell 2010) according to the equation:

$$A = R.K.LS.C.P \quad (1)$$

where A is average annual soil loss per unit area, ( $\text{Mg ha}^{-1} \text{ yr}^{-1}$ ); R is rainfall erosivity, ( $\text{MJ mm ha}^{-1} \text{ h}^{-1} \text{ year}^{-1}$ ); K is the soil erodibility, ( $\text{Mg h}^{-1} \text{ MJ}^{-1} \text{ mm}^{-1}$ ); LS is the topographical factor, dimension less; C is the soil use and management factor, dimension less; and P is the conservation practice factor, dimension less (Wischmeier and Smith 1978).

Also the 28S54 image obtained from the Shuttle Radar Topography Mission (SRTM), available at <http://www.dsr.inpe.br/topodata>, was used to prepare the land slope map.

To estimate the water requirements of crops, the dual crop coefficient method outlined in FAO 56 bulletin (Allen et al. 1998) was used. This approach describes the relationship between crop evapotranspiration ( $ET_c$ ) under standard condition and reference evapotranspiration ( $ET_o$ ), by separating the crop coefficient ( $K_c$ ) into basal crop coefficient ( $K_{cb}$ ) and soil evaporation coefficient ( $K_e$ ) according to the following equation:

$$ET_c = (K_{cb} + K_e) * ET_o \quad (2)$$

The  $ET_o$  was calculated using FAO Penman-Monteith method (Allen et al. 1998), selected as the method by which the evapotranspiration of the reference surface ( $ET_o$ ) can be

determined unambiguously using weather data, giving consistent  $ET_o$  values for all regions and climates. The FAO Penman-Monteith equation is given as:

$$ET_o = \frac{0.408\Delta(R_n - G) + \gamma \frac{900}{T + 273} u_2 (e_s - e_a)}{\Delta + \gamma(1 + 0.34u_2)} \quad (3)$$

Where  $ET_o$  is reference evapotranspiration ( $\text{mm d}^{-1}$ );  $R_n$  is net radiation on the surface ( $\text{MJ m}^{-2} \text{d}^{-1}$ );  $G$  is soil heat flux density ( $\text{MJ m}^{-2} \text{d}^{-1}$ );  $\gamma$  is the psychrometric constant ( $\text{kPa}^\circ\text{C}^{-1}$ );  $T$  is air temperature at 2 m height ( $^\circ\text{C}$ );  $u_2$  is wind speed at 2 m height ( $\text{m s}^{-2}$ );  $e_s$  is saturated vapor pressure (kPa);  $e_a$  is the actual vapor pressure (kPa);  $e_s - e_a$  is the saturation vapor pressure deficit (kPa); and  $\Delta$  is the slope of the vapor pressure curve ( $\text{kPa}^\circ\text{C}^{-1}$ ).

In order to integrate remote sensing data to the FAO approach, the  $K_{cb}$  and  $K_c$  coefficients in Equation 2 were obtained from the NDVI values. The  $K_{cb}$  was estimated via NDVI ( $K_{cb \text{ VI}}$ ) using the methodology proposed by Allen and Pereira (2009) and Pôças et al. (2015).

### ***Crop and meteorological data***

Meteorological data of minimum and maximum air temperature, relative humidity, vapor pressure, wind speed and solar radiation and precipitation were obtained from a meteorological station belonging to the National Institute of Meteorology (INMET), installed in the vicinity of the study area. The crop data is a function of the irrigation management system (Sistema Irriga ®), a web-based support for farm irrigation scheduling in Brazil. Thus, information on crop type, time of sowing, growth stages, soil moisture and yield were organized in a spreadsheet and then imported as tables to the SPRING database.

### ***Association of tables with objects***

Any table introduced in the database will be associated with the graphical elements of each pivot (line, point or polygon) via a common column, repeated in each of the tables and the object. Once this step is taken, the connection between the object (table rows) containing the information for each pivot and the corresponding polygon was made.

## **RESULTS AND DISCUSSION**

The different tables with data on areas irrigated by center pivot system were organized within a GIS, thus a geo-relational database was created. An example of a table inserted into the geo-

relational data base is shown in Figure 2, where the statistical analysis obtained through NDVI values can be observed. Moreover, the satellite images used allowed the visualization of the locations of the center pivots and creation of graphics capable of being associated with the table information, allowing the simultaneous perception of the locations as well as the magnitude of the variables analyzed.

Figure 3 shows the results of geo-relational data base, where we have a table showing the number of each pivot, represented by the column in yellow color, and the values of each variable. Also it was possible to view the satellite image, with the identification and location of the 30 pivots analyzed. When a center pivot in the image or map to be analyzed is selected, it is shown in lime green color, alternately, if table values can be used, the simple thing to do is to select the correspond in grow in the table and the pivot will be automatically appeared on the image or map, which will also be lime Green in color. It was observed that the center pivots 4, 7 and 28 were not selected in the table and therefore appeared as blue color on the map (Figure 3).

To check for variables that could be used to make a pattern, for example, precipitation values for a given date, simply select check attributes in the relational data base, where the established parameters are listed as shown in Figure 4. From this figure, it is clear that for the date in question, the pivots 1, 2 and 3, located in the eastern part of the area, did not receive rainfall, or in other words, rainfall amount is zero (Figure 5). This procedure can be applied to all images, dates of acquisition and all variables.

In agriculture, the need for weather information is becoming increasingly important. The length of the growing season of different species or varieties of plants depends directly on the climatic conditions and water availability, which determines the geographic distribution of risk to plant development (Carvalho et al. 2012), thus allowing for proper planning of irrigated areas. The efficiency of water usage can be defined by the amount and frequency of rainfall associated with the soil water holding capacity (Bergamaschi et al. 1992). On the other hand, periods of drought during the rainy seasons, called indian summers, contribute greater risk to agricultural production in the world (Lana et al. 2006).

Dados Não Espaciais

Tabela... DADOS\_NDVI

Manipulação dos Dados

	PI	POLIGONO	NPIXEL	MINIMO	MAXIMO	AMPLITUDE	MEDIA	VARIANCIA	DESVIOPADRAO	ASSIMETRIA	CURTOSE	COEFVARIACAO	MEDIAN
1	01012004_NDVI	1	815	0.426645	0.678171	0.251526	0.545775	0.001163	0.034104	0.012668	3.003409	6.248713	0.547006
2	01012004_NDVI	2	434	0.438183	0.786398	0.348214	0.694804	0.001736	0.041671	-2.241891	11.973982	5.997471	0.700039
3	01012004_NDVI	3	424	0.617431	0.766492	0.14906	0.702529	0.000778	0.0279	-0.361105	3.164534	3.971426	0.703389
4	01012004_NDVI	4	1191	0.202846	0.612996	0.41015	0.321668	0.004126	0.064233	1.484942	5.53337	19.968864	0.30983
5	01012004_NDVI	5	653	0.519051	0.785878	0.266827	0.736782	0.001074	0.032778	-3.351717	17.980627	4.448762	0.742561
6	01012004_NDVI	6	1027	0.231745	0.772261	0.540517	0.342011	0.003977	0.063061	3.962626	21.234821	18.438271	0.329449
7	01012004_NDVI	7	574	0.684991	0.797559	0.112569	0.760268	0.000201	0.014184	-0.72223	4.623105	1.865658	0.76033
8	01012004_NDVI	8	164	0.534017	0.779684	0.245667	0.67752	0.004492	0.067025	-0.216179	1.855926	9.892757	0.67567
9	01012004_NDVI	9	605	0.561255	0.764758	0.203504	0.696982	0.003332	0.057723	-0.546456	1.657089	8.281861	0.73459
10	01012004_NDVI	10	340	0.638377	0.814239	0.175862	0.790575	0.000413	0.020316	-4.350525	28.4213	2.569819	0.795067
11	01012004_NDVI	11	642	0.489038	0.694566	0.205528	0.621732	0.001726	0.041543	-0.659659	2.983229	6.681872	0.627191
12	01012004_NDVI	12	588	0.366181	0.622848	0.256667	0.480434	0.001936	0.043999	-0.112259	2.49451	9.158076	0.485265
13	01012004_NDVI	13	603	0.752571	0.807469	0.054898	0.782724	7.2e-05	0.008513	-0.179222	3.109581	1.087669	0.782197
14	01012004_NDVI	14	463	0.50853	0.782737	0.274207	0.711005	0.002363	0.048608	-1.545326	5.702939	6.836557	0.719131
15	01012004_NDVI	15	485	0.770191	0.823271	0.05308	0.797358	0.000103	0.010128	-0.105665	2.536529	1.270133	0.797329
16	01012004_NDVI	16	188	0.581362	0.704751	0.123389	0.660802	0.000688	0.026225	-0.606492	2.923066	3.968673	0.663363
17	01012004_NDVI	17	307	0.575185	0.806051	0.231767	0.753117	0.001530	0.030000	-1.52013	5.022246	5.108541	0.763152

Metadados... Fechar Ajuda

Figure 2. Table of non-spatial data from SPRING software.

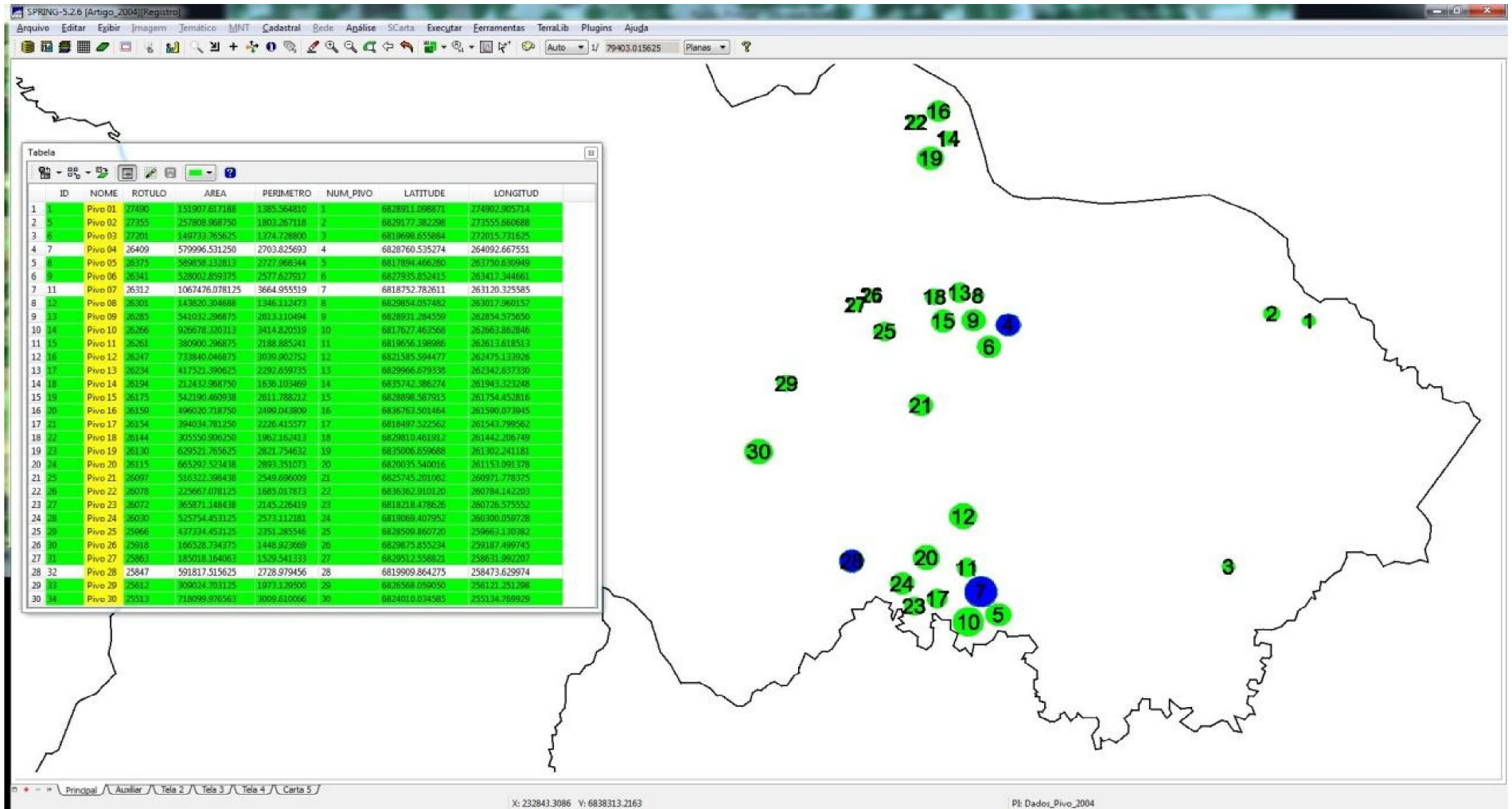


Figure 3. Geo-relational database from SPRING software.

The quantification of rainfall distribution during the year is important to define a region as being of greater or lesser economic risk to the development of a given crop, and thus could also set the implementation of irrigation systems. Measurement and records of rainfall data have been used to: estimate crop production, establish the management of water resources, evaluate the environmental performance, protect soils against erosion, and assess current and future climate risks. Also, obtaining the correct spatial distribution of rainfall is paramount to agricultural planning, especially with regard to annual crops, where excess or lack of water can undermine or derail the entire production system (Carvalho et al. 2012).

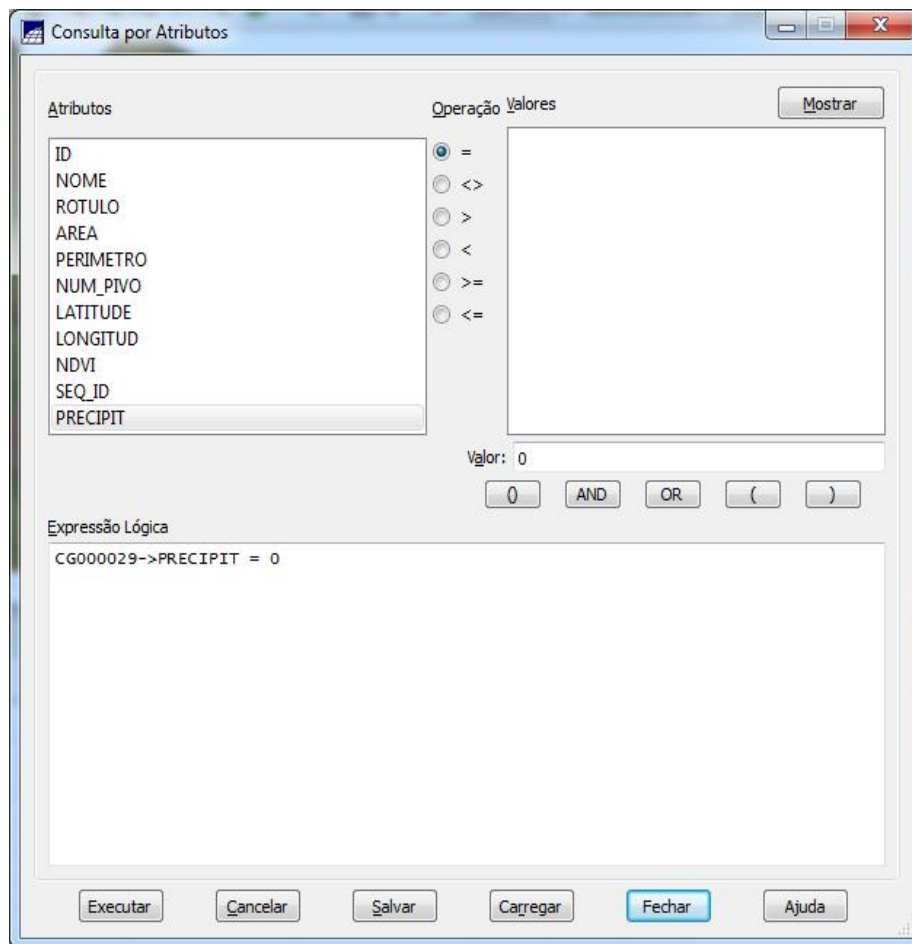


Figure 4. Attributes checking – Precipitation = 0 (zero).

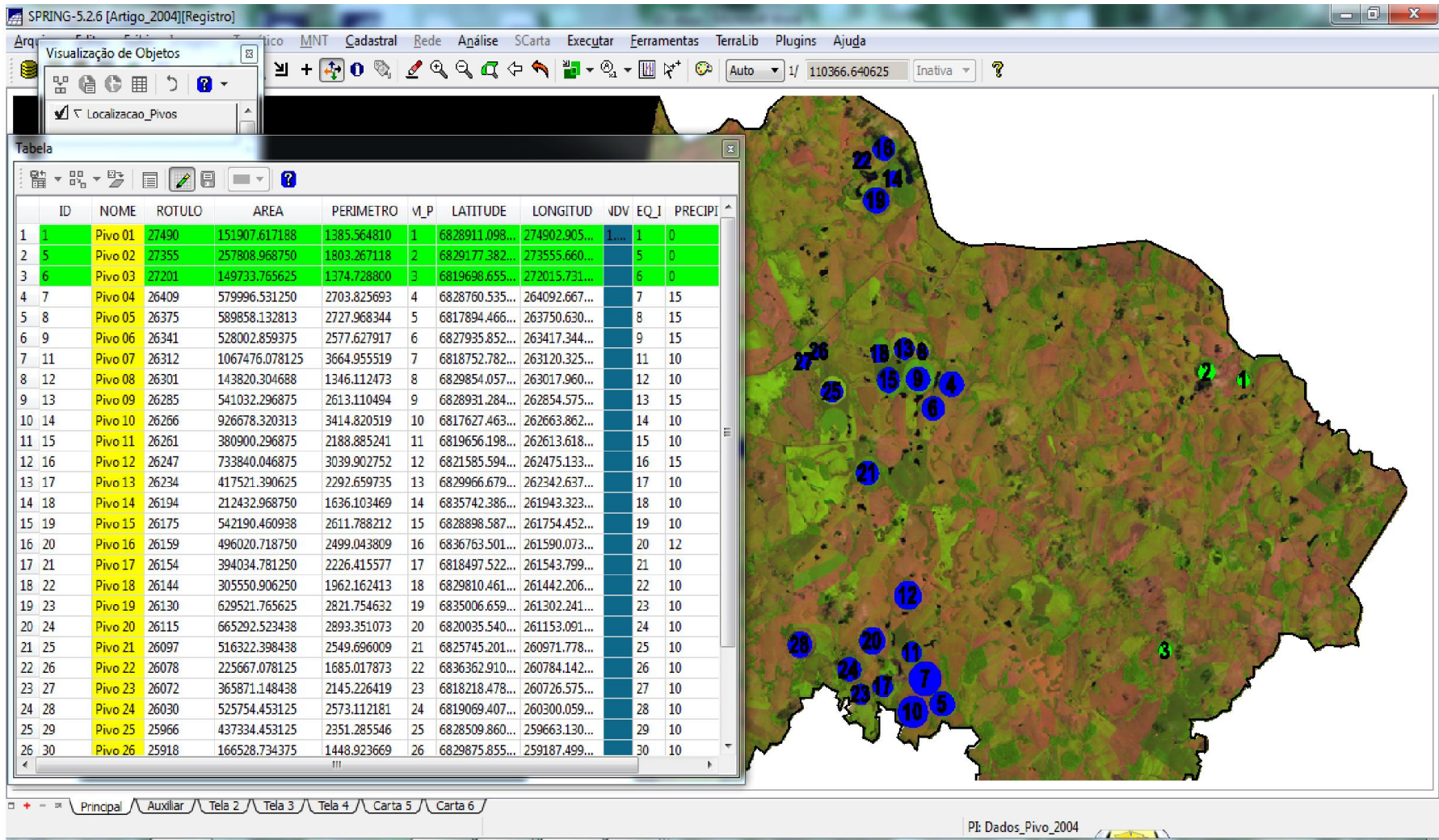


Figure 5. Results of geo-relational database check.  
Central pivots with precipitation=0(zero) are highlighted in lime green color.



The procedures for checking and handling of meteorological data, characteristics and aspects of crops and remote sensing information associated with geographic information are the essence of geo-relational database developed within the GIS in the SPRING software. What distinguish the GIS from other information systems are the functions that enable the realization of spatial analysis. These functions use the spatial and non-spatial attributes of graphic entities stored in the spatial database; with a view to make simulations (models) about the phenomena of the real world, its aspects or parameters (INPE 2015).

Integrated planning of management, monitoring and soil conservation, water and vegetation are now enhanced with the use of geotechnology. The use of GIS stands out as a tool to map and get solutions to various questions about data collected from physical, environmental and agricultural platform, especially when describing the mechanisms of changes in the environment, and assist in the planning and management of existing resources (Magalhães Filho et al. 2014).

The most fundamental aspect of processing data in GIS environment is the dual nature of information: a geographic data has a geographic location (expressed as coordinates on a map) and descriptive attributes (which can be represented in a conventional database). Another very important aspect is that spatial data do not exist alone in space: as important as to locate them, also to be able to discover and represent the relationships between the various data (INPE 2015).

The potentials of a geo-relational database for the management and planning of irrigated areas by center pivot are diverse, but its applicability and effectiveness will depend on the interpretation of the information that the analyst will insert and thereafter consult to solve or view potential problems associated with the system. Some of the situations that the analyst might be interested in pursuing within the GIS are presented in Table 1.

In this study, the identification of crops and growth stages were obtained through records of monitoring and management of irrigated areas under rural properties, which were integrated into the GIS. Several studies have also demonstrated the potentials of remote sensing for the identification of agricultural crops; (Antunes et al. 2012; Risso et al. 2012), as well as for the discrimination of crop phenological stages (Picoli et al. 2012). The use of remote sensing techniques has also contributed to accelerate the process of manipulation, analysis and spatial distribution data in order to reduce running costs, such as in soil survey. In this context, the digital elevation models (DEM) and the morphometric terrain attributes were employed. There is a growing demand for elevation models and derived morphometric

attributes for continuous representation of the land in digital format, which have been widely used in landscape analysis and other applications. The DEM obtained by remote sensing are available worldwide, with large area covered by imagery and low cost of processing; however, the quality of the information depends on surface roughness and land slope (Pinheiro et al., 2012).

For this study, the land slope map (Figure 6) was developed using digital models derived from the *Shuttle Radar Topography Mission* (SRTM), available at <http://www.dsr.inpe.br/topodata>.

Slope is the inclination of land in the region. It is observed that the area under study had slopes between 0 and 30%, in which major percentage of the area having slope ranging between 0 and 10%, classified as flat to gently undulating relief and with areas having slopes between 15 and 30 %, classified as gently to strongly undulating relief (EMBRAPA 1999). The areas having slopes between 15 and 30% were identified in pivots No. 1, 5, 6, 7, 10, 11, 12, 15, 16, 17, 19, 21, 24, 25, 26 and 28, which could impair the optimization of the operation of the center pivot systems. However, it is interesting to note that this observation did not prevent the installation of the center pivot irrigation systems, shown by the large number of pivot units, including possibilities for expansion, because the relief did not show any limitation.

Apart from relief and climate, land use characteristics and occupation are also important information for the planning and management of irrigated areas, since it can be used to identify the productive regions historically. In this context, the procedure of supervised classification of the region in the images of 1991, 2001 and 2011 was applied. In this way, it was possible to identify the productive potential of the region under study that shows agricultural history of 20 years (Figure 7).

The supervised classification by region (SCR) constitutes an important tool within the GIS, since it allows the identification of crop type, acreage, permanent protection areas, thus assists in the estimation of production and the environmental behavior of the past, present and future trends. This is all possible because this classification is based on grouping of pixels, that is, from image segmentation (Fernandes et al. 2012). For the Landsat 5/TM satellite imagery, each pixel is 900m<sup>2</sup> in area. The image segmentation is the primary step in SCR because it divides the image into continuous and homogeneous objects however the accuracy of segmentation directly affects the performance of the classification (Yang et al. 2006). This classification has been considered as an important tool because it has been used to delineate soil use classes and land cover effectively (Duveiller et al. 2008).

Table 1. Examples of potential spatial analysis in the geo-relational database of irrigation.

<b>Analysis</b>	<b>General question</b>	<b>Example</b>
Condition	What is ...?	What kind of culture and developmental stage that is the pivot 07 on 10/12/2010?
Answer:	The pivot number 07 has soy with 11 cm in vegetative stage V3 and 37 days after sowing (DAS).	
Location	Where is...?	What are the as with slopes above 15%?
Answer:	The pivots n°1, 5, 6, 7, 10, 11, 12, 15, 16, 17, 19, 21, 24, 25, 26 and 28 show areas of slope above 15%, as illustrated in Figure 6.	
Trend	What changed...?	These lands were productive for 20, 10 and 5 years ago?
Answer:	Yes. Figure 7 shows the classification of land use for the years 1991, 2001 and 2011.	
Routing	Where?	What are the Best pivots to plant soybeans during 2012 cropping season?
Answer:	The better pivots for growing soybeans during the 2012 cropping season are pivot No.1, 2, 5, 6, 7, 8, 10, 11, 13, 14, 15, 16, 17, 18, 19, 20, 21, 22, 23, 24, 25, 26, 27, 28, 29 and 30, i.e. those where there was no soybean during 2011 season.	
Standards	What is the standard...?	What is the distribution of NDVI values and the phenological stages present in the number of pivot 13 in November 2005?
Answer:	The pivot point 13 has a distribution of valore NDVI between -0.1 to 0.3 indicating that this part of the pivot without vegetation and part of this transition period between vegetative and reproductive, as illustrated in Figure8.	
Model/Scenario	What happens if...?	What is the most erosion vulnerable area on an occurrence of rain for the pivot number 13 in November, 2005?
Answer:	The red area indicated in the erosion risk map (Figure 9) is more likely to erodibility.	
Model/Scenario	What is the need for...?	What is the water need for the maize crop cultivated in the central pivots by January 26, 2005?
Answer:	There is no need for irrigation on January 26, 2005 due to accumulated rainfall on days 24 and 25 which was of 15 mm in addition to the $ET_c$ had been averaging 3 mm.	

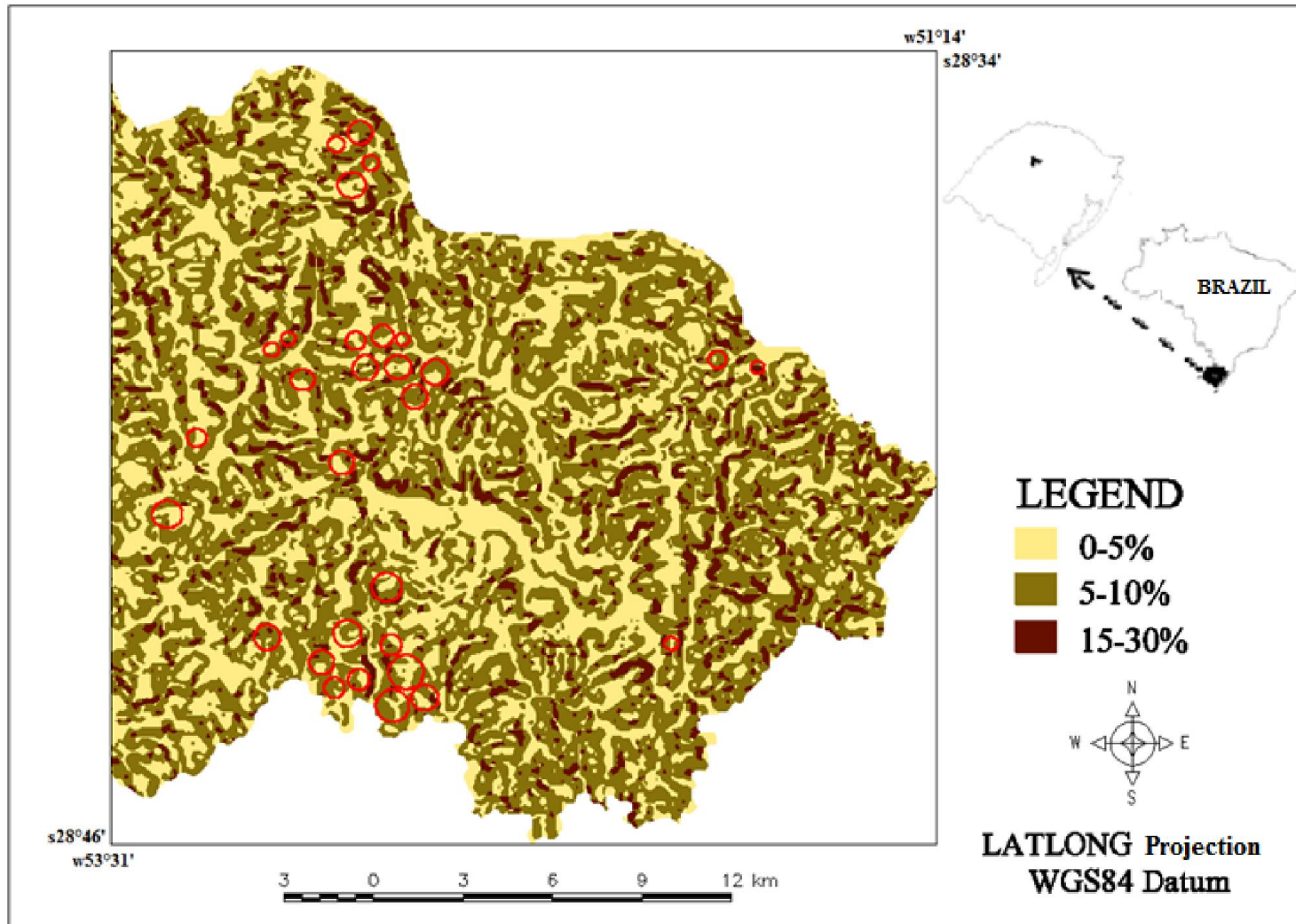


Figure 6. Land slope map showing the identified center pivot irrigation locations (red circles).

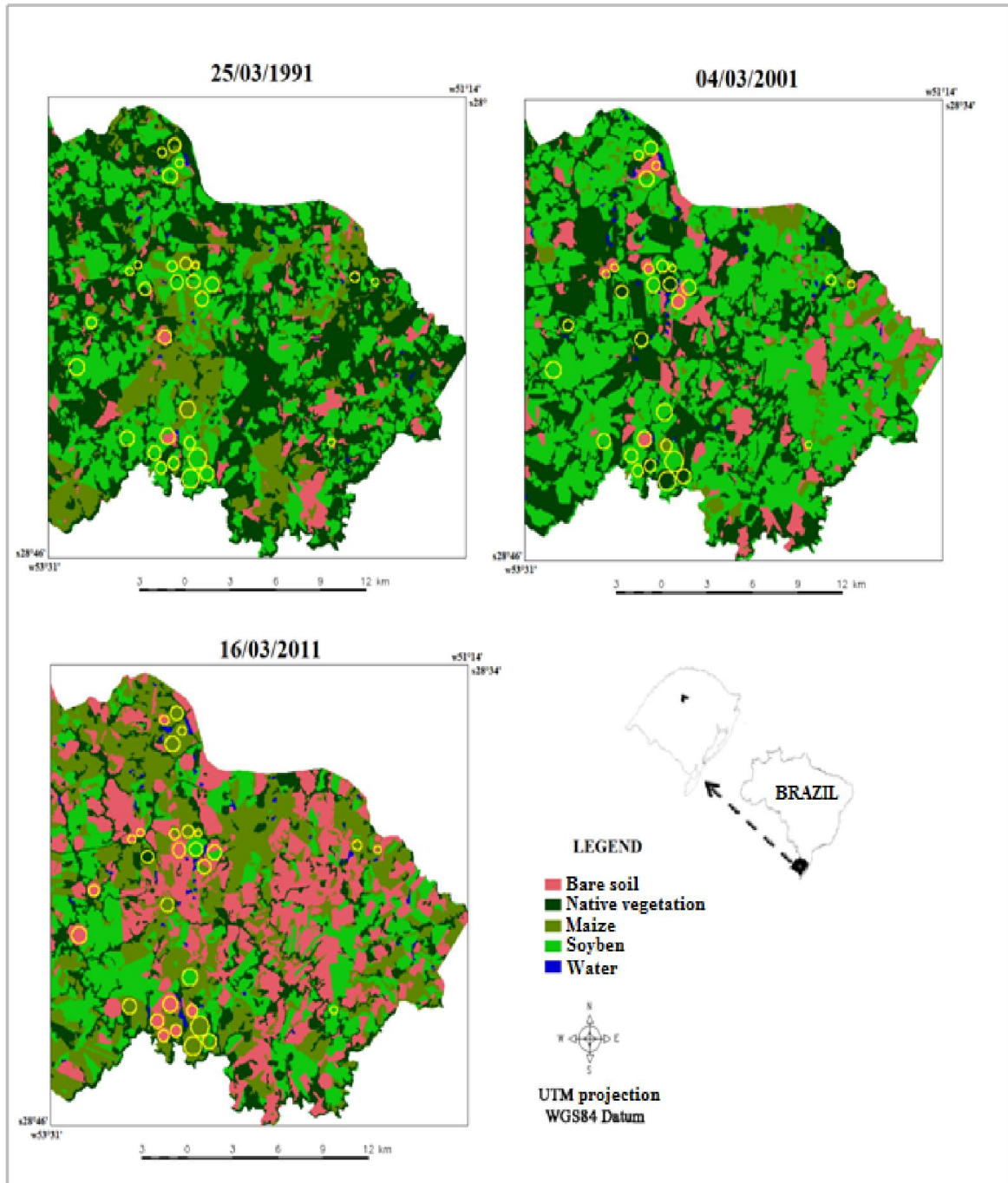


Figure 7. Soil use map for the years 1991, 2001 and 2011.

Thus, through the images of the satellite Landsat 5/TM sensor, processed by remote sensing techniques, it was possible to create maps that record the status of soil use in the region at the time of satellite pass. Each pixel in the image contains information related to the position of points and radiation characteristics (reflectance) of the land surface imaged by the sensor. However, the raw image is difficult to interpret for a non-expert user, therefore,

"principal component analysis", which produces a "highlight" of the characteristics of each target, and then "supervised classification by regions" procedures were applied to transform the original image into an easily interpretable map for users.

In addition to the potential visualization, the procedure also allows for numerical assessments of land use in the study area, because the program emits a report that describes the areas occupied by each chosen class in the classification. Using this capability, a comparison between the results of land use obtained from the images of years 1991, 2001 and 2011, corresponding to the 1990, 2000 and 2010 cropping seasons, was performed. This serves to provide an indication of the trends that had happened in the region, which exemplifies a typical situation of obtaining information for the management of the territory, permitting an integrated analysis for the planning of expansion of irrigated areas in a sustainable manner, taking into account several factors inherent to the region under study. In Figure 7, we can see the growth of cropped areas and water courses for the past 20 years.

Table 2 shows the comparison of land use classes analyzed for the years 1991, 2001 and 2011. The area was divided into five classes: a) water reservoir; b) soybean; c) maize; d) native vegetation; and e) bare soil. The water reservoir class increased by 33% due to construction of dams and water reservoirs for irrigation; soybeans class showed an increase of 24.5% during the first decade (year 2001), occupying more than 50% of the area under study, but during the second decade, there was a decrease of 23.6%, leading to an expansion of only 0.9% for the 20 years (after 2011) analyzed. For corn occupying 19.8% of the planted area in 1991, the planted area fell to 4.18% in 2001, however for the year 2011, there was an increase of 32.7% in planted area, occupying about 37% of the total area, and this fact is associated with the high productivity obtained from the maize crop when subjected to irrigation (Rodrigues et al., 2013), which did not occur 20 years ago. The native vegetation class showed a decrease of about 32% after 20 years. In 1991, it occupied about 47% of the total area under study but in 2011, it could only occupy 14.8%. For bare soil class, representing bare soil or with straw, there was an increase of 13.5% for the 20 years analyzed. This may be associated with the harvest period of some cultivars such as maize and soybeans from March.

In addition to the numerical assessments carried out by the integration of information in the GIS, one also locate the areas planted to soybean, for instance in pivots 3, 4, 9 and 12, for the 2010/2011 cropping season. Therefore, to obtain the best yield for soybean in the 2011/2012 season, it is required that other pivots were not planted to the crop in the 2010/2011 season other than to be grown with legumes, that is adherence to crop rotation system (Thomas and Costa 2010).

Table 2. Comparison of land use classes analyzed between the years 1991, 2001 and 2011.

Soil use class	Area occupied in percentage (%)		
	1991	2001	2011
Water reservoirs	0.13	0.30	0.46
Soybean	25.86	50.32	26.78
Maize	19.82	4.18	36.86
Native vegetation	47.03	37.63	14.79
Bare soil	6.96	7.05	20.45

Another important aspect to obtain good yields is the practice of efficient irrigation. However this requires adequate monitoring of climate as well as crop phenology (Martins et al. 2012, 2013); within the irrigation system. In this context, the management of irrigated areas via remote sensors enables efficient visualization of the distribution of the phenomena under studied. In Figure 8, it is observed that pivot No. 13 presented different crop growth stages. The west side of the pivot has an area without vegetation, which covers almost 50% of the central pivot area. In a longitudinal section at the central area of this pivot, there is a small area showing transition between growth stages, having pixels with vegetative stages and to the east side, a region with reproductive stage (Figure 8). This phenomenon may be attributed to the time of harvest of some maize crop that occurred in January, which corresponds to the image data (26/01/2005) evaluated.

On the other hand, the survey of USLE factors showed a valuable tool that could provide necessary data for the physical diagnosis of the management plan of the area under study. With the USLE, it was possible to identify areas with steep slope according to LS factor; the type of soil of the region can be identified and consequently its agricultural potential by factor K, and also the uses and management of the soil, according to factor C (Magalhães Filho et al. 2014). With this information, it is possible to map soil losses and identify areas susceptible to erosion, which will assist the rural entrepreneur in choosing management practices consistent with the environmental situation of the enterprise. Therefore, the integration of USLE in a GIS constitutes a further approach to environmental planning and irrigation.

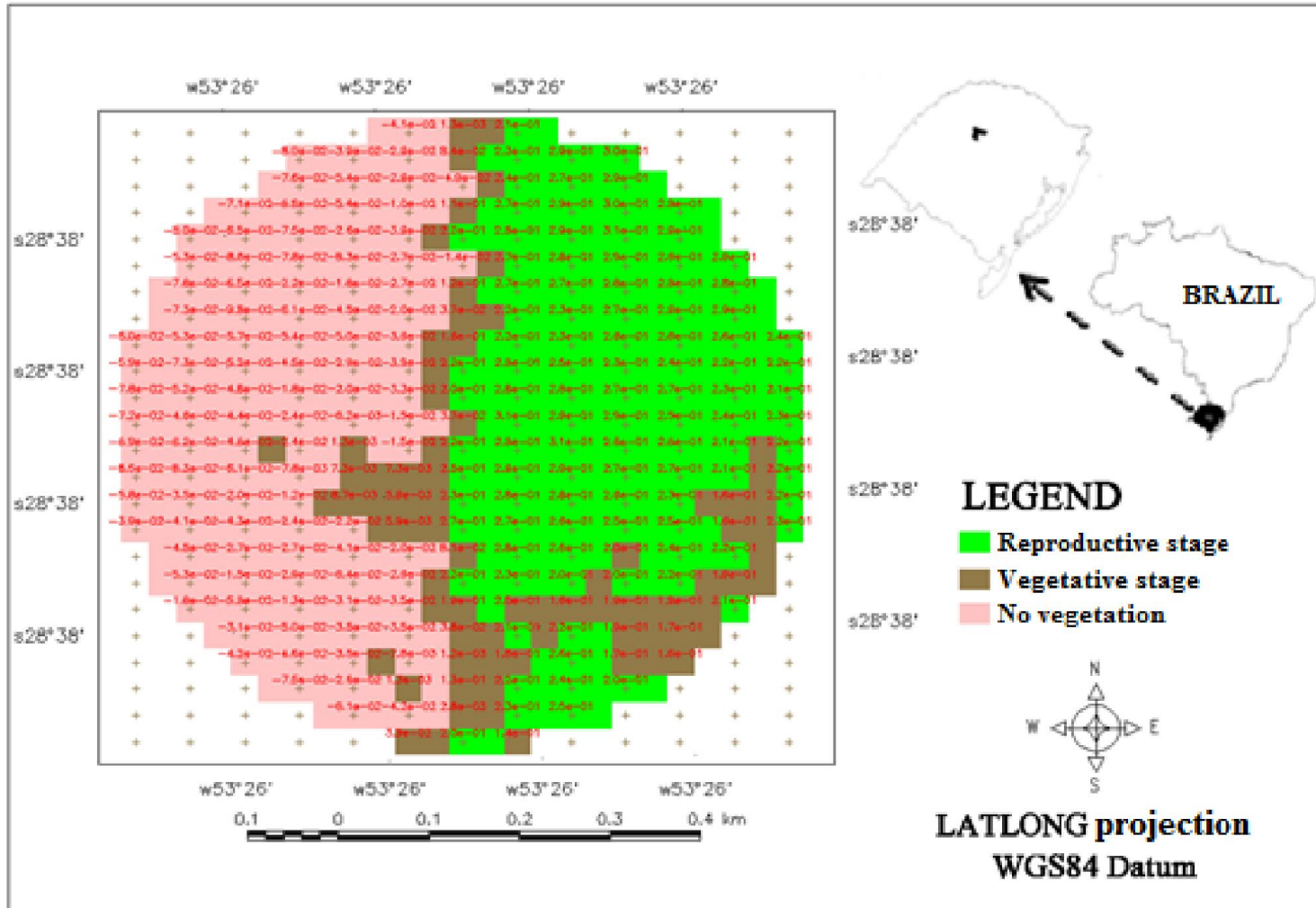


Figure 8. Map of the spatial distribution of NDVI values and their growth stages for pivot No. 13 using the satellite image obtained on 13th January 2005.



Because the relief of the landforms control the direction and the intensity of surface water flow, the knowledge and analysis of the spatial behavior of soil characteristics become extremely important as it is directly related to surface processes of soil loss, transport and deposition of materials (Leão et al. 2010). Once areas of potential soil loss is mapped, it becomes easier to control the soil loss by adopting some management practices, such as the use of terraces and contour farming, which possess high potential in reducing soil losses by erosion (Albuquerque et al. 2005; Inácio et al. 2007). The intrinsic characteristics of each type of soil also interfere with erosion, especially when associated with the relief (Bueno and Stein 2004), which acts significantly in the remaining soil loss factors (Campos et al. 2008; Weill and Sparovek 2008).

Considering the wide variability of soil loss factors and the great influence of relief and of rainfall erosivity on erosive processes (Miqueloni et al. 2012), the application of USLE to the study of soil loss in central pivots can assist in the visualization of potentially vulnerable areas and vulnerability to erosive processes at plot level. Figure 9 shows the erosion risk map for pivot No. 13 after the application of USLE model in LEGAL. The pivot has an area of about 41.75 ha, and out of these, about 0.8 ha under high erosion risk, identified by red color on the map, with soil loss having the potential of reaching up to  $16 \text{ Mg ha}^{-1} \text{ y}^{-1}$ . The region classified as medium erosion risk, identified by brown color on the map, was approximately 36% of the total area, having soil loss between 4 and  $8 \text{ t ha}^{-1} \text{ y}^{-1}$ . The remaining area, about 62% of the total area of the pivot presents soil loss considered low and very low (Bertoni and Lombardi Neto 2005), and are represented by yellow and beige colors.

In the case of the need for irrigation there was an average  $\text{ET}_c$  of 3 mm and cumulative rainfall of 15 mm which sets up in a decision not to irrigate at the date of January 26, 2005. The  $\text{ET}_c$  values for the seven analyzed pivots are shown in Table 3.

Table 3. Evapotranspiration of corn in the seven analyzed pivots on the date of January 26, 2005.

<b>Pivot</b>	<b><math>K_{cb \text{ VI}}</math></b>	<b><math>\text{ET}_c</math></b>
01	0.24	1.47
02	0.20	1.22
06	0.98	6.04
08	0.51	3.14
13	0.47	2.88
25	0.77	4.73
27	0.24	1.47
<b>Average</b>	<b>0.20</b>	<b>3.00</b>

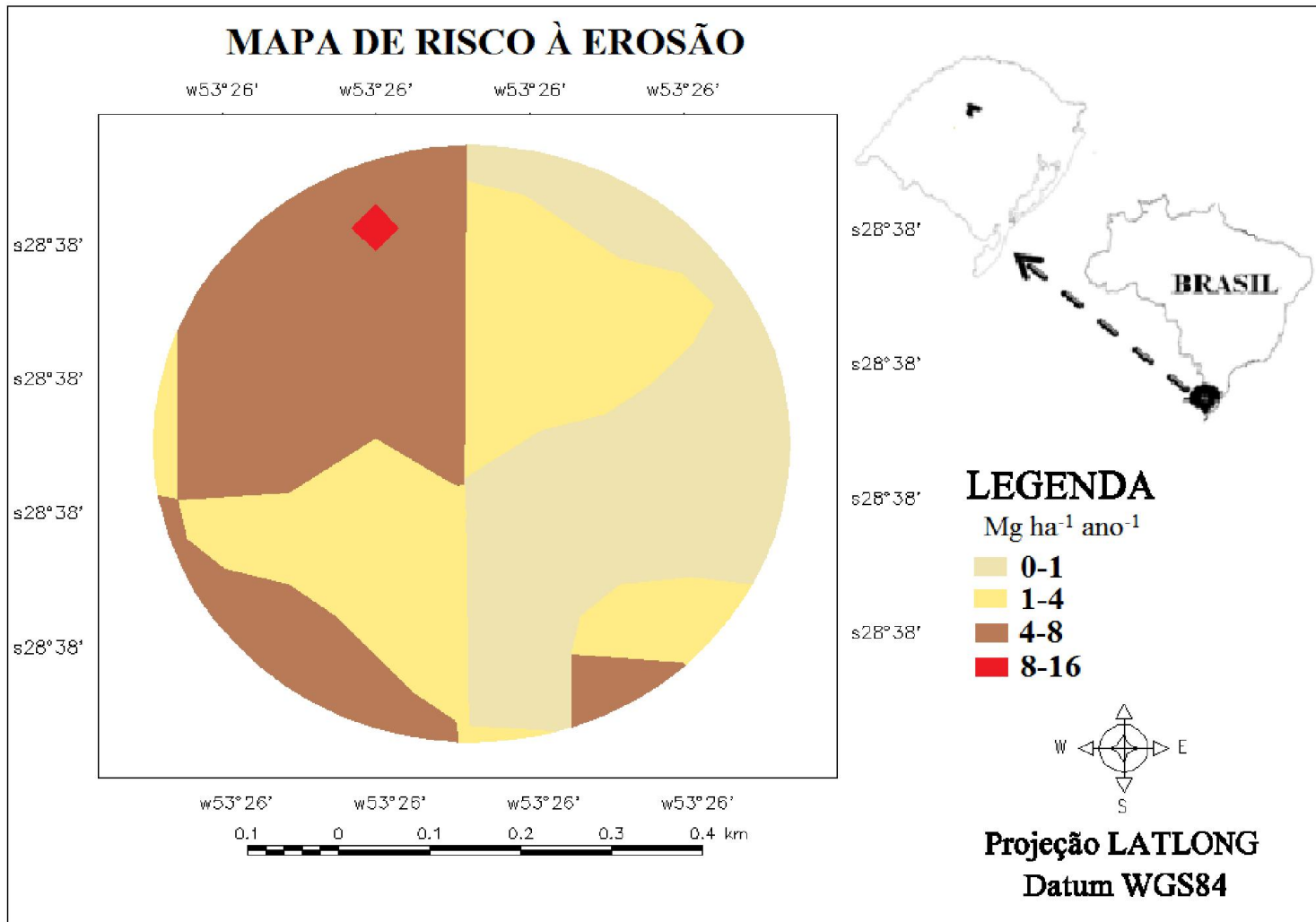


Figure 9. Erosion risk map for the pivot No. 13 for the image obtained on November 13, 2005.

The use of remote sensing products integrated into a Geographical Information System (GIS), allows for generate digital maps of crop water requirements. These maps can be used to distribute irrigation scheduling information. Yet at the same time, they offer the opportunity to modify the entire system and procedures of information generation and distribution opening the door to a further wide range of improvements in systems for irrigated areas monitoring (BELMONTE et al., 2005).

## CONCLUSIONS

The geo-relational database was organized and run successfully using data obtained from field records, weather stations and images of Landsat 5/TM satellite. The geoprocessing of information, integrated with GIS, enabled the assessment and visualization of information, and provided better understanding of the dynamics of vegetation, soil, rainfall and crop water demands.

The GIS created was able to identify:

- i) the spatial distribution of rainfall, at any time, for each pivot monitored through satellite images or maps of the area combined with weather data obtained from nearest weather stations;
- ii) crops and distinct growth stages within the center pivots, and their spatial distribution through the NDVI values;
- iii) land use classes by supervised classification of the satellite images by regions; and
- iv) erosion risk areas as well as the agricultural potentials of the region through models, computations and combining of information obtained through remote sensing.

There is evidence, therefore, that the geo-relational database of SPRING software could be a support tool for irrigation management, which would facilitate decision making as a result of the possibility of obtaining information on spatial and temporal scales.

## REFERENCES

- Albuquerque, A. W., M. Filho, G., Santos, J. R., Costa, J. P. V., Souza, J. L. 2005. "Determinação de fatores da equação universal de perda de solo em Sumé, PB." **Revista Brasileira de Engenharia Agrícola e Ambiental** 9: 153-160.
- ANA. Agência Nacional de Águas. 2014. *Relatório de Conjuntura dos Recursos Hídricos*. <http://www2.ana.gov.br/Paginas/default.aspx>
- ANA. 2015. *Agência Nacional de Águas*. <http://www2.ana.gov.br/Paginas/default.aspx>

- Antunes, J. F. G., Mercante, E., Esquerdo, J. C. D. M., Lamparelli, R. A. C., Rocha, J. V. 2012. "Estimativa de área de soja por classificação de imagens normalizada pela matriz de erros." **Pesquisa Agropecuária Brasileira** 47: 1288-1294.
- Belmonte, A. C., Jochum, A. M., García, A. C., Rodríguez, A. M., Fuster, P. L. 2005. "Irrigation management from space: Towards user-friendly products". **Irrigation and Drainage Systems** 19: 337-353.
- Bergamaschi, H. 1992. *Agrometeorologia aplicada à irrigação*. Porto Alegre: UFRGS.
- Bernardo, S., Soares, A. A. Mantovani, E. C. 2008. *Um modelo para a determinação de irrigação suplementar*. Viçosa: UFV.
- Bertoni, J., Lombardi Neto, F., 2005. *Conservação do solo*. Piracicaba: Ícone
- BRASIL. *Lei Nº 9.433, de 8 de Janeiro de 1997 da Política Nacional de Recursos Hídricos*. Congresso Nacional. Brasília. 1997.
- BRASIL. 2009. *Conjuntura dos recursos hídricos no Brasil*. Brasília: Agência Nacional de Águas.
- Bueno, C. R. P., Stein, D. P. 2004. "Potencial natural e antrópico de erosão na região de Brotas, Estado de São Paulo." **Acta Scientiarum Agronomy** 26: 1-5. doi: 10.4025/actasciagron.v26i1.1946
- Câmara, G., Souza, R. C. M., Freitas, U. M., Garrido, J. C. P. 1996. "Intergrating remote sensing and GIS by object-oriented data modeling." **Computers & Graphics** 20: 395-403. doi:10.1016/0097-8493(96)00008-8.
- Câmara, G., Davis, C., Monteiro, A. M. 2001. *Introdução à Ciência da Geoinformação*. São José dos Campos:INPE.
- Campos, M. C. C., Marques Júnior, J., Martins Filho, M. V., Pereira, G. T., Souza, Z. M., Barbieri, D. M. 2008. "Variação espacial da perda de solo por erosão em diferentes superfícies geomórficas." **Ciência Rural** 38: 2485-2492.
- Carvalho, J. R. P., Assad, E. D., Hilton, S. P. 2012. "Interpoladores geoestatísticos na análise da distribuição espacial da precipitação anual e de sua relação com altitude." **Pesquisa Agropecuária Brasileira** 47: 1235-1242.
- Christofidis, D. 2007. "Agricultura irrigada sustentável no semi-árido e no Rio Grande do Norte." **Revista Item** 6: 62-67.
- Duveiller, G., Defourny, P., Desclée, B., Mayaux, P. 2008. "Deforestation in Central Africa: estimates at regional, national and landscape levels by advanced processing of systematically-distributed Landsat extracts." **Remote Sensing of Environment** 112: 1969-1981.
- EMBRAPA. *Sistema Brasileiro de Classificação de Solos*. Rio de Janeiro: Brasília: Embrapa Produção de Informação, 1999. 412 p.
- EMBRAPA, ANA. 2013. *Água na Agricultura. Mapeamento da Agricultura Irrigada do Brasil por Pivôs Centrais*. <https://www.embrapa.br/agua-na-agricultura/mapas-sobre-irrigacao>
- Fernandes, R. R., Nunes, G. M., Silva, T. S. F. 2012. "Classificação orientada a objetos aplicada na caracterização da cobertura da terra no Araguaia." **Pesquisa Agropecuária Brasileira** 47: 1251-1260.
- Inácio, E., Cantalice, J. R. B., Nacif, P. G. S., Araujo, Q. R., Barreto, A. C. 2007. "Quantificação da erosão em pastagem com diferentes declives na microbacia do Ribeirão Salomea." **Revista Brasileira de Engenharia Agrícola e Ambiental** 11: 355-360.

- INPE - Instituto Nacional de Pesquisas Espaciais. 2015. *Tutoriais Geoprocessament*. <http://www.dpi.inpe.br/spring/portugues/tutorial/estatistica.htm>
- Jacinto, L. U. A. 2001. "Pecuária do futuro com a ajuda da irrigação." **Irrigação e Tecnologia Moderna** 51: 50-54.
- Kinnell, P. I. A. 2010. "Event soil loss, runoff and the Universal Soil Loss Equation family of models: a review." **Journal of Hydrology** 385: 384-397.
- Lana, X., Martínez, M. D., Burgueño, A., Serra, C., Martín-Vide, J., Gómez, L. 2006. "Distributions of long dry spells in the Iberian Peninsula, years 1951-1990." **International Journal of Climatology** 26: 1999-2021.
- Leão, M. G. A., Marques Júnior, J., Souza, Z. M. 2010. "Variabilidade espacial da textura de um latossolo sob cultivo de citros." **Ciência e Agrotecnologia** 34: 121-131.
- Magalhães Filho, F. J. C., Ayres, F. M., Sobrinho, T. A. 2014. "Integrando SIG e USLE para mapeamento da perda de solo em área de proteção ambiental." **Revista Agrarian** 7: 552-559.
- Martins, J. D., Carlesso, R., Aires, N. P., Gatto, J. G., Dubou, V., Fries, H. M., Scheibler, R. B. 2012. "Irrigação deficitária para aumentar a produtividade da água na produção de silagem de milho." **Irriga (UNESP Botucatu)** 1: 192-205.
- Martins, J. D., Rodrigues, C. G., Paredes, P., Carlesso, R., Oliveira, Z., Knies, A., Petry, M., Pereira, L. S. 2013. "Dual crop coefficients for maize in southern Brazil: Model testing for sprinkler and drip irrigation and mulched soil." **Biosystems Engineering** 115: 291-310. doi:10.1016/j.biosystemseng.2013.03.016.
- Miqueloni, D. P., Bueno, C. R. P., Ferraudo, A. S. 2012. "Análise espacial dos fatores da equação universal de perda de solo em área de nascentes." **Pesquisa Agropecuária Brasileira** 47, 1358-1367.
- Picoli, M. C. A., Lamparelli, R. A., Sano, E. E. 2012. "Imagens multipolarizadas do sensor Palsar/Alos na discriminação das fases fenológicas da cana-de-açúcar." **Pesquisa Agropecuária Brasileira** 47: 1307-1316.
- Pinheiro, H. S. K., Chagas, C. S., Carvalho Júnior, W., Anjos, L. H. C. 2012. "Modelos de elevação para obtenção de atributos topográficos utilizados em mapeamento digital de solos." **Pesquisa Agropecuária Brasileira** 47: 1384-1394.
- Pires, R.C. M., Arruda, F.B., Sakai, E., Calheiros, R. O., Brunani, O. 2008. "Agricultura Irrigada." **Revista Tecnologia & Inovação Agropecuária** 6: 98-111.
- Risso, J., Rizzi, R., Rudorff, B. F. T., Adami, M., Shimabukuro, Y. E., Formaggio, A. R., Epiphanyo, R. D. V. 2012. "Índices de vegetação Modis aplicados na discriminação de áreas de soja." **Pesquisa Agropecuária Brasileira** 47: 1317-1326.
- Rodrigues, G. C., Martins, J. D., Silva, F. G., Carlesso, R., Pereira, L. S. 2013. "Modelling economic impacts of deficit irrigated maize in Brazil with consideration of different rainfall regimes." **Biosystems Engineering** 116: 97-110.
- SABESP. 2015. *Companhia de Saneamento Básico do Estado de São Paulo*. <http://site.sabesp.com.br/site/Default.aspx>
- Thomas, A. L., Costa, J. A. 2010. *Soja: Manejo para alta produtividade de grãos*. Porto Alegre: Evangraf.
- USGS. 2004. *GLCF: Landsat GeoCover Mosaic. Global Land Cover Facility*, <http://glcf.umd.edu/data/mosaic/>

Vönösmarty, C. J.; Green, P.; Salisbury, J.; Lammers, R. B. 2000. "Global Water Resources: Vulnerability from Climate Change and Population Growth". **Science** 289: 283-288. DOI: 10.1126/science.289.5477.284

Weill, M. D. A. M., Sparovek, G. 2008. "Estudo da erosão na Microbacia do Ceveiro (Piracicaba, SP). I – Estimativa das taxas de perda de solo e estudo de sensibilidade dos fatores do modelo EUPS." **Revista Brasileira de Ciência do Solo** 32: 801-814.

Wischmeier, W. H., Smith, D. D. 1978. *Predicting rainfall erosion losses: a guide to conservation planning*. U.S. Department of Agriculture.

Yan, G., Mas, J. F., Maathuis, B. H. P., Xiangmin, Z., Van Dijk, P. M. 2006. "Comparison of pixel-based and object-oriented image classification approaches – a case study in a coal fire area, Wuda, Inner Mongolia, China." **International Journal of Remote Sensing** 27: 4039-4055.

## **ARTIGO III - SENSORIAMENTO REMOTO PARA MONITORAMENTO DE MILHO E SOJA IRRIGADOS POR PIVÔ-CENTRAL NO RIO GRANDE DO SUL**

### **Remote sensing for monitoring maize and soybean under center-pivot irrigation in Rio Grande do Sul**

Abstract - In this study, the Normalized Difference Vegetation Index (NDVI) generated from satellite images was applied to study the crop's growth cycle of soybean and maize in 28 center-pivot irrigated areas in Cruz Alta Region, RS, Brazil. The NDVI was computed from surface reflectance data of LANDSAT5/TM images for several dates throughout the crop cycle, using SPRING GIS - INPE software. The Analysis of Variance (ANOVA) and Tukey Honestly Significant Difference (HSD) test comparing the NDVI sets of values for each pivot showed a sensitivity of 0.02 NDVI units that was enough for the recognition of phenological stages of soybean and maize in a days after sowing (DAS) scale. The results allowed the determination of the following NDVI intervals: between 0 to 0.24 in soybean and 0 to 0.3 in maize for the initial period stages; between 0.24 to 0.81 in soybean and 0.3 to 0.71 in maize for the crop development stages; between 0.81 to 1.0 (soybean) and 0.71 to 1 (maize) for the mid-season period; between 0.81 to 0.3 (soybean) and 0.71 to 0.3 (maize) for the end season period. Crop monitoring and irrigation models can use this information for operational adjustment.

Index terms: phenology, Tukey, NDVI, SPRING GIS, Landsat.

#### **Introduction**

In southern Brazil, as in many other places in the world, irrigation management networks have been organized, driven by the traditional FAO56 methodology (Allen et al., 1998). According to this approach, the evapotranspiration from agricultural fields is estimated by multiplying the weather-based reference evapotranspiration ( $ET_o$ ) by a crop coefficient ( $K_c$ ), determined according to the crop type and the crop growth stage (Allen et al., 1998; Pereira et al., 2015a). However, there are typically some uncertainties regarding whether the crops conditions and growth are comparable to those represented by the  $K_c$  values tabulated. In addition, it is difficult to predict the correct crop growth stage dates for large populations of crops and fields (Allen & Pereira, 2009). That affects the accuracy of the input data for irrigation models like SIMDUALKc and AQUACROP used for irrigation management (Pereira et al., 2015b).

Remote sensing based approaches potentially enable timely estimation of crop water use for resource monitoring and irrigation scheduling adjustment (Hornbuckle et al., 2009; Johnson & Trout, 2012). A key advantage of remote sensing is the ability to monitor crop

development over time and space, and hence reducing the need for idealized growth stage assumptions or intensive field monitoring (Dengsheng, 2006; Mateos et al., 2013).

From this point of view, there is an increasing interest in mapping detailed phenological stages and cycles of vegetation by remote sensing, demanding a data quality adequate to the needs of irrigated crop management, monitoring of natural resources and water consumption regulation, among other applications (Calera et al., 2005; Dengsheng, 2006).

This work presents a case study of the application of NDVI calculated from Landsat imagery to detect the phenological stages of maize and soybean in pivot irrigated areas, its variability within crop fields and the time intervals used for irrigation management adjusted locally. The present work may contribute in defining important characteristics of space-assisted agricultural management specifically related to the use of NDVI to support local irrigation modeling and management. In particular, the sensitivity of NDVI for crop cycle description and for phenological stages detection is assessed for the specific conditions of central pivot irrigated maize and soybean in the study region.

## **Materials and Methods**

### **Study area**

The study area is located in Cruz Alta, in the northwestern part of the Rio Grande do Sul State, Brazil, between 28° 34' to 28° 45" S and 53° 30' to 53° 14' W (Figure 1). The geology is predominantly igneous rock, especially basalt, with the remaining soil developed from Botucatu's sand stone or mixture of this with basalt (Streck et al., 2008a). A typical soil in the region can be described as: Rhodic Hapludox (FAO) or Typic Haplorthox (US Soil Taxonomy), argillaceous and deep with an inclination of 1%.

This is a subtropical humid region, with mean annual precipitation of 1755 mm. Rainfall is distributed in the four seasons. Water stress occurs in the summer due to increased evaporative demand. Considering a 30 years series of data, the average monthly rainfall is 135 mm with standard deviation of 20 mm. The maximum temperature (37-38°C) occurs in



December to March and the minimum (0 to -4.5) occurs in May to September. Weather data is available from the National Institute of Meteorology (INMET), which has a station located inside the study site (28.63°S, 53.6°W and 472.5 m altitude). The region has a relatively high density of central pivot irrigated areas, 28 of which were selected for this work due to the presence of soybean or maize as planted crops. The area of the irrigated fields varied between 10 and 100 hectares and the plants density ranged from 70.000 to 75.000 plants ha<sup>-1</sup> for maize and 260.000 to 340.000 plants ha<sup>-1</sup> for soybean.

### **Remote sensing data and products**

The images used in this study were obtained from the TM (Thematic Mapper) sensor aboard Landsat 5 for path/row 222/80 and 223/80 which overlap in the study area. The dates of image acquisition considered in this study cover the period from January to December 2004, totalizing 12 images (Table 1).

The digital processing of the bands of Landsat 5 images for each date was done in SPRING software, version 5.2.6 (Câmara et al., 1996), with projection set to UTM system with reference to WGS84 datum. Image processing included geo-referencing adjustment to less than 0.5 pixel error, creation of image compositions for false color RGB543 combination, vector editing of pivot's limits, inspection of occurrence of clouds or image failures in the pivot areas, reflectance computation, atmospheric correction, classification for crop identification, NDVI calculation, descriptive statistics and thematic images production. Some routines in the internal processing language LEGAL were adapted for the execution of the procedure.

The conversion of digital numbers (DN) into radiance was made according to the procedure described by Markham & Barker (1987a). The calibration coefficients used for the conversion to reflectance was extracted from Chander et al. (2009); Markham & Barker (1987b). The atmospheric correction of the images was made according to Chavez (1996).

The NDVI was computed according to Rouse et al. (1974).

The average NDVI for each pivot was plotted against a temporal scale for the visualization of the crop cycle. Additionally, a first derivative analysis (Viña et al., 2004) was used to help in the determination of the NDVI intervals corresponding to the main stages of irrigated agriculture management defined by FAO 56. The NDVI sets of the pivots were then classified according to the intervals obtained in this work.

### **Field monitoring system information**

Field data referring to crop type, sowing date, phenological stage, plant height, planting density, soil moisture in different layers, soil physical characteristics, frequency and amount of irrigation, rain, and meteorological data (minimum humidity, wind speed, reference evapotranspiration) were obtained for some of the pivots from the database of a local enterprise dedicated to irrigation management and monitoring - Sistema Irriga® – that is related to the Federal University of Santa Maria (UFSM), Brazil, aimed to improve crop water irrigation management. Currently the system monitors more than 120.000 ha every year in different regions of Brazil.

Pivots number 09, 13 and 18 were planted with soybean during 2004/2005 growing season, and pivots number 04, 06, 08, 19, 25, 27 and 30 were cultivated with maize during the same growing season. A procedure of image classification for different dates was used for radiometric recognition of the crops planted in pivots where field information was not available. A supervised classification with the maximum likelihood algorithm was applied, and the pixels from pivots 04, 06, 08, 09, 13, 18, 19, 25, 27, and 30 were used as training set for the classification. Additionally, the qualitative analysis of the NDVI curve profile along the crop cycle (days of the year) showed a characteristic “fingerprint” that allowed identification of the crops and some cultivars. The cultivars of maize were identified as early

or late considering time for physiological maturity and time for flowering. No other specific information about the cultivars was available.

### **Phenology**

The phenological stages for soybean used were the Fehr & Canivess (1977) scale and for maize we used the scale proposed by Ritchie et al., (1986). The stages considered were the vegetative and reproductive stages, represented by V and R, respectively, followed by numerical indices that identify the specific stages. Emergency was designated as VE, and cotyledon stages for soybean were VC. The additional nomenclature V0 was used for pre-emergence stages. The sequential stages V1, V2, ..., Vn correspond to the number of vegetative nodes in soybean, and the number of leaves in maize.

To establish a relationship between NDVI and phenology, the average NDVI for each pivot, corresponding to a specific crop or cultivar were first plotted in a days after sowing (DAS) scale and adjusted by the coincidence of the rapid growth edge. This procedure diminishes the propagation of the uncertainty associated with the duration of the initial period to the average curve. Then a sigmoid curve was adjusted to the initial, rapid growth and mid-season periods. Analog sigmoid adjustment was made with the field height registers of each crop. Finally, the DAS, adjusted height, adjusted NDVI and phenological stage information of each crop were unified and consisted in a common time scale, selecting the most frequent stage for the set of pivots in each time period.

### **Sensitivity of the NDVI to phenological stage identification: Tukey difference**

The sensitivity of NDVI - minimum significative difference in NDVI as the plants grow - was calculated using the Tukey's Honestly Significant Difference Test (Tukey's HSD test) after analysis of variance (ANOVA). The results also included the probability (p-value) of the difference being obtained by random variation and not due to real differences in plant growth, under the selected confidence interval for the test (95%). For this analysis, the matrix

of the NDVI values per pixel for each pivot was exported and organized in columns corresponding to each pivot in each date. R statistical software was used (R D. C. T., 2011) for ANOVA and Tukey test execution, analyzing the significative differences between NDVI average values for different pivots in the same date, and also the same pivot in different dates.

The derivative of the NDVI vs DAS curve was used as a measure of the variation of the NDVI sensitivity with time. The derivative was calculated using the approximation  $(y_n - y_{n-1}) / (x_n - x_{n-1})$ . A positive/negative value indicated the amount of increase/decrease in NDVI per day, and the variability in this rate was analyzed in the time plot of the derivative.

### **Validation of the average curve and phenology model**

The leave one out cross-validation method was used to evaluate the reliability of the correlation between NDVI, DAS and phenological stage. In the application of this method the NDVI values of the complete cycle for each pivot were sequentially reserved for comparison with the values of the average curve, which represents the local model of crop cycle for a specific crop cultivar (Pereira et al., 2015a). Several indicators were used to evaluate the goodness of fit of the results: root mean square error (RMSE), regression coefficient forced through origin (b), determination coefficient ( $R^2$ ), ratio of RMSE to standard deviation (RSR), average absolute error (AAE), average relative error (ARE), percent bias (PBIAS), modelling efficiency (EF). For a discussion of the application of these goodness of fit indicators in irrigation modelling see Pereira et al. (2015b).

For the phenology comparison between the average model and the field specifications, the sequential stages of plant development were assigned with a number. The comparison between the numbers obtained in the average model and the ones from field determinations, corresponding to the same DAS, were then compared using the same indicators already mentioned.

## **Results and Discussion**

### **Geographic data base and image processing**

The complete set of NDVI thematic images (Figure 2) shows the temporal evolution of the NDVI values inside the pivots. The dates correspond to the satellite imaging day. The label maize or soybean appears in the dates in which the culture was present in the pivot, giving an idea of the extent of the cultural cycle. The presence of sectors in some pivots was generally associated to management processes as sowing or harvesting that were in progress in that date. Yet, pivots number 4, 27 and 30 were planted in only half the area with maize. These images were useful for checking the causes of anomalous behavior in NDVI average along time, and contributed to the adjustment of representative vectorial limits of the culture inside the pivot, which were essential for a precise calculation of the NDVI statistical parameters.

The identification of crops per pivot was done using the field information available for 10 pivots and through the results of the radiometric classification procedure and was further confirmed by the NDVI vs DAS profile recognition procedure. The maize crop was identified in pivots number 1, 2, 4, 6, 7, 8, 13, 15, 19, 21, 22, 25, 27, 30; and soybean crop in pivots number 5, 9, 11, 12, 14, 16, 17, 18, 20, 23, 24, 26, 28, 29. The cross-linking of the information from the different procedures allowed minimizing the uncertainty associated to the application of a single procedure.

### **Statistical processing of NDVI pixel's values**

The descriptive statistics applied to the NDVI values of the pixels in each pivot showed a reasonable Gaussian behavior and a maximum value of 0.1 for the standard deviation, compatible to results by Kamble et al. (2013) or Maxwell & Sylvester (2012).

As stated by Allen et al. (2005) referring to random errors associated with calculations derived from satellite images, the random error will tend to reduce in proportion to the square

root of the number of images processed and integrated in the calculations. The same reasoning is valid for pixels' integration or plants' integration in the calculation. According to this rule, as we generally have more than 100 independent pixels in each pivot image, the random error of the Pivot's NDVI will be reduced by a factor over 10 compared with individual pixels.

On the other hand, comparing to the phenology field characterization, which is made in individual plants, the random variation can be diminished by a factor equal to the square root of the number of plants integrated in the image of the pivot's area. Each pixel of the Landsat 5 TM images corresponds to 0.09 ha and contains the average radiometric signal of around 7000 to 8000 maize plants or 26000 to 34000 soybean plants. Applying the square root rule, we see that the procedure is likely to reduce the NDVI and phenology determination variability for maize by a factor between 84 to 89 and between 161 to 184 for soybean, comparing the information contained in one pixel with that of an individual plant, with an additional factor of more than ten times when considering the information of a typical pivot in the region.

These considerations support the possibility of higher NDVI sensibility for phenological stage monitoring of fields when compared with individual plant visualization or measurement.

### **ANOVA and Tukey Honestly Significant Difference Test**

The results of ANOVA test applied to the pivots allowed to conclude that the NDVI average values for the pivots were significantly different between image dates, with 95% confidence, and p-values  $\approx 0$ . The Tukey HSD test allowed determining the lowest significative difference between pivot's average NDVI values. The minimal time interval (between satellite images of 2004/11/23 and 2004/12/02) of 9 days corresponded to the minimum difference observed in this study between pivot's average NDVI values (ranging from 0.01 to 0.03 NDVI units with p-value of around  $3 \times 10^{-7}$ ). These results indicate that a

value of sensitivity of 0.02 units can be considered as an achievable limit of sensitivity for the differentiation of NDVI values in central pivot irrigated facilities for maize and soybean crops in sub-tropical climate. This can be interpreted as “growth sensitivity”, in the sense that two pivots with a difference in NDVI of 0.02 units can be considered to have a different growth state of the plants. This important conclusion could not be found clearly stated in the literature, but can also be deduced from the information of other authors (Hatfield & Mayers, 2010; Scanlon et al. (2002). This good sensitivity is favored by the greater uniformity of crop development in irrigated lands, and by the great number of pixels that can be averaged for the calculations.

### **NDVI vs DAS curves**

#### **Profile and sub-division of the curves**

From the average NDVI values for each pivot in different image dates, we could construct the individual NDVI vs DAS (days after sowing) curves for both soybean and maize. The profiles of the curves for the several pivots showed the same characteristics for the same cultivar of crop, as can also be observed in the work of Tasumi and Allen (2007) and Hatfield & Prueger (2010). Evident differences are visible between different cultivars of maize, as can be seen in Figure 3, where the time scale for each plot was already adjusted in a days after sowing base. The characteristic profiles seen for each crop in this study have also been observed in previous studies (e.g., Calera et al., 2004; Wang et al., 2016, Tasumi and Allen, 2007; Martin et al.,2007).

Cross-linking the NDVI profile information with field information, three cultivars of maize could be differentiated, some of them adapted for a shorter crop cycle. In the case of soybean, no field information was available for the identification of different cultivars. The maize early-flowering cultivar in Figure 3b) shows a decreasing positive slope (derivative) earlier than the late-flowering cultivars in Figure 3a) and 3c). The comparison of the periods

required to maturity is obscured due to the low frequency of satellite imaging in the late season.

The average NDVI values of the several soybean (or maize) pivots were used to obtain a representative curve, in a DAS time scale, typical of the regional agricultural practice (Figure 4). This curve can be used for monitoring purposes, as a reference to identify different growing patterns or stress (Wang et al., 2016). Or can also be associated with the phenological information obtained from the field monitoring database of the irrigation management system that operates in the study region. The results are shown in Figure 4 a) and 4 b) for soybean and maize, respectively, and are compatible with the study of Hatfield & Prueger (2010) or Martin et al. (2007).

One important observation is that the curves are smooth and monotonic, without noise, in all cases (Figure 4a and 4b), with clear features and sensitivity enough for the visual recognition of the growth periods and important points for crop management, e.g., the typical 60 days after sowing detasseling event of maize, which was clearly visible in all individual curves and the average curve in Figure 4b. Tasumi and Allen (2007) found similar curves when about 3095 irrigated fields were analyzed. Other studies had even used filters with monotonic criteria to eliminate low quality data (Wang et al., 2016).

### **Phenology and NDVI**

The phenologic stage information from field monitoring was organized and consisted in a DAS scale for each type of crop. This scale allowed the evaluation of the sensitivity of NDVI for phenology differentiation. The graph showing the NDVI vs DAS curve in conjunction with the phenological stages is presented in Figure 4. The results are compatible with the ones from Hatfield & Prueger (2010), Martin et al. (2007) and Raun et al. (2005).

The height of the plants, adjusted to a sigmoid, was considered as an intermediate calibration parameter because of its correlation with the phenological stages, and as a



quantitative field determined variable to help in the determination of the daily stages and the internal consistency of the information.

The results presented in Figure 4 indicate that a growth sensitivity of 0.02 for the differentiation of NDVI from pivots allows the detection of all the phenological states. Obviously, the smaller intervals corresponding to the first vegetative stages (VE, VC, V1-V3), have higher probability of confusion as they correspond to five different stages with low NDVI variation and short time interval. Other vegetative stages (V4-V9) correspond to NDVI variation much larger than the sensitivity and can be more easily resolved. For the reproductive stages, as the NDVI initiates a tendency to remain constant, during the so called mid-station period, the identification of the phenological stage is dependent on the DAS value, in particular with reference to the beginning of the reproductive period. That means that the knowledge of the DAS corresponding to the beginning of the reproductive phase can be used for the identification of the phenological stages during the mid-season, in conjunction with the NDVI value. In this sense, it is a 2 variables function: Phenology = function (NDVI, DAS). Previous studies, e.g. Viña et al., (2004) or Hatfield & Prueger (2010) have also reported high variation of NDVI with time when the vegetation is green at moderate to high height, as found during vegetative (V4-V9), while in the period of maximum canopy expression, as in the reproductive stages, the variation is lower.

### **FAO56 Irrigation management stages**

To improve the ability to identify the key points that separate the intervals that should be defined for FAO56-like irrigation approach we can use the derivative of the NDVI vs DAS curve, as shown in Figure 5. It shows the magnitude and sign of the variation of the NDVI value per day for soybean and maize. This can also be seen as a “temporal sensitivity” of NDVI, in (NDVI units)/day. As the derivative is the slope of the curve, we can clearly differentiate 4 time intervals: the initial period with a horizontal plane slope, the growing

period with a positive and high value of the slope, the mid-season with a nearly horizontal slope but with possible up-down features, and the end-season with a high negative slope. Other studies (e.g., Viña et al., 2004) have also used first derivative analysis for the detection of phenology variation.

The initial period is characterized by a low NDVI value and a zero or low value of the derivative. As the end of the initial period is defined by a 10% of vegetation cover, we can consider an increase of 10% of the total NDVI variation as reasonable end value criteria for the initial period, together with a low value of the derivative, and the same criteria was used for the other limits. The rapid growth period is characterized by the maximum positive derivative of around  $0.015 \sim 0.02$  NDVI/day. This value of maximum variation of NDVI per day obviously allows better phenological stages discrimination, improving the time resolution of the model. The mid-season is characterized by an almost null derivative, with almost constant NDVI around its maximum value, which can be sensible to management operations or plant variations. In this region, any NDVI variation of more than 0.02 would appear as transitory negative or positive variations in the value of the derivative, as can be seen in the “detasseling peak” in Figure 5. The end-season is initiated by the senescence, and is represented by a constant decline in the NDVI which derivative is less significative because it is highly dependent on the imaging frequency in the period. From the above criteria, the NDVI intervals determined for soybean and maize for the several periods of crop management, in the region of study, are presented in Table 3.

The definition of these intervals, derived from NDVI information of the local pivots, have the advantage of being adjusted to the local crop, soil and climate characteristics, when compared to the general guides of FAO56, for example. This can permit a higher accuracy in the definition of the intervals, which can improve the quality of the input data used in irrigation management models and potentially improve the accuracy of strategic outputs like

irrigation constants or evapotranspiration (e.g., Tasumi & Allen, 2007; Pôças et al., 2015). Remote sensing techniques associated with a GIS environment are a powerful tool to improve agricultural management (Bastiaanssen et al., 2000), and the connection between NDVI and phenology can be explored for this purpose. The predicted daily variation of NDVI, also of around 0.02 (NDVI units/day), show the possibility of detecting almost daily variations in plant growth with this method, provided the NDVI information could be acquired in a daily basis.

We shall make a comment, in this point, about the saturation of NDVI that is generally accepted to happen over a leaf area index (LAI) value of 4 that corresponds to mid-season period saturation. The lower sensitivity of the NDVI in this period can be overcome, for operational monitoring purposes, with the use of the DAS variable of the Phenology (NDVI, DAS) calibrated function. The development of new leaves in the crop, for example, would not change the NDVI value in that saturated region, but the DAS variable can be fine tuned with phenology through the sharp rapid growth period and through the variation of slope due to reproductive stages in the beginning of the mid-season. On the other hand, for irrigation applications regarding crop basal coefficient ( $K_{cb}$ ) calculation, the saturation effect is less important as the  $K_{cb}$  also saturates in the same LAI interval (Duchemin et al., 2006).

### **Validation of the phenology general calibration curve**

The goodness of fit parameters for some representative pivots, comparing the individual NDVI curves and the average curve with the average fit are shown in Table 4.

As an average, for the crops analyzed (soybean; maize), we can conclude that the pivots' indicators behave almost linearly ( $b=0.99$ ), with a 97 to 99 percent of the variation observed in the individual curves registered in the average curve as shown by  $R^2=(0.97;0.99)$ . The root mean square error of around 4% ( $RMSE=(0.03; 0.04)$ ), and its quotient with the standard deviation, RSR, show a reasonable low value ( $RSR=(0.036;0.06)$ ). Similar

conclusions arise from the errors, being especially clear in the absolute relative error, ARE of the individual pivots and the average values around 7%. Similar research for comparison could not be found in the literature for soybean and maize in irrigated fields. The quality of the correlation could have been further improved through the use of an additional normalization both of the pivot's NDVI (eliminating the base variation with  $NDVI_{norm} = (NDVI - NDVI_{min}) / (NDVI_{max} - NDVI_{min})$ ), and with a days after emergence (DAE) scale, however, it was preferred the choice of using typical local values of NDVI, adjusted to the regional agricultural practice.

For the comparison of the field phenology and the model prediction, the parameters of Table 5 indicate a good adjustment, with  $R^2 = 0.92$  and relative error ARE = 11.95% for soybean, or  $R^2 = 0.94$  and relative error ARE = 13.48% for maize. The other parameters confirm this tendency.

### **GIS Thematic Maps for Crop Stage Monitoring**

As an application of the NDVI FAO56-like-intervals for irrigation management as defined in Table 3 for soybean and maize, we can obtain, in GIS environment, the resulting thematic maps of crop stage for each pivot as shown in Figure 6 for three dates during the 2004/2005 growing season. In this figure we can see the crop development stage that is predominant in each pivot as well as its spatial distribution, giving useful information for site-specific management decisions related with irrigation.

The phenology(NDVI, DAS) general relationships established for the region appear valuable for monitoring the phenology in a DAS scale, which is important for management purposes. As crop development depends on temperature and photoperiod and the genetic response to these environmental factors (Thomas & Costa, 2010; Tojo Soler et al., 2005), the phenology (DAS) curve can have considerable uncertainty. This statement does not apply to

the phenology (NDVI) relationship, that can be considered independently from DAS and has lower uncertainty, as discussed in this work.

In other words, a general reference curve relating phenological stages with DAS may not fulfill the requirements of accuracy necessary for good agricultural management if it is not adjusted with local information, making it necessary extensive and expensive field monitoring for decision support (Gitelson et al., 2012). The phenological stages may not be easily determined in a field basis due to the presence of a distribution of stages that will be found in any field (Streck et al., 2008b; Risso et al., 2012). The stage to be considered for management purposes in a field will generally be defined by the prevalence of 50 % of the plants, and this evaluation can increase the operational costs of field work due to its characteristics (Thomas et al., 2010).

According to Bastiaanssen et al. (2000), remote sensing has several advantages over field measurements. First, measurements derived from remote sensing are objective; they are not based on opinions. Second, the information is collected in a systematic way which allows time series and comparison between schemes. Third, remote sensing covers a wide area such as entire river basins. Ground studies are often confined to a small pilot area because of the expense and logistical constraints. Fourth, information can be aggregated to give a bulk representation, or disaggregated to very fine scales to provide more detailed and explanatory information related to spatial uniformity. Fifth, information can be spatially represented through geographic information systems, revealing information that is often not apparent when information is provided in tabular form. These considerations remark the interest of this work to analyze the contribution to agricultural management that could be achieved by means of a NDVI locally adjusted relationship that could associate the phenological stages and DAS between adequate operational limits.

## Conclusions

1) A locally calibrated phenology (NDVI, DAS) function, with sensitivity of 0.02 NDVI units was obtained for the recognition of phenology, allowing the phenological stage monitoring and the determination of the periods recommended by FAO56 irrigation management schedule. The intervals of NDVI values per period were obtained: between 0.17 to 0.24 in soybean and 0.21 to 0.3 in maize for the initial period stages; between 0.24 to 0.82 in soybean and 0.3 to 0.71 in maize for the crop development stages; between 0.81 to 1.0 (soybean) and 0.71 to 1 (maize) for the mid season period; between 0.81 to 0.3 (soybean) and 0.71 to 0.3 (maize) for the end season period.

2) A local average NDVI vs DAS curve for a certain cultivar with average error (ARE) around 7% or less can be determined and used as information input for irrigation planning and modeling. These curves also showed a kind of fingerprint of the local crop varieties and agricultural management habits.

3) The functional relation between Phenology, NDVI and time for the pivots in the study region could model the phenology with an average relative error, ARE ~ 12% for soybean and ARE ~ 13% for maize, with a coefficient of variation  $R^2=92\%$  and  $94\%$  respectively. The final precision and accuracy are dependent on the quality of the field phenology monitoring during the calibration period of this function for a specific crop variety. The absolute error was around 1 phenological stage for both crops.

4) As the Phenology (NDVI, DAS) curve has a slope of 0.015 ~ 0.02 NDVI units/day during the vegetative growth in the crop development period, a daily NDVI monitoring can potentially detect significant differences in that period that could trigger management procedures. This is less probable with satellite data, but can be feasible using unmanned aerial vehicles equipped with sensors (Tojo Soler et al., 2005).

5) The last statement is also valid for the reproductive stages during the mid-season period, even though the slope is around zero and NDVI saturates with regards to LAI. In fact, any variation in NDVI greater than 0.02 can be detected in any growth period. For example, the detasseling management operation produced a variation of around 0.06, clearly discriminated in the individual and general curves for maize.

6) The uniformity of central pivot irrigated fields ( $\sigma < 0.1$ ), and the great number of plants per pixel, and pixels per pivot, reduce the random NDVI error in a factor between 840 to 890 for maize and between 1610 to 1840 for soybean, playing an important role in the precision of 0.02 obtained in the pivots' average NDVI measurements.

7) The results are appropriate for its use in GIS environment, where thematic maps of the different phenological stages can be readily prepared.

8) With the advent of unmanned aerial vehicles, together with satellite information and modeling, these results show a promissory future for assisting crop monitoring and irrigation management.

### References

- ALLEN, R. G.; PEREIRA, L. S. Estimating crop coefficients from fraction of ground cover and height. **Irrigation Science**, v.28, p. 17-34. 2009.
- ALLEN, R. G.; PEREIRA, L.; RAES, D.; SMITH, M.. FAO Irrigation and drainage paper No. 56. **FAO, Food and Agriculture Organization of the United Nations**, p. 26-40. Rome. 1998.
- ALLEN, R. G., TASUMI, M., MORSE, M., TREZZA, R. A Landsat-based energy balance and evapotranspiration model in Western US water rights regulation and planning. **Irrigation and Drainage Systems** 19: 251-268. 2005. doi: 10.1007/s10795-005-5187-z.
- BASTIAANSEN, W.G.M.; MOLDEN, D. J.; MAKIN, I. W. Remote sensing for irrigated agriculture: examples from research and possible applications. **Agricultural Water Management**, v. 46, p. 137-155. 2000.
- CALERA, A.; GONZÁLEZ-PIQUERAS, J.; MELIA, J. Monitoring barley and corn growth from remote sensing data at field scale. **International Journal of Remote Sensing**, v.25 p. 97-109, 2004.
- CALERA, A. B.; JOCHUM, A. M.; CUESTA, G. A.; MONTORO, A. L. Irrigation management from space: towards user-friendly products. **Irrigation Drainage**, v.19, p. 337-353, 2005.

CÂMARA, G.; SOUZA, R. C.; FREITAS, U. M.; GARRIDO, J. C. Intergrating remote sensing and GIS by object-oriented data modeling. **Computers & Graphics**, v. 20 (3), 395-403, 1996.

CHANDER, G.; MARKHAN, B. L.; HELDER, D. L. Summary of current radiometric calibration coefficients for Landsat MSS, TM, ETM+, and EO-1 ALI sensors. **Remote Sensing of Environment**, v.113, p. 893-903, 2009.

CHAVEZ, J. Image-based atmospheric corrections – revisited and improved. **Photogrammetric Engineering and Remote Sensing**, v.62(9), p. 1025-1036, 1996.

DENGSHENG, L. Irrigation management from space: towards user-friendly products **International Journal of Remote Sensing**, v.19, p. 1297-1328, 2006.

DUCHEMIN, B.; HADRIA, R.; ERRAKI, S.; BOULET, G.; MAISONGRANDE, P.; CHEHBOUNI, A.; ESCADAFAL, R.; EZZAHAR, J.; HOEDJES, J. C. B.; KHARROU, M. H. Monitoring wheat phenology and irrigation in Central Morocco: On the use of relationships between evapotranspiration, crops coefficients, leaf area index and remotely-sensed vegetation indices. **Agricultural Water Management**, v. 79, p. 1-27, 2006.

FEHR, W. R.; CANIVESS. **Stages of soybean development**. (D. o. Technology, Ed.) Ames: Iowa State University, 1977.

GITELSON, A. A.; PENG, Y.; MASEK, J. G.; RUNDQUIST, D. C.; VERMA, S.; SUYKER, A.; BAKER, JOHN M.; HATFIELD, J. L.; MEYERS, T. Remote estimation of crop gross primary production with Landsat data. **Remote Sensing of Environment**, v. 121, p. 404-414, 2012.

HATFIELD, J. L.; PRUEGER, J. H. Value of using different vegetative indices to quantify agricultural crop characteristics at different growth stages under varying management practices. **Remote Sensing**, v. 2, p. 562-578, 2010.

HORNBUCKLE, J. W.; NICHOLAS, J. C.; EVAN, W.; CHRISTEN, T.-M. S.; WILLIAMSON, B. Irrigation water management by satellite and SMS - A utilization framework. **Report CSIRO**. 2009.

JOHNSON, L. F.; TROUT, T. J. Satellite NDVI Assisted Monitoring of Vegetable Crop. **Remote Sensing**, v.4(2), p. 439-455, 2012. DOI:10.3390/rs4020439

KAMBLE, B.;IRMAK, A.; HUBBARD, K. Estimating Crop Coefficients Using Remote Sensing-Based Vegetation Index. **Remote Sensing**, v.5, p. 1588-1602, 2013. DOI:10.3390/rs5041588.

MARKHAM, B. L.; BARKER, J. L. Radiometric Properties of U.S. processes Landsat MSS data. **Remote Sensing of Environment**, v.17, p. 39-71, 1987a.

MARKHAM, B. L.; BARKER, J. L. Thematic Mapper bandpass solar exoatmospherical radiances. **International Journal or Remote Sensing**, v.8(3), p. 517-523, 1987b.

MARTIN, K. L.; GIRMA, K.; FREEMAN, K. W.; TEAL, R. K.; TUBANA, B.; ARNALL, D. B.; CHUNG, B.; WALSH, O.; SOLIE, J. B.; STONE, M. L. Expression of variability in corn as influenced by growth stage using optical sensor measurements. **Agronomic Journal**, v. 99, p. 384-389. 2007

MATEOS, L.; GONZÁLEZ-DUGO, M. P.; TESTI, L.; VILLALOBOS, F. J. Monitoring evapotranspiration of irrigated crops using crop coefficients derived from time series of satellite images. I. Method. **Agricultural Water Management**, v.125, p. 81-91, 2013.



- MAXWELL, K.S.; SYLVESTER, M. K. Identification of “ever-cropped” land (1984–2010) using Landsat annual maximum NDVI image composites: Southwestern Kansas case study. **Remote Sensing Environment**, v. 121, p. 186-195, 2012.
- PEREIRA, LUIS S., ALLEN, G. RICHARD, SMITH, MARTIN, RAES, DIRK. Crop evapotranspiration estimation with FAO56: Past and future. **Agricultural Water Management** v. 147, p. 4-20. 2015a.doi:10.1016/j.agwat.2014.07.031.
- PEREIRA, L. S.; PAREDES, P.; RODRIGUES, G. C.; NEVES, M. Modeling malt barley water use and evapotranspiration partitioning in two contrasting rainfall years. Assessing AquaCrop and SIMDualKc models. **Agricultural Water Management**, v.159, p. 239-254, 2015b.
- PÔÇAS, I.; PAÇO, T.A.; PAREDES, P.; CUNHA, M.; PEREIRA, L.S. Estimation of Actual Crop Coefficients Using Remotely Sensed Vegetation Indices and Soil Water Balance Modelled Data. **Remote Sensing**, p. 1-29, 2015.
- RAUN, W.R., SOLIE, J.B.; MARTIN, K.L.; FREEMAN, K.W.; STONE, M.L.; JOHNSON, G.V.; MULLEN, R.W. Growth stage, development, and spatial variability in corn evaluated using optical sensor readings. **J. Plant Nutr**, v. 28, p.173-182. 2005.
- R, D. C. T. (2011). A language and environment for statistical computing. **R Foundation for statistical computing**. Vienna, Austria.
- RISSE, J.; RIZZI, R.; RUDORFF, B.F.T.; ADAMI, M.; SHIMABUKURO, Y.E.; FORMAGGIO, A.R.; EPIPHANIO, R.D.V. Índices de vegetação Modis aplicados na discriminação de áreas de soja. **Pesquisa Agropecuária Brasileira**, v. 47, p. 1317-1326, 2012.
- RITCHIE, S. W.; HANWAY, J. J.; BENSON, G. O. **How a Corn Plant Develops**. Iowa State University of Science and Technology Cooperative Extension Service, Ames, Iowa, Special Report No. 48, p. 1-21. 1997 (reprinted).
- ROUSE, J. W.; HAAS, R. H.; SCHELL, J. A.; DEERING, D. W. Monitoring Vegetation Systems in the Great Plains with ERTS. In: Third Earth Resources Technology Satellite-1 Symposium. **Proceedings**. Greenbelt: NASA, 1974.
- SCALON, T. M.; ALBERTSON, J. D; CAYLOR, K. K.; WILLIAMS, C. A. Determining land surface fractional cover from NDVI and rainfall time series for a savanna ecosystem. **Remote Sensing of Environment**, v. 82, p. 376-388. 2002.
- STRECK, E.V.; KAMPF, N.; DALMOLIN, R. S.; KLAMT, E.; NASCIMENTO, P. C.; SCHNEIDER, P. **Solos do Rio Grande do Sul**. Porto Alegre: EMATER/RS, 2008a. 222p. (UFRGS. Departamento de Solos. Faculdade de Agronomia).
- STRECK, N.A.; LAGO, I.; GABRIEL, L.F.; SAMBORANHA, F.K. Simulating maize phenology as a function of air temperature with a linear and a nonlinear model. **Pesquisa Agropecuária Brasileira**, v. 43, p.449-455, 2008b.
- TASUMI, M.; ALLEN, R. G. Satellite-based ET mapping to assess variation in ET with timing of crop development. **Agricultural Water Management**, v.88, p. 54-62, 2007.
- THOMAS, A. L; COSTA, J. A. **Soja: Manejo para alta produtividade de grãos**. Porto Alegre: Evangraf, 2010. 248p.
- TOJO SOLER, C. M.; SENTELHAS, P. C; HOOGENBOOM, G. Thermal time for phenological development of four maize hybrids grown off-season in a subtropical environment. **Journal of Agricultural Science**, v. 143, p. 169-182, 2005.

VIÑA, A.; GITELSON, A.; RUNDQUIST, D.; KEYDAN, G.; LEAVITT, B.; SCHEPER, J. Monitoring Maize (*Zea mays* L.) Phenology with Remote Sensing. **Agronomy Journal**, v. 96, p. 1139-1147, 2004

WANG, R.; CHERKAUER, K.; BOWLING, L. Corn Response to Climate Stress Detected with Satellite-Based NDVI Time Series. **Remote Sensing**, v. 8, p. 1-22. 2016.

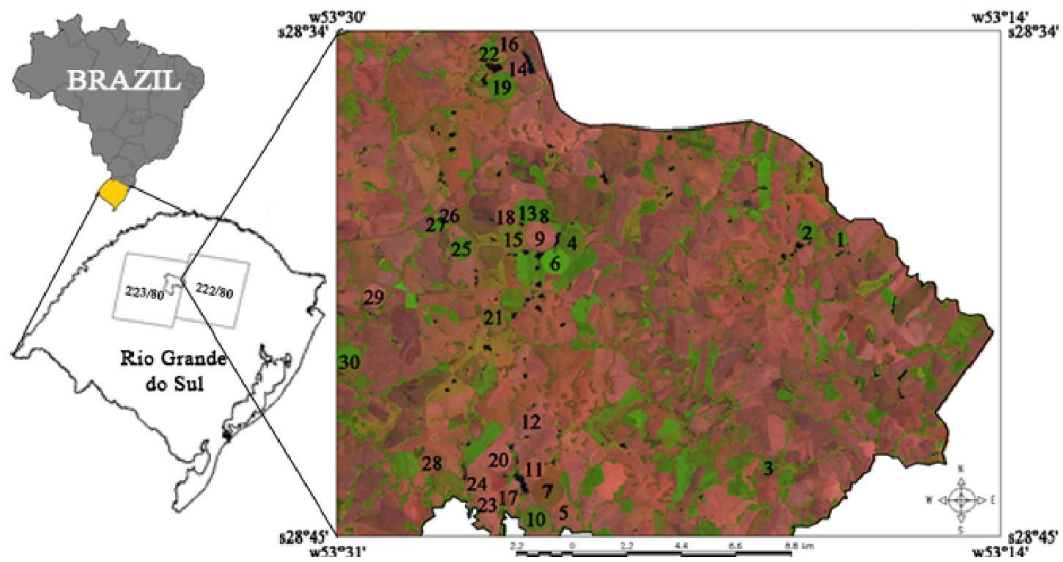


Fig 1. Location and number of the centered pivots in Cruz Alta, Rio Grande do Sul, Brazil. The Landsat paths 222 and 223 row 80 overlap in the region.

Tab 1. Information of the path and date (for row 80) of the Landsat5/TM images analyzed.

<b>Date</b> <b>2004/2005</b>	4/9	29/9	6/10	15/10	7/11	23/11	2/12	18/12	26/1	27/2	8/3	2/5
<b>Path</b>	223	222	223	222	223	223	222	222	223	223	222	223
<b>Day of Year</b>	248	272	280	289	312	328	337	353	26	58	67	122

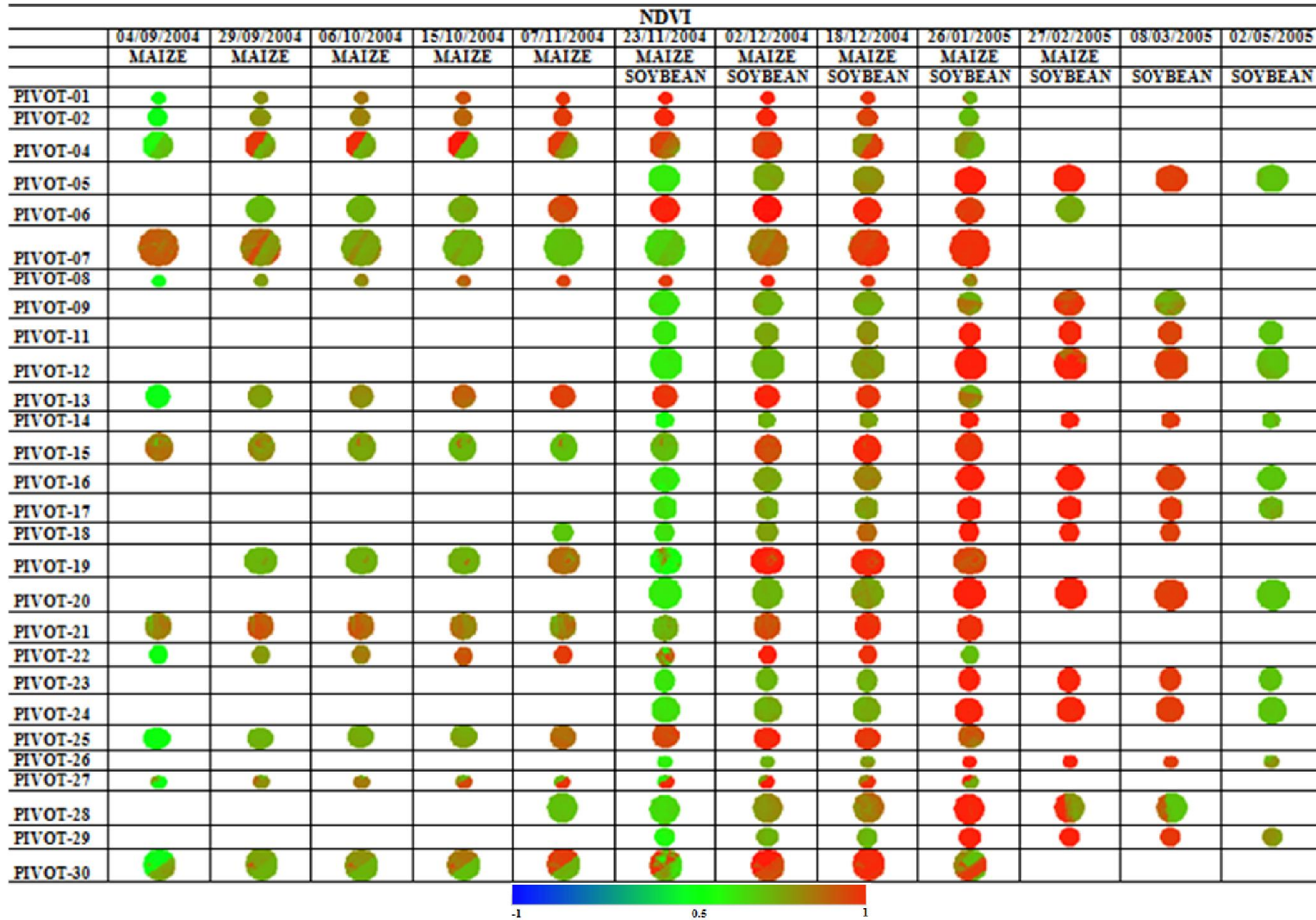


Fig 2. Thematic maps resulting from the NDVI values during the crop cycle.

Tab 2. Exemplification of the output of Tukey's HSD tests for the identification of significative differences between pivots' average NDVI. "Date" includes the dates of the pair of images compared; "diff" shows the corresponding difference between the average NDVI of the pivot's pixels in each date; "lwr" and "upr" are the 95% probability limits, and p value is the probability of the difference being due to randomness. All dates showed significant difference in NDVI.

<b>Date</b>		<b>diff</b>	<b>lwr</b>	<b>upr</b>	<b>p value</b>
18/12/2004	08/03/2005	-0.08	-0.09	-0.07	0.E+00
21/12/2004	08/03/2005	-0.15	-0.16	-0.14	0.E+00
23/11/2004	08/03/2005	-0.17	-0.18	-0.16	0.E+00
26/01/2005	08/03/2005	0.46	0.45	0.47	0.E+00
27/02/2005	08/03/2005	0.31	0.30	0.32	0.E+00
02/12/2004	18/12/2004	-0.07	-0.08	-0.06	0.E+00
23/11/2004	18/12/2004	-0.09	-0.10	-0.08	0.E+00
26/01/2005	18/12/2004	0.54	0.53	0.55	0.E+00
27/02/2005	18/12/2004	0.39	0.38	0.40	0.E+00
23/11/2004	02/12/2004	-0.02	-0.03	-0.01	3.E-07
26/01/2005	02/12/2004	0.61	0.60	0.62	0.E+00
27/02/2005	02/12/2004	0.46	0.45	0.47	0.E+00
26/01/2005	23/11/2004	0.63	0.62	0.64	0.E+00
27/02/2005	23/11/2004	0.48	0.47	0.49	0.E+00
27/02/2005	26/01/2005	-0.15	-0.16	-0.14	0.E+00

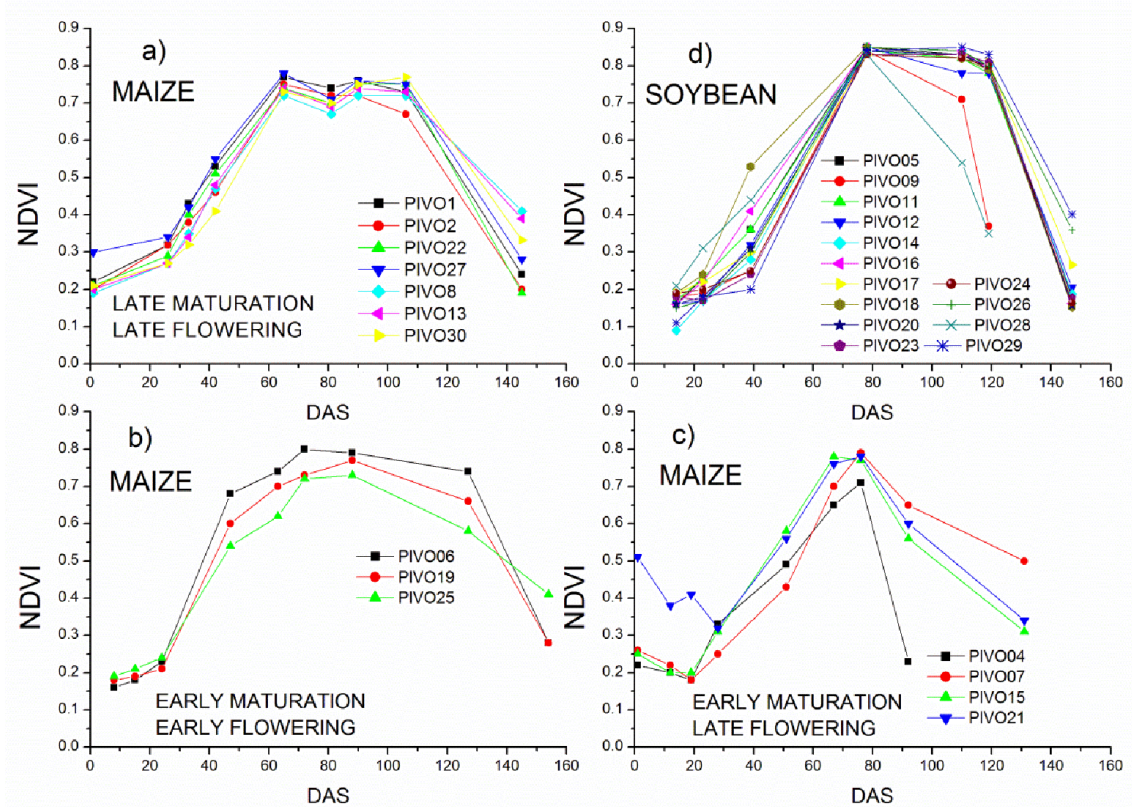


Fig 3. NDVI profile for maize and soybean along the crop cycle (Days After Sowing, DAS). Crop cycles for three maize cultivars and for soybean are registered in the NDVI vs DAS plots corresponding to the irrigated central pivots. The cultivars differ in the time needed for maturation and flowering, classified as early or late. The profile can be considered as a fingerprint of the crop and used for recognition, modeling and management purposes.

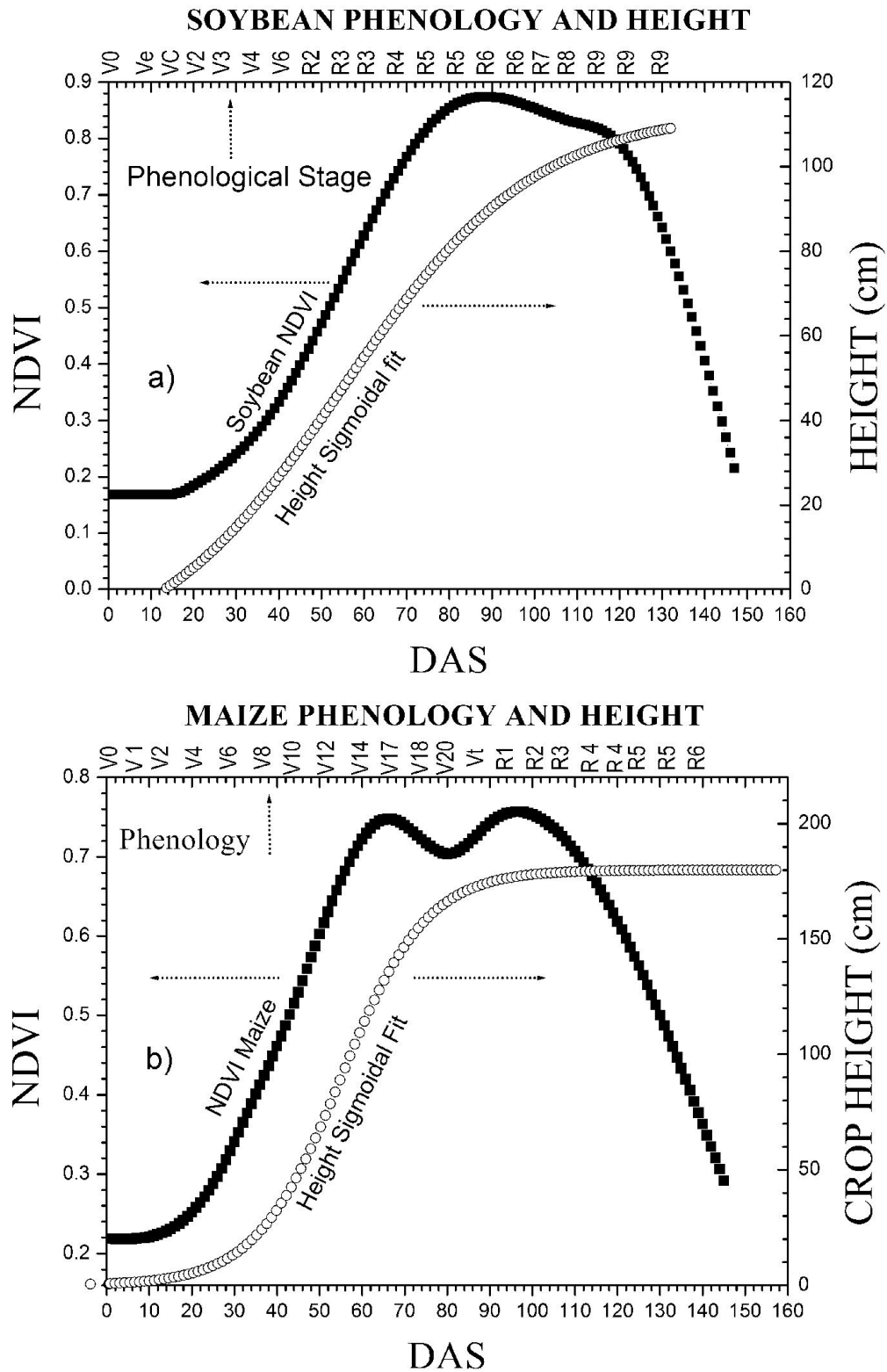


Fig 4. Relation between NDVI, Phenology, Height and Days After Sowing for Soybean a) and maize b). The field height data was adjusted to a sigmoid, and consisted with the phenology and NDVI as a function of DAS.

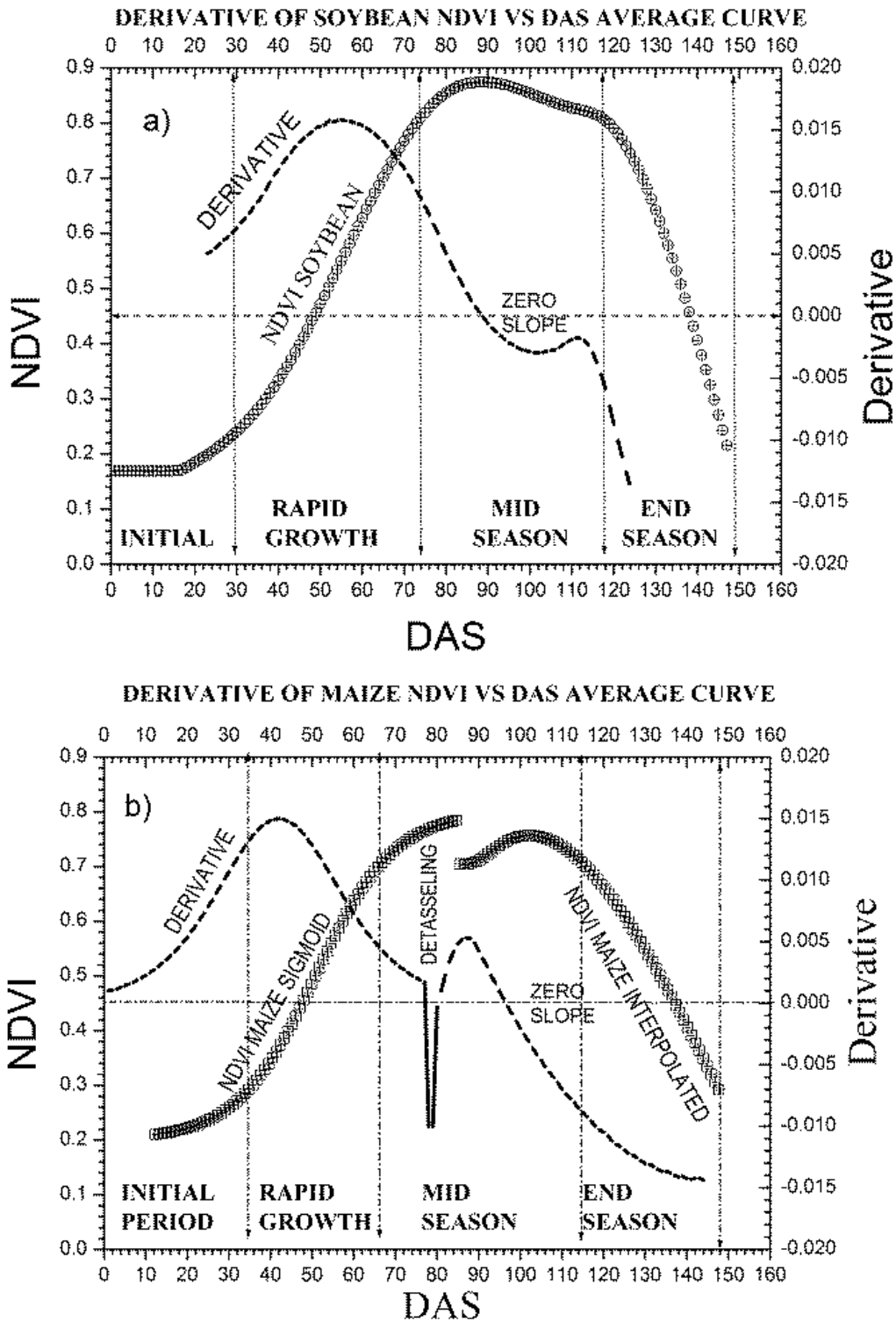


Fig 5. The first derivative analysis helps in the definition of the stages of the crop cycle. NDVI Derivative maxima can indicate a point of inflexion in plant development, as well as a near zero derivative indicates a stable situation or saturation. The detasseling procedure in maize appeared as a sharp peak in the derivative, once the NDVI growing edge was adjusted to a sigmoid and extrapolated to the date of the next satellite image.



Tab 3. NDVI intervals for development periods determined for soybean and maize.

Period	Soybean NDVI Interval	Days Interval	Maize NDVI Interval	Days Interval
Bare soil	0 to 0.17	variable	0 to 0.21	variable
Initial	0.17 to 0.24	30-0=30	0.21 to 0.3	25-0=25
Crop development	0.24 to 0.82	74-30=44	0.3 to 0.71	58-25=33
Mid season	0.81 to 1	118-74=44	0.71 to 1	109-58=51
Late season	0.81 to 0.3	144-118=26	0.71 to 0.3	145-109=36
Harvesting	<0.3	variable	<0.3	variable

Tab 4. Statistical indicators for the comparison of the average curve with the individual pivots' curve.

SOYBEAN										
	b	R <sup>2</sup>	RSR	PBIAS	RMSE	EF	d	E <sub>max</sub>	AAE	ARE
Pivot 05	1.01	1	0.03	-2.7	0.02	0.99	1	0.06	0.01	5.65
Pivot 11	1	0.99	0.032	-1.4	0.03	0.99	1	0.05	0.02	7
Pivot 12	0.98	0.99	0.032	1.6	0.03	0.99	1	0.05	0.02	5.96
Pivot 14	1	1	0.037	2.7	0.03	0.99	1	0.07	0.02	9.74
Pivot 16	1.02	0.98	0.052	-3.5	0.04	0.98	1	0.11	0.03	0.95
Pivot 17	1.01	0.99	0.044	-3.9	0.04	0.99	1	0.09	0.02	11.4
Pivot 20	1	1	0.014	1.1	0.01	1	1	0.02	0.01	3.77
Pivot 23	0.99	0.99	0.035	2.5	0.03	0.99	1	0.07	0.02	6.95
Pivot 24	0.99	0.99	0.033	1.7	0.03	0.99	1	0.06	0.02	7.79
AVRGE	0.99	0.99	0.036	-0.28	0.03	0.99	0.99	0.07	0.03	6.55
MAIZE										
	b	R <sup>2</sup>	RSR	PBIAS	RMSE	EF	d	E <sub>max</sub>	AAE	ARE
Pivot 1	1.04	0.98	0.053	-3.8	0.03	0.97	0.99	0.05	0.03	6.97
Pivot 2	0.97	0.98	0.058	3.1	0.04	0.97	0.99	0.08	0.03	6.51
Pivot 8	0.98	0.95	0.075	1.2	0.05	0.95	0.99	0.13	0.03	9.42
Pivot 13	1	0.97	0.061	-0.1	0.04	0.97	0.99	0.11	0.02	7.18
Pivot 15	1.06	0.98	0.042	-0.7	0.03	0.98	1	0.05	0.02	6.23
Pivot 22	1	0.98	0.054	0.3	0.03	0.97	0.99	0.09	0.02	5.5
Pivot 27	1.05	0.99	0.072	-7.1	0.05	0.95	0.99	0.09	0.04	10.6
Pivot 30	0.99	0.97	0.06	1.6	0.04	0.97	0.99	0.07	0.03	6.96
AVRG	0.99	0.98	0.06	-1.54	0.04	0.97	0.99	0.09	0.03	8.11

Tab 5. Validation of the phenology calibration.

SOYBEAN										
	b	R <sup>2</sup>	RSR	PBIAS	RMSE	EF	d	E <sub>max</sub>	AAE	ARE
		0.9								
AVRGE	1.05	2	0.040	-4.9	1.46	0.90	0.98	2.00	0.92	11.95
MAIZE										
	b	R <sup>2</sup>	RSR	PBIAS	RMSE	EF	d	E <sub>max</sub>	AAE	ARE
AVRG	0.98	0.94	0.021	2.2	2.33	0.94	0.98	1.00	1.46	13.48

## SPATIAL DISTRIBUTION MAP OF DEVELOPMENTAL STAGES OF AGRICULTURAL CROPS

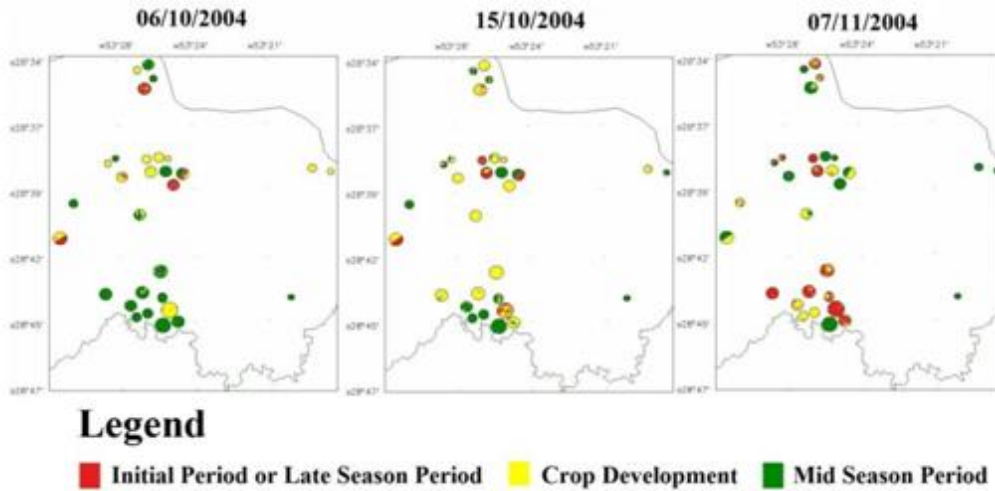


**Figure 6.** Thematic Map of Phenology for Irrigation Management. Distribution of NDVI classes for soybean and maize crops, obtained through satellite images for 28 center pivot irrigation sites in Cruz Alta, RS, Brazil. The red color corresponds to the “initial period” of early vegetative growth or to the “late season period” of physiological maturity; yellow corresponds to “crop development period” of active crop growth; while the green colors represent NDVI values which correspond to “mid season period” of stable growth phase (see Table 3).

## ARTIGO IV - ASSIMILAÇÃO DO NDVI PARA A ESTIMATIVA DE COEFICIENTES DE CULTURA BASAIS PARA SOJA E MILHO IRRIGADOS POR PIVÔS CENTRAIS NO SUL DO BRASIL

### Assimilation of NDVI to estimate basal crop coefficients for soybean and maize under central pivot irrigation in southern Brazil

#### ABSTRACT

In the last two decades, different approaches have been developed and implemented for estimating  $K_c$  or  $K_{cb}$  directly from vegetation indices (VI) and these approaches have been based on the classical FAO 56 dual crop method. This study aimed to determine the  $K_{cb}$  for the corn and soybeans crops cycle using NDVI (Normalized Difference Vegetation Index) in twenty-eight (28) irrigated areas, with fourteen (14) fields grown with maize and the other fourteen (14) grown with soybean. Twelve (12) Landsat 5/TM satellite images of paths 222/80 and 223/80 with field monitored information for the soil, crop, weather and irrigation were used. The NDVI values were correlated with the potential and actual  $K_{cb}$  simulated using the soil water balance in SIMDualKc model, adjusted using the field information. Equations for estimating  $K_{cb}$  via NDVI were generated, and the resulting assimilated average and individual pivot  $K_{cb}$  derived from NDVI were compared, and also with those simulated by SIMDualKc model. The efficiency of model prediction (EF) was 0.93 and 0.78 for soybean and maize potential  $K_{cb}$ , respectively, and 0.90 and 0.74 for the actual  $K_{cb}$  in the same order. The Average Relative Error between the average  $K_{cb}$  NDVI model for the region and the  $K_{cb}$  SIMDualKc was under 30%. This study showed that estimating  $K_{cb}$  by NDVI could be an alternative for planning and supporting irrigation management in southern Brazil.

**Keywords:** Remote sensing, NDVI, crop coefficient, SIMDualKc, Landsat

#### INTRODUCTION

The intensification of irrigated agriculture associated with increased scarcity of water is a current concern in many regions of the world. Approximately 18% of the cultivated areas on our planet are irrigated and account for 44% of world agricultural production (UNESCO WWAP, 2015). In Brazil, it is estimated that 16% of the total food production comes from irrigated areas and these are expanding (BRASIL, 2013). The irrigated area in 2012 was approximately 5.8 million ha, about 20% of the national potential of 29.6 million ha. In recent decades, there has been a significant increase in irrigated agriculture in Brazil, with growing rates higher than the growth of the total planted area (ANA, 2014).

With the expansion of irrigated areas, crop productivity has increased and the farmers can maintain agricultural activities even in conditions of severe drought. Currently, the risks of frustrations resulting from insufficient rainfall and drought are increasing due to climate change resulting in high cost of agricultural production in the country. By means of irrigation, farmers have a much higher probability of good productivity.

Moreover, irrigation is responsible for 70% of the consumption of fresh water globally (FAO, 2012). Thus, it is necessary to seek alternative strategies for the management, monitoring and support of irrigation with a focus in efficient use of water resources without affecting crop production or deteriorating the environment, thus ensuring sustainability in irrigated agriculture.

Several different approaches can be found in literature to estimate the water needs of crops, such as: i) the widely used approach adopted from FAO 56 guidelines (ALLEN et al., 1998), where the reference evapotranspiration ( $ET_o$ ) is multiplied by crop coefficient ( $K_c$ ) to obtain the crop evapotranspiration,  $ET_c$  ( $ET_c = ET_o * K_c$ ); ii) computation directly from terrestrial observations with weather stations installed in crop fields using equations based on physical principles such as the Penman-Monteith equation (SHUTTLEWORTH and WALLACE, 2009; CAMPOS et al., 2012), or eddy covariance (PADILLA et al., 2011.) or direct measurements using lysimeter; iii) through energy balance on the surface models using remote sensing data combined with ground meteorological data (BASTIAANSEN et al., 1998; ALLEN et al., 2007) and iv) through meteorological information and modeling of the water balance in the soil associated with field monitoring of the amount of water at different soil depths and of other soil and vegetation parameters (HUNSAKER et al., 2005; ROSA et al., 2012), with calibration depending on field observations of crop phenological stages and other crop parameters and management practices.

Approaches (ii) and (iii) are considered complex and difficult to apply in the operational context of agricultural common practices; the ease of use and applicability can be limited to researchers or professionals with specialized training. On the other hand, approach (i) combined with (iv) has a long history of use both for operational objectives of agricultural production and for research, thus allowing its use and applicability by people with varying degrees of technical know-how. Approach (iv) is very sensitive, requiring an estimate of the depth corresponding to the crop root zone, and depends critically on soil physical data, length of each developmental stage of the crop as well as rainfall and irrigation frequency; these characteristics stimulate the search for approaches that could improve the quality of the data used, specially aiming adaptation to prevailing local conditions (PEREIRA et al., 2015a).

In recent years, due to the increasing availability of free satellite images, the applicability of remote sensing has been explored combined with the application of FAO 56 methodology and soil water balance models for estimating  $ET_c$  (e.g., PÔÇAS et al., 2015). In the application of FAO 56 method, the dual crop coefficient approach option uses  $K_c$  separated into basal crop coefficient ( $K_{cb}$ ), representing the crop transpiration component, and

an evaporation coefficient ( $K_e$ ), which expresses the soil evaporation (ALLEN et al., 1998). The  $K_{cb}$  has been related to vegetation indices (VI) ( $K_{cb\ VI}$ ), calculated from the surface reflectance at different wavelengths of the electromagnetic spectrum, obtained by remote sensing (PEREIRA et al., 2015a). This type of approach to estimate  $K_{cb}$  is based on the strong correlation between various VI and biophysical parameters of the plant, including the leaf area index, crop developmental stages and physiological processes depending on light absorption by crop canopy, as is the case of evapotranspiration (GLENN et al., 2008, 2011; JOHNSON and TROUT, 2012). The most commonly used VI in this type of approach is the normalized difference vegetation index (NDVI; ROUSE et al., 1974) and the soil adjusted vegetation index (SAVI; HUETE, 1988). On the other hand,  $K_e$  can be obtained from soil water balance models or from the satellite band in the thermal region.

The remote sensing approach, which produces the so generically referred  $K_{cb\ VI}$ , has been used extensively by several authors (HUNSAKER et al., 2005; ER-RAKI et al., 2013; MATEOS et al., 2013; PÔÇAS et al., 2015; CAMPOS et al., 2012) with promising results, although there is a need to account for modeling differences in local conditions as climate, soil types, cultural practices, common cultivars and so on.

One advantage of the  $K_{cb\ VI}$  approach is that it allows better visualization of spatial variation of  $K_{cb}$  (and subsequently  $K_e$ ) in agricultural areas, due to differences in planting dates, row spacing, differences between cultivars and other factors relating to management (PEREIRA et al., 2015a). This type of data can be easily integrated into geographic information systems (GIS) and mathematical models, to obtain an estimate of  $K_e$  and  $ET_c$  in time and space, in a given geographic distribution in matrix form (TODOROVIC & STEDUTO, 2003; EL NAHRY et al., 2010; RAZIEI & PEREIRA, 2013).

Several relations between  $K_{cb}$  ( $K_c$ ) and VI have been established, however, there is not yet an agreement on the nature and generality of these relationships (GONZÁLEZ-DUGO & MATEOS, 2008). While some studies established linear relations between  $K_{cb}$  and VI (e.g., GONZALEZ-PIQUERA et al., 2003; DUCHEMIN et al., 2006; CAMPOS et al., 2010), others have presented more complex relationships (e.g., HUNSAKER et al., 2003, 2005; ER-RAKI et al., 2007; GONZÁLEZ-DUGO & MATEOS, 2008). In some cases, such as Pôças et al. (2015) and Mateos et al. (2013), the information on VI is integrated to  $K_{cb}$  through the soil cover fraction or the coefficient of vegetal density ( $K_d$ ) (e.g., ALLEN & PEREIRA, 2009), to allow better fitting of  $K_{cb}$  for crops where the soil is not fully covered or during crop developmental stage in which the vegetation do not entirely cover the soil.

There is also big concern about the inaccuracies associated with the estimation of  $K_{cb}$  or evapotranspiration (ET) by root water balance, as stated by Allen et al. (2011a, 2011b), which described the sources of inaccuracies that can be involved in the related measurements. For example it is expected an important random error caused by large spatial and vertical variability of bulk density and water holding characteristics of the soil so that discrete measurements do not represent the integrated volume of soil and/or the full root zone depth. Also inaccuracies in measuring precipitation and irrigation additions or unrepresentativeness of data are considered a big factor, together with differential spatial wetting of soil, deep percolation losses, spatial variation in root systems, calibration of sensors, systematic or random errors when obtaining samples or taking readings, or altering density, aeration and infiltration characteristics of the surface of soil from foot traffic, excavation or backfilling (ALLEN ET AL., 2011a).

Therefore, the establishment of methodologies that allow more accurate relationships between crop coefficient and VI is a research topic still in progress, being the objective of this study to locally calibrate the  $K_{cb}$  from NDVI data obtained by remote sensing for maize and soybean irrigated by center pivot systems, using as reference,  $K_{cb}$  values obtained through SIMDualKc model, in order to obtain estimates of  $K_c$  and  $ET_c$  closest to the reality of soil and climate for crops established in a humid subtropical region of southern Brazil.

## MATERIALS AND METHODS

### Study area

The area under study is located in the northwest region of Rio Grande do Sul, in the municipality of Cruz Alta (Figure 1), between latitudes  $28^{\circ} 34' 05''$  and  $28^{\circ} 45' 14''$  S and longitude  $53^{\circ} 14' 22''$  to  $53^{\circ} 30' 33''$  W. The climate is "Cfa" by Koppen classification (KOTTEK et al., 2006), corresponding to subtropical humid, with average annual rainfall of 1755 mm, evenly distributed throughout the year. A typical soil in the region can be described as: Rhodic Hapludox (FAO) or Typic Haplorthox (US Soil Taxonomy), argillaceous and deep with an inclination of 1%. According to Brazilian Soil Classification (EMBRAPA, 2006) the major soil types in the region are "Latossolo vermelho distrófico". The agriculture is characterized by the growing of commercial crops, mainly soybean, maize, sunflower, beans and wheat. This study analyzed twenty-eight (28) areas irrigated by center pivot system, where fourteen (14) fields were cultivated with maize while the remaining with soybean, with pivots 1, 2, 4, 6, 7, 8, 13, 15, 19, 21, 22, 25, 27 and 30 identified for maize, while pivots 5, 9, 11, 12, 14, 16, 17, 18, 20, 23, 24, 26, 28 and 29 were identified for soybean (Figure 1).

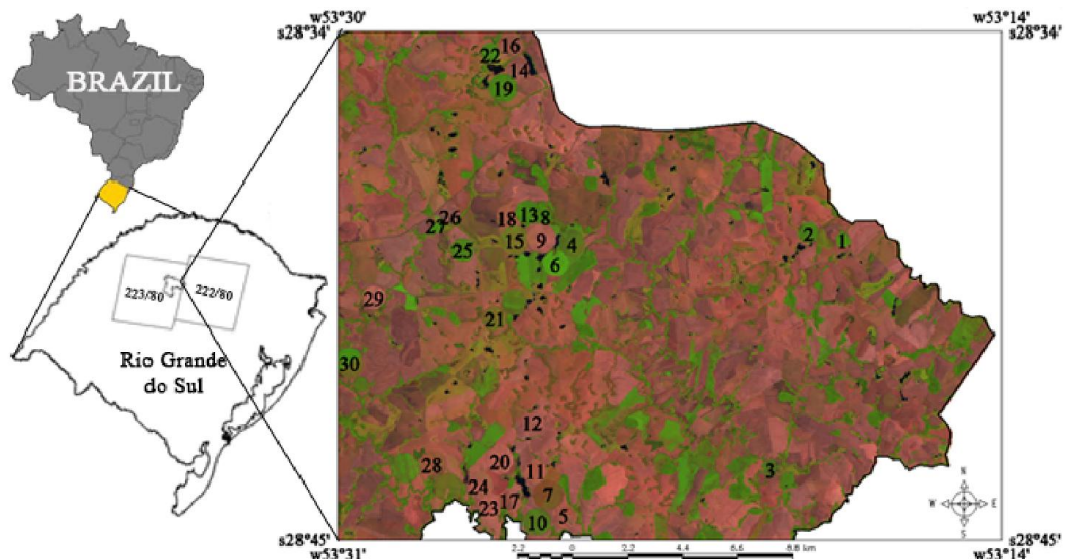


Fig. 1. Location of the study area. The rectangle is in the overlapped region of the paths 222/80 and 223/80 of the Landsat 5 satellite imagery.

### Field monitoring

Field information including crop type, sowing date, phenological stage, plant height, planting density, soil moisture in different layers, soil physical characteristics, irrigation depth, rainfall and meteorological data were provided by Sistema Irriga®, Federal University of Santa Maria (UFSM), Santa Maria, Brazil. The meteorological data include hourly and daily records of relative humidity, air temperature, wind speed, solar radiation, rainfall and atmospheric pressure, which were used for the  $ET_o$  determination.

According to information obtained from Sistema Irriga®, pivots 09, 13 and 18 were planted with soybeans, while pivots 04, 06, 08, 19, 25, 27 and 30 were cultivated with maize during the 2004/2005 growing season, used in this study. The field size ranges from 10 to 100 ha, with plant population between 70,000 and 75,000 plants  $ha^{-1}$  for maize plants and from 260,000 to 340,000 plants  $ha^{-1}$  for soybeans.

The data collected on plant height, stage of development, rainfall, irrigation and soil moisture content were used to calibrate the SIMDualKc model (MARTINS et al., 2013; PAREDES et al., 2014; PEREIRA et al., 2015b) and the vegetation index values, particularly the NDVI, obtained were evaluated. The crop development stages were defined as suggested by ALLEN et al. (1998) as: (i) initial phase, starting from sowing/planting up to 10% ground cover (Ini); (ii) rapid developmental stage, from 10% soil cover to maximum vegetal cover (Dev); (iii) intermediate phase, during maximum vegetal cover, including flowering (Mid);

and (iv) maturation phase, from the beginning of senescence and yellowing of leaves to harvesting (Late).

### **Crop Identification in GIS and geographic database**

From the field information on the type of crop planted in some pivots and with the registers of the duration of soybean and maize cycle it was possible to associate the crop characteristics with the spectral characteristics of the NDVI image pixels. That was made for each culture in various stages of the cycle, allowing the completion of supervised classification procedures to identify the same crop in other unmonitored pivot fields. It was also possible to identify the graphic profile characteristics of NDVI as a function of time. This process materialized a characteristic curve of the time series of NDVI for some crop cultivars at each pivot in the studied region. This profile also serves as an effective means of identification.

### **SIMDualKc**

The SIMDualKc is a model and corresponding software directed to irrigation planning and scheduling (ROSA et al., 2012), that uses the approach of dual crop coefficients for  $K_c$  (ALLEN et al., 1998, 2005b), focusing on the estimated  $ET_o$  and the water balance in the soil. Following the dual  $K_c$  approach,  $K_{cb}$  and  $K_e$  are considered separately (PEREIRA et al., 2015b), thus allowing a better assessment of irrigation management practices.

The SIMDualKc model has been successfully applied to estimate ET and  $K_c$  for a wide range of agricultural crops (e.g., PAREDES et al., 2014; PEREIRA et al., 2015b; PÔÇAS et al., 2015). In the present work, the  $K_{cb}$  output data obtained in SIMDualKc ( $K_{cb}^{SIMDual}$ ), previously calibrated in the region (MARTINS et al., 2013) was used as a basis for assimilation of NDVI data through correlation equations, and also as a reference for establishing comparisons with a FAO56-like methodology. This approach was developed for the crops of soybean and maize in southern Brazil.

The  $K_{cb}$  calculation in SIMDualKc is done by the following equation (ALLEN & PEREIRA, 2009; ROSA et al., 2012), where the impacts on the density of the plants and/or the leaf area are taken into consideration by a density coefficient:

$$K_{cb} = K_{cmin} + K_d(K_{cbfull} - K_{cmin}) \quad (1)$$



Where  $K_d$  is the coefficient of density,  $K_{cb \text{ full}}$  is the value when the plant reaches the peak of its growth, under soil cover conditions almost full (or  $LAI > 3$ ),  $K_{c \text{ min}}$  is the minimum, when the soil is uncovered, i.e., in the absence of vegetation. The minimum  $K_c$  value can vary for (0.0 to 0.15) depending on the crop or vegetation and the frequency of rainfall or irrigation.  $K_{cb}$  is corrected by the model for local climatic conditions when the minimum relative humidity ( $RH_{\text{min}}$ ) differs from 45% and/or when the average wind speed is different to  $2 \text{ m}\cdot\text{s}^{-1}$  (ALLEN et al., 1998; ALLEN & PEREIRA 2009; ROSA et al., 2012). The  $K_d$  is calculated with equation (2) as proposed by ALLEN & PEREIRA (2009) and represents the combined effects of soil fraction effectively covered by culture,  $f_{c \text{ eff}}$  [0.01-1], and plant height (h); the multiplier  $M_L$  describes the effect of canopy density on shading and of maximum relative ET per fraction of ground shaded:

$$K_d = \min \left( 1, M_L f_{c \text{ eff}}, f_{c \text{ eff}}^{\left(\frac{1}{1+h}\right)} \right) \quad (2)$$

$K_e$  is calculated by a daily water balance in the evaporable layer of soil that is characterized by its depth ( $Z_e$ , m), total evaporable water (TEW, mm) and the readily evaporable water (REW, mm). TEW is the maximum depth of water that can be evaporated from the evaporable layer of soil when completely wet, and REW is the depth of water that can be evaporated without water restrictions (ALLEN et al., 1998, 2007a). The maximum soil evaporation ( $E_s$ ) occurs when the soil is wet by rain or irrigation and with minimum shadowing of the culture, which occurs during the early development stages of the crop. Minimum  $E_s$  occurs when the culture fully shades the soil and the energy available for evaporation is minimal (PEREIRA et al., 2015).

When the soil is wet  $K_e$  is maximum, but is limited by the available power on the soil surface and its value cannot exceed the difference  $K_{c \text{ max}} - K_{cb}$ . As the soil dries, less water is available for evaporation and there is a decrease in  $E_s$  in proportion to the amount of water that remains in the soil surface layer. Thus,  $K_e$  is expressed by:

$$K_e = K_r(K_{c \text{ max}} - K_{cb}) \quad K_e \leq f_{ew}K_{c \text{ max}} \quad (3)$$

where  $K_r$  is the evaporation reduction coefficient, dependant of water depletion in the soil surface ( $\leq 1, 0$ ),  $K_{c \text{ max}}$  is the maximum value of  $K_c$ , for example, when  $K_{cb} = K_c + K_e$  following a rain or irrigation event, and  $f_{ew}$  is the fraction of soil that is exposed to radiation and wetting

by rain or irrigation, which depends on the fraction of soil covered by crop ( $f_c$ ).  $K_r$  is calculated using the approach of the drying cycle in 2-stages (ALLEN et al., 1998).

When there is occurrence of water deficit in the soil a stress coefficient ( $K_s$ ) is calculated by the model for the whole root zone.  $K_s$  is expressed as a linear function of the depletion in the root zone  $D_r$  (ALLEN et al., 1998; ALLEN et al., 2005a):

$$K_s = \frac{TAW - D_r}{TAW - RAW} = \frac{TAW - D_r}{(1-p)TAW} \quad D_r > RAW \quad (4a)$$

$$K_s = 1 \quad D_r \leq RAW \quad (4b)$$

where TAW and RAW are respectively the total available and readily available soil water (mm),  $D_r$  is the depletion in the root zone (mm), and  $p$  is the fraction depleted for no stress.  $K_{cb}$  is multiplied by  $K_s$  to account for the effects of water deficiency stress to obtain the actual coefficient  $K_{cb \text{ act}}$ .

$$K_{cb \text{ act}} = K_s K_{cb \text{ pot}} \quad (4c)$$

The detailed calculation of  $K_{cb}$ ,  $K_e$  and  $K_s$  in SIMDualKc is described in ROSA et al. (2012).

The calibration of SIMDualKc is focused in optimizing the crop parameters and  $K_{cb}$  and  $p$  for the various growth stages of the crop and also the soil evaporation parameters, deep percolation parameters and the flow curve, using trial and error procedures until small errors are found (ROSA et al., 2012). As input data for SIMDualKc modeling of irrigated areas, it is needed information regarding i) type of crop, as sowing time, crop cycle duration and lengths of development stages and harvest period; ii) soil, as permanent wilting point and field capacity at different depths, percentage of clay and sand; iii) irrigation, as irrigation depth (mm), and iv) weather, such as rainfall,  $ET_o$ , minimum relative humidity and wind speed, as well as location and altitude of the weather station providing the data.

As input data for SIMDualKc modeling of the pivots that had no field data available, it was used weather, soil and irrigation data of the monitored pivots, adopting the criterion of proximity between them. Thus, it is considered that the soil characteristics in the pivots number 4 , 5, 6, 8 , 9, 11 , 12, 13, 14 , 15, 16, 17 , 18, 19, 20, 21, 23 , 24, 26, 28 , 29 and 30 are sandy clay, the pivot 25 is sandy clay loam and pivots 1, 2, 7 ,22 and 27 are clay . The average soil water content at field capacity (FC) and wilting point (WP) for the pivots with sandy clay soil was, respectively,  $0.33 \text{ cm}^3 \cdot \text{cm}^{-3}$  and  $0.16 \text{ cm}^3 \cdot \text{cm}^{-3}$ ; to the sandy clay loam soil  $0.31$  and  $0.16 \text{ cm}^3 \cdot \text{cm}^{-3}$ ; and the clay soil was  $0.37$  and  $0.19 \text{ cm}^3 \cdot \text{cm}^{-3}$ . The sandy clay soil and clay soil have  $105 \text{ mm} \cdot \text{m}^{-1}$  TAW while the sandy clay loam soil has  $95 \text{ mm} \cdot \text{m}^{-1}$  TAW.

The sowing dates and duration of the stages of the crop cycle were adjusted in SIMDualKc model based on the periods observed in the NDVI curves as a function of days on each pivot, but in accordance with the development and crops cycle length obtained by field monitoring. Such cross information from field visits and remote sensing allowed performing verification mechanisms that improved the quality of the input data used.

### **Products and remote sensing data**

Images of TM sensor (Thematic Mapper) on board of Landsat 5 satellite were used in this study, covering the period from September to December 2004 and January to March 2005, totalizing 12 images in the paths 222/80 and 223/80. The existence of an overlap area ( $\approx 15$  km) between the two orbits inside the study area (Figure 1) assured a shorter revisiting time, thereby improving the temporal resolution. In this way, a relatively regular imaging of the entire maize and soybean crop cycle was achieved. For maize, ten dates of images were considered: 04/09/2004, 24/09/2004, 06/10/2004, 15/10/2004, 07/11/2004, 23/11/2004, 02/12/2004, 18/12/2004, 26/01/2005, and 27/02/2005. For the soybean crop, seven dates of images were considered: 23/11/2004, 02/12/2004, 18/12/2004, 26/01/2005, 27/02/2005, 08/03/2005 and 02/05/2005.

The Landsat 5 images were obtained via Internet at the site of the Brazilian Space Institute, INPE: <http://www.dgi.inpe.br/CDSR/>. A search was made on the images database, looking for the target path and orbit of the Landsat5 images, looking for coincidence with the time period where field monitoring information was available. The selected images were those that showed clouds coverage ratio less than 10 % in the quadrant corresponding to the study area. Digital processing of the images included: geometric correction, radiometric calibration, atmospheric correction, vectoring, cutting and extraction of NDVI. The radiometric calibration followed the procedures and calibration parameters described in Chander et al. (2007, 2009). The atmospheric correction was made in accordance with the simplified method proposed by Chavez (1996) and Gürtler et al. (2005). This processing was done in the SPRING GIS software version 5.2.6 (CÂMARA, 1996). The calculation of NDVI was made according to the equation proposed by Rouse et al. (1974).

### **Statistical analysis**

Linear regression analysis was performed by least squares method obtaining the line of best fit between the values of  $K_{cb}$  obtained from the output of SIMDualKc model

( $K_{cbSIMDual}$ ) and the average pivot NDVI values obtained from satellite images at the corresponding dates. The SIMDualKc model provides a matrix with output data for each day of the cycle. On the other hand, the average NDVI values for each pivot corresponding to the same variety of maize or soybean were obtained from remote sensing data only in the satellite passage dates, and then interpolated for the remaining days of the cycle. Both sets of data were compared using statistical indicators. A description about the use of these indicators in watershed modeling is found in Moriasi et al. (2007), and for irrigation modeling we refer to Pereira et al. (2015b).

As goodness of fit indicators between  $K_{cb SIMDual}$  and NDVI, the regression coefficient ( $b_0$ ) and the coefficient of determination ( $R^2$ ) were used, which are calculated as:

$$b_0 = \frac{\sum_{i=1}^n O_i P_i}{\sum_{i=1}^n O_i^2} \quad (5)$$

$$R^2 = \left\{ \frac{\sum_{i=1}^n (O_i - \bar{O})(P_i - \bar{P})}{[\sum_{i=1}^n (O_i - \bar{O})^2]^{0.5} [\sum_{i=1}^n (P_i - \bar{P})^2]^{0.5}} \right\}^2 \quad (6)$$

A regression coefficient  $b_0$  near 1 indicates that the values provided by SimDualKc are statistically close to the NDVI and a coefficient of determination  $R^2$  close to 1.0 indicates that most of the variance calculated by the model is also present in the NDVI values.

To better evaluate the effect of NDVI assimilation to the  $K_{cb SIMDual}$ , the output from that model was compared to the  $K_{cb NDVI}$  obtained by the correlation equation with the NDVI. For this, we used a set of additional residual estimation error indicators which are described hereinafter.

The root mean square error (RMSE), expresses the magnitude of the average residual error according to equation 7:

$$RMSE = \left[ \frac{\sum_{i=1}^n (O_i - P_i)^2}{n} \right]^{0.5} \quad (7)$$

It can vary between 0, when a perfect fit occurs, and a positive value, expectedly lower than the average of the observations.

The RSR rate of the RMSE to the standard deviation of the observed data (sd), standardizes RMSE for comparison, as a relative value that can be converted to %:

$$RSR = \frac{[\sum_{i=1}^n (O_i - P_i)^2]^{0.5}}{[\sum_{i=1}^n (O_i - \bar{O})^2]^{0.5}} \quad (8)$$

The ideal value of RSR is 0.0, which indicates a perfect simulation model; the lower RSR values, the better the simulation model performance.

The average absolute error (AAE), which expresses the average size of the error estimates:

$$AAE = \frac{1}{n} \sum_{i=1}^n |O_i - P_i| \quad (9)$$

The average relative error (ARE), which expresses the calculation errors as a percentage of observation values

$$ARE = \frac{100}{n} \sum_{i=1}^n \left| \frac{O_i - P_i}{O_i} \right| \quad (10)$$

The percentage of polarization (PBIAS) which measures the average trend of simulated data to be higher or lower than their corresponding observations:

$$PBIAS = 100 \frac{\sum_{i=1}^n (O_i - P_i)}{\sum_{i=1}^n O_i} \quad (11)$$

The ideal value of PBIAS is 0.0; values close to 0.0 indicate an exact concurrence of  $K_{cb \text{ SIMDual}}$  and  $K_{cb \text{ NDVI}}$ . Positive or negative values refer to the occurrence of a sub or over-estimation respectively.

The modeling efficiency (EF), which is used to determine the relative magnitude of the residual variance of  $K_{cb \text{ SIMDual}}$  compared to the variance of the  $K_{cb \text{ NDVI}}$  data. This is defined as:

$$EF = 1.0 - \frac{\sum_{i=1}^n (O_i - P_i)^2}{\sum_{i=1}^n (O_i - \bar{O})^2} \quad (12)$$

The target value is 1.0. Values closer to 1.0 indicate that the variance of the residuals is much less than the variance in observations, so that the model performance is very good.

Conversely, when EF is close to 0 or negative, this means that there is no gain in using the model, so the average of the observations is as good predictor or better than the model.

## RESULTS AND DISCUSSION

### Basal crop coefficient ( $K_{cb}$ ) derived from NDVI

For agricultural planning purposes in the region, it is important the availability of general models that estimate the  $K_{cb}$  during the growing cycle for each variety of crop. From the data corresponding to all the pivots of the same crop variety, average curve models for the growing cycle of a given crop in the region were obtained.

To estimate  $K_{cb}$  from NDVI, linear correlation was conducted between NDVI values and potential  $K_{cb}$  obtained by SIMDualKc model ( $K_{cb\ pot\ SIMDual}$ ), for the two crops under study. The same procedure was repeated for actual  $K_{cb}$  ( $K_{cb\ act\ SIMDual}$ ) and NDVI. Ninety-six (96)  $K_{cb}$  values were considered for soybean crop and one hundred and twenty-six (126)  $K_{cb}$  values were considered for maize. The resulting plots and equations for the crop are shown in Figure 2.

From the equations obtained, a new set of  $K_{cb}$  general values that follow the smooth and continuous curve of the NDVI vs DAS plot could be generated, in a scale adjusted to the  $K_{cb}$  of the particular crop. In this way, through the linear equations, it is possible to assimilate the information contained in the NDVI to  $K_{cb}$ , obtaining a new set of values for the crop basal coefficient designated as  $K_{cb\ NDVI}$ .

The equations of the linear correlation to estimate potential crop coefficient from NDVI ( $K_{cb\ pot\ NDVI}$ ) are expressed by equation (13) for the soybean crop and equation (14) for the maize crop, with the corresponding coefficient of determination:

$$K_{cb\ pot\ NDVI\ soybean} = 1.225*NDVI-0.043 \quad R^2=0.93 \quad (13)$$

$$K_{cb\ pot\ NDVI\ maize} = 1.648*NDVI-0.204 \quad R^2=0.82 \quad (14)$$

On the other hand, the equations generated to estimate the actual crop coefficient ( $K_{cb\ act}$ ) from NDVI for soybean and maize are expressed by equations 15 and 16, respectively.

$$K_{cb\ act\ NDVI\ soybean} = 1.12*NDVI-0.027 \quad R^2=0.85 \quad (15)$$

$$K_{cb\ act\ NDVI\ maize} = 1.578*NDVI-0.188 \quad R^2=0.78 \quad (16)$$

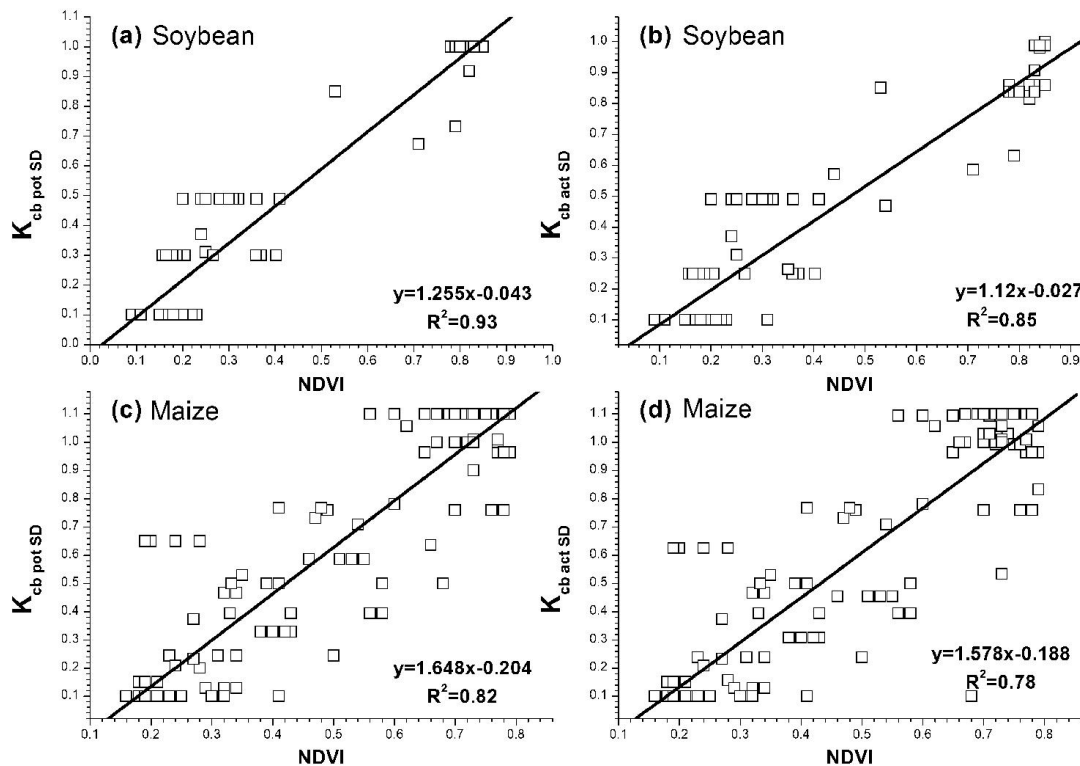


Fig. 2. Linear relationships between the NDVI and K<sub>cb</sub> SIMDual for soybean [2 (a) and 2 (b)], and maize [2 (c) and 2 (d)] crop cycles. The equations are included to show the functional correlation between the potential and actual K<sub>cb</sub> SIMDual and NDVI. The values of the coefficient of determination are also presented.

The results showed that 93% of the variability in K<sub>cb pot</sub> for soybean values can be explained by the variability of NDVI values. This indicates that modeling of the potential K<sub>cb</sub> for soybean is accurate, and fits well to the profile of the growth cycle produced by NDVI. Uniform characteristics of crop management in central-pivot irrigated areas may be important causes of this good fit.

To give a further step in the estimate of the actual water need from the crops we can use the K<sub>cb act</sub> correlation. The coefficient of determination  $R^2 = 0.85$  indicates a slightly lower adjustment with NDVI comparing to the  $R^2 = 0.93$  of the potential value.

As the  $K_{cb act SIMDual} = K_s * K_{cb pot SIMDual}$  (Equation 4c) and as K<sub>cb pot</sub> SIMDual had good fit with NDVI ( $R^2 = 0.93$ ), it is obvious that the lower adjustment of K<sub>cb act</sub> SIMDual with NDVI was due to the effect of the water stress coefficient, K<sub>s</sub>, computed by the model.

This effect can be associated to a temporal difference in the response of NDVI to water stress conditions. While SIMDualKc model reveals immediately the water stress

condition through the soil water balance, the NDVI does not reveal water stress immediately because it depends on plant response. In other words, coefficients of stress based in the soil water balance show possibility of plant stress, while the NDVI only reveals actual conditions of water stress.

It should be noted that, on one hand, there is the interest of no reduction in productivity while, on the other, there is the interest of maximum efficiency of water use. While the SIMDualKc model met the first interest by showing the stress situation immediately, the NDVI met the second interest by showing the real effects in plants. The assimilation of the two sources of information led to a compromise between these two trends, and provides a better model fit considering crop reality, because the stress may not manifest, even if there is probability of stress.

Some authors have stated that most of the vegetation indices follow the effects of water stress in the long run, but do not allow early detection of water stress (STAGAKIS et al., 2012). However, the low temporal or spatial resolution of satellite images commonly used in NDVI calculations, or the greater variability of NDVI in not irrigated vegetation may have imposed a limit of sensibility to monitor the effects of water stress, and this topic is matter of current research (WANG et al., 2016).

For maize crop, the coefficient of determination ( $R^2 = 0.82$ ) from equation 14, shows a good fit of  $K_{cb\ pot}$  and NDVI. This was lower compared with the result obtained by Gonzalez-Piquera et al. (2003) ( $R^2 = 0.94$ ). The lower  $R^2$  obtained may be due to the wider variety of conditions sampled in this study, the higher number of pivots considered and also due to the higher number of maize cultivars grown by farmers, causing distinct estimation of  $K_{cb}$  by SIMDualKc model with respect to individual cases. The  $K_{cb\ act\ NDVI}$  for maize also shows the same trend observed in soybean, with slightly lower values than the potential ones. It should also be stated that the adjustment of the SIMDualKc model to the Brazilian sub-tropical conditions found in this study is recent and still in progress (MARTINS et al., 2013).

The difference of adjustment between  $K_{cb}$  derived from NDVI and  $K_{cb}$  derived from SIMDualKc was observed to be sometimes greater for individual pivots, as is shown in Table 1.

Tab. 1. Comparison of  $K_{cb\ pot\ NDVI}$  with  $K_{cb\ pot\ SIMDual}$  and  $K_{cb\ act}$  derived from NDVI ( $K_{cb\ act\ NDVI}$ ), with  $K_{cb}$  obtained from SIMDualKc ( $K_{cb\ SIMDual}$ ) for the soybean crop cycle and maize in twenty eight pivots analyzed. Coefficient of determination ( $R^2$ ) and the forced-by-origin angular coefficients (b) are presented.

---

**Soybean**

---



<b>Pivot</b>	<b>R<sup>2</sup> (K<sub>cb pot</sub>)</b>	<b>b<sub>0</sub> (K<sub>cb pot</sub>)</b>	<b>R<sup>2</sup> (K<sub>cb act</sub>)</b>	<b>b<sub>0</sub> (K<sub>cb act</sub>)</b>
05	0.96	1.03	0.90	0.98
09	0.95	0.98	0.89	1.02
11	0.95	1.03	0.90	0.98
12	0.97	1.04	0.91	0.97
14	0.96	0.94	0.90	0.91
16	0.96	1.02	0.90	0.98
17	0.96	1.05	0.91	1.02
18	0.87	0.91	0.79	1.05
20	0.96	0.97	0.93	0.95
23	0.93	0.96	0.80	0.94
24	0.92	0.98	0.76	0.95
26	0.96	1.04	0.91	0.99
28	0.94	1.04	0.81	1.02
29	0.90	0.95	0.78	0.91
<b>AVERAGE</b>	<b>0.94</b>	<b>1.00</b>	<b>0.86</b>	<b>0.98</b>

<b>Maize</b>				
<b>Pivot</b>	<b>R<sup>2</sup> (K<sub>cb pot</sub>)</b>	<b>b<sub>0</sub> (K<sub>cb pot</sub>)</b>	<b>R<sup>2</sup> (K<sub>cb act</sub>)</b>	<b>b<sub>0</sub> (K<sub>cb act</sub>)</b>
01	0.80	1.00	0.80	1.01
02	0.78	1.01	0.72	1.01
04	0.91	1.17	0.91	1.14
06	0.90	0.95	0.63	0.71
07	0.84	0.98	0.73	0.97
08	0.93	0.92	0.90	0.92
13	0.92	0.89	0.90	1.08
15	0.73	0.89	0.71	0.88
19	0.91	0.90	0.90	0.97
21	0.70	1.12	0.71	1.12
22	0.71	0.96	0.70	0.97
25	0.92	1.13	0.90	1.13
27	0.70	1.11	0.70	1.12
30	0.92	0.99	0.90	0.99
<b>AVERAGE</b>	<b>0.83</b>	<b>1.00</b>	<b>0.79</b>	<b>1.00</b>

In Table 1 it can be seen that the coefficient of determination exceeded the 90% threshold in 20 pivots, averaging 0.94 for potential  $K_{cb}$  and 0.86 for actual  $K_{cb}$  for soybean, and averaging 0.83 for potential  $K_{cb}$  and 0.79 for actual  $K_{cb}$  for maize. It was also observed that most of the forced-by-origin angular coefficients (b) were close to 1, indicating a standard statistical variation equivalent of  $K_{cb NDVI}$  and  $K_{cb SIMDual}$ , for both actual and potential crop coefficient in each pivot.

Nevertheless, some lower adjustments are also visible in Table 1, which were associated with the  $K_s$  stress factor internal multiplication with  $K_{cb pot SIMDual}$  already mentioned. So it was decided to also test a different assimilation procedure, by extracting  $K_s$

from SIMDualKc and multiplying it directly to  $K_{cb\ pot\ NDVI}$ , that is:  $K_{cb\ act\ NDVI} = K_{cb\ pot\ NDVI} * K_s$  (Equation 4c), as has also been reported by PÔÇAS et al. (2015).

The assimilation of NDVI data analyzed here can be made either through  $K_{cb\ pot}$  (Equations 13 and 15 for soybean and maize, respectively) or through  $K_{cb\ act}$  (Equations 14 and 16 for soybean and maize, respectively) or via  $K_s * K_{cb\ pot\ NDVI}$ . To further compare these procedures, additional statistical parameters were calculated and the results are presented in Table 2.

For the complete set of  $K_{cb}$  values calculated for soybean and maize for all the pivots in each imaging data, six comparisons were made: 1)  $K_{cb\ pot}$  assimilated from NDVI against  $K_{cb\ pot}$  from SIMDualKc; 2)  $K_{cb\ act}$  assimilated from NDVI against  $K_{cb\ act}$  from SIMDualKc; 3)  $K_{cb\ pot\ NDVI}$  multiplied by stress coefficient  $K_s$  (obtained from SIMDualKc) against  $K_{cb\ act}$  SIMDual.

The regression coefficient,  $b_0 = 1.00$ , for the tested crops shows that both the actual and potential values of  $K_{cb\ NDVI}$  are statistically close to the  $K_{cb}$  values obtained from SIMDualKc, in other words, similarity between the two set of data. For the potential  $K_{cb}$ , the  $R^2$  of 0.93 (soybean) and 0.82 (maize) in Table 2(a) are within the range of values reported by Pôças et al. (2015) which compared  $K_{cb\ SIMDual}$  with  $K_{cb\ VI}$  derived from NDVI and SAVI for annual and perennial crops.

Table 2 - Statistical parameters for the comparison between the potential and actual crop coefficients calculated by NDVI and SIMDualKc.

Cultura	$b_0$	$R^2$	RMSE	RSR	PBIAS	AAE	ARE	EF
(a) $K_{cb\ pot\ NDVI}$ VS $K_{cb\ pot\ SIMDual}$								
Soja	1.00	0.93	0.10	0.027	0.0	0.08	28.61	0.93
Milho	1.01	0.82	0.17	0.042	-1.2	0.12	33.64	0.78
(b) $K_{cb\ act\ NDVI}$ VS $K_{cb\ act\ SIMDual}$								
Soja	1.00	0.85	0.10	0.032	0.1	0.09	29.45	0.86
Milho	1.01	0.78	0.19	0.049	-1.0	0.14	35.02	0.71
(c) $K_s * K_{cb\ pot\ NDVI}$ VS $K_{cb\ act\ SIMDual}$								
Soja	1.00	0.92	0.08	0.030	1.0	0.07	28.23	0.91
Milho	1.01	0.80	0.16	0.044	0.3	0.11	34.39	0.74

For the actual  $K_{cb}$  in Table 2b, on the other hand, the  $R^2$  of 0.85 and 0.78 for soybean and maize, respectively, were lower than the  $R^2$  of Table 2c, when  $K_s$  obtained from SIMDualKc model was multiplied directly to the  $K_{cb\ pot}$  assimilated from NDVI in equations (15) and (16). This is related to the characteristics of water stress function  $K_s$ , which has a narrow sharp peaks irregular pattern influenced by rainfall and irrigation.

The wetting events increase rapidly the TAW, and these intense peaks of short duration create a "noisy" pattern which is internally passed in SIMDualKc model for the

$K_{cb \text{ act SIMDual}}$  without any smoothing. This is unlike the  $K_{cb \text{ pot SIMDual}}$  characteristics that are continuous, monotonous and smooth just as the NDVI.

For those reasons, the product of  $K_{cb \text{ pot NDVI}} * K_s$  has a better adjustment, reflected by  $R^2$  of Table 2c in comparison to Table 2b. That is,  $K_{cb \text{ pot NDVI}} * K_s \text{ SIMDual} = K_{cb \text{ act NDVI}}$  can be considered a better assimilation procedure for obtaining the actual values of basal crop coefficient in the presence of water stress.

The other indicators of model adjustment were further analyzed, considering only cases (a) and (c) of Table 2. The RMSE between  $K_{cb \text{ pot NDVI}}$  and  $K_{cb \text{ pot SIMDual}}$  for the set of images considered was 0.10 for soybean and 0.17 for maize, while the RMSE between  $K_{cb \text{ act NDVI}}$  and  $K_{cb \text{ act SIMDual}}$  was 0.17 and 0.19 for soybean and maize, respectively. These results were lower than the average of observations, indicating that there may be small residual errors and a better fit may be occurring for the cultivation of soybean compared to maize, as the soybean crop had lower RMSE for both potential and actual crop coefficients. The RSR indicator (0-1) indicated that both the potential and actual  $K_{cb}$  for soybean (0.027 and 0.030 for potential and actual  $K_{cb}$ , respectively) and maize (0.042 and 0.044 for potential and actual  $K_{cb}$ , respectively) showed residual errors that are a small fraction of the variance. The PBIAS (%) indicates a good fit of both the potential and actual  $K_{cb}$  for both crops, with an overestimation of the assimilated model around 1% and 0.3% against the actual  $K_{cb \text{ SIMDual}}$  of soybean and maize respectively. This can be probably related to the water stress effect already explained. The efficiency of model prediction, EF, was 0.93 and 0.78 for soybean and maize potential  $K_{cb}$ , respectively, and 0.91 and 0.74 for the actual  $K_{cb}$  in the same order. This shows that the variance of residuals had good agreement, with slightly higher values in soybean compared to maize. Finally, the average absolute error, AAE, around 0.1 units of  $K_{cb}$ , and the average relative error, ARE, of about 30% show the proximity of the models.

In short, Table 2 showed that the assimilation processes of NDVI on  $K_{cb \text{ SIMDual}}$  produced  $K_{cb \text{ NDVI}}$  assimilated values that are slightly different, but we can expect to be more representative of the crop water requirement in the field, due to the additional information contained in the NDVI. Due to the characteristics of the stress coefficient  $K_s$ , the preferred procedure for calculation of  $K_{cb \text{ act NDVI}}$  is the product  $K_s * K_{cb \text{ pot NDVI}}$ , especially when stress is manifested.

This indicates a possible management of irrigation systems through potential and actual  $K_{cb}$  obtained using models such as SIMDualKc adjusted with NDVI and assimilated as proposed. This is valid for irrigated areas with similar characteristics to the ones found in the

center pivot irrigation system evaluated in this study, and can potentially produce better information on the real crop evolution throughout the growing cycle.

Complementary, Figures 4 and 5 show the seasonal curves of  $K_{cb\ pot}$  obtained from SIMDualKc and the  $K_{cb\ pot\ NDVI}$  curves obtained using equations 13 and 14 for the soybean and maize growing period, respectively.

In general, the results obtained for soybean show a good fit between the  $K_{cb\ pot\ NDVI}$  and  $K_{cb\ pot\ SIMDual}$  throughout the growing period in various pivots (Figure 3). A comparison of the actual and potential Kcb curves obtained from SIMDualKc model shows the occurrence of little or no stress during mid-season growth stage of the crop in all the pivots, and a slightly higher stress in the end-season, where irrigation can be sometimes relaxed.

For most of the pivots, the  $K_{cb\ NDVI}$  values for soybean were between 0.10 and 0.20 for the initial stage, from 0.15 to 1.0 for the rapid developmental stage, 0.95-1.1 for the mid-season stage and 0.5-0.3 at harvest, depending on the situation at the satellite image data. These results are consistent with the values tabulated in Allen et al., (1998) for  $K_{cb}$  at initial, mid-season and harvest (end) stages ( $K_{cb\ ini}=0.15$ ,  $K_{cb\ mid}=1.10$  e  $K_{cb\ end}=0.30$ ).

For maize, the  $K_{cb\ pot\ NDVI}$  curves for most pivots follow a similar pattern as the  $K_{cb\ pot\ SIMDual}$  curves and also very close to those of  $K_{cb\ act\ SIMDual}$ . This is coherent with only limited stress occurrences detected in short periods during the crop cycle (Figure 4). The  $K_{cb\ NDVI}$  values for the set of pivots grown to maize ranged from 0.10 to 0.25 for the initial stage, between 0.2 and 1.0 for the crop developmental stage, between 0.95 and 1.2 for the mid-season, and between 1.0 and 0.5-0.2 for the late stage. These results are similar to the values tabulated in Allen et al. (1998) for  $K_{cb}$  at initial stage, mid-season stage and at harvest ( $K_{cb\ ini} = 0.15$ ,  $K_{cb\ mid} = 1.15$  and  $K_{cb\ end} = 0.15-0.50$ ), as well as in accordance with the values of  $K_{cb}$  approximated from SAVI by Padilla et al. (2011).

It shall be noted that the values of the  $K_{cb\ NDVI}$  for the late season are highly dependent on management conditions, including the moisture conditions at which the grains were harvested and the fluctuations in the temporal resolution of the satellite images, which may not coincide with the time of harvest. Comparing the results of this study with the findings of Pôças et al. (2015), who used vegetation indices by a procedure based on the vegetation density coefficients, the  $K_{cb\ act\ NDVI}$  obtained for the mid-season stage was slightly higher while the range of values for the crop developmental and late stages are wider. Moreover, the  $K_{cb\ NDVI}$  values obtained in this study correspond to climatic and regional conditions which are quite different.

With the correlations between the NDVI values obtained for soybean and maize and the potential values of  $K_{cb}$  from SIMDualKc model for the entire crop cycle and for 28 pivots evaluated in southern Brazil, it was possible to generate functions (Equations 13 and 14) which shall be seen as  $K_{cb}$  values from FAO 56 guidelines calibrated with local information about the growth of the crops contained in NDVI.

It is also concluded from the study that actual values of crop coefficient,  $K_{cb \text{ act NDVI}}$  can be obtained by the product  $K_s * K_{cb \text{ pot NDVI}}$ , with  $K_s$  extracted from SIMDualKc model.

In most of the pivots evaluated, the assimilation using SIMDualKc model produced results that did not differ by more than 30% of the value obtained by FAO methodology.

Although comparison with absolute standards was not performed in this study, the assimilation of information contained in NDVI, directly related to the actual plant growth stage, is expected to improve the accuracy of estimating  $K_{cb}$  especially when stress conditions are present.

The overall results showed that the main contribution of assimilation would be in a better adjustment to local plant conditions represented by the NDVI, and also mitigating the effect of water stress which arises from the soil water balance, and depends on experimental or general information that can have considerable random error or uncertainties.

These results indicate the possibility of a better fit for the determination of water requirement of crops in the region under study, in operational context, by means of assimilation of FAO56 crop basal coefficient calculated by SIMDualKc with local NDVI, using the proposed algorithm.

# Soybean

## Day Of the Year (DOY)

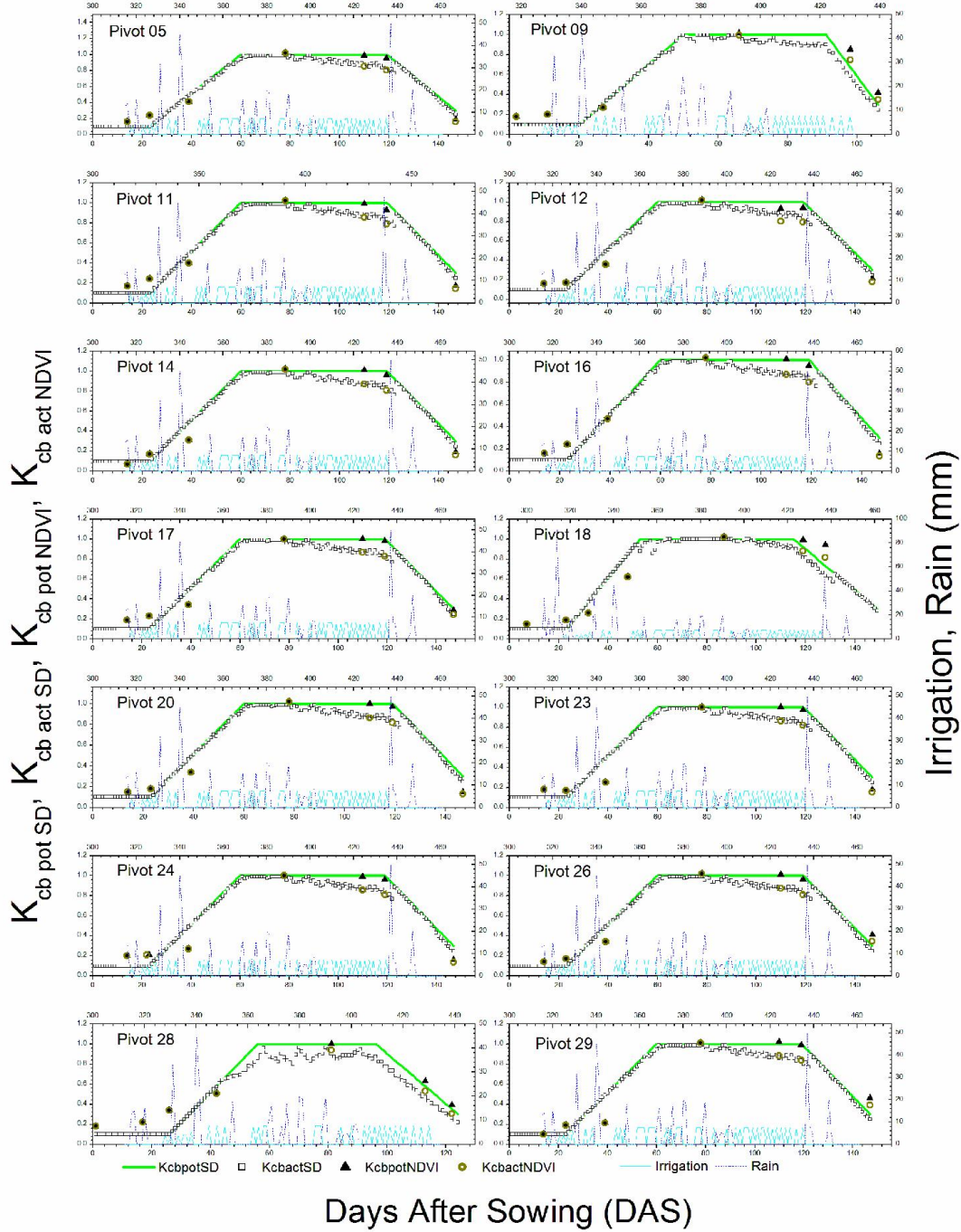


Fig. 3. Seasonal variation of the daily basal crop coefficients obtained from SIMDualKc model for both potential ( $K_{cb\ pot\ SIMDual}$ ) and actual ( $K_{cb\ act\ SIMDual}$ ) conditions and those obtained from the NDVI ( $K_{cb\ pot\ NDVI}$ ) as well as the precipitation and irrigation during the soybean crop cycle (November to May).

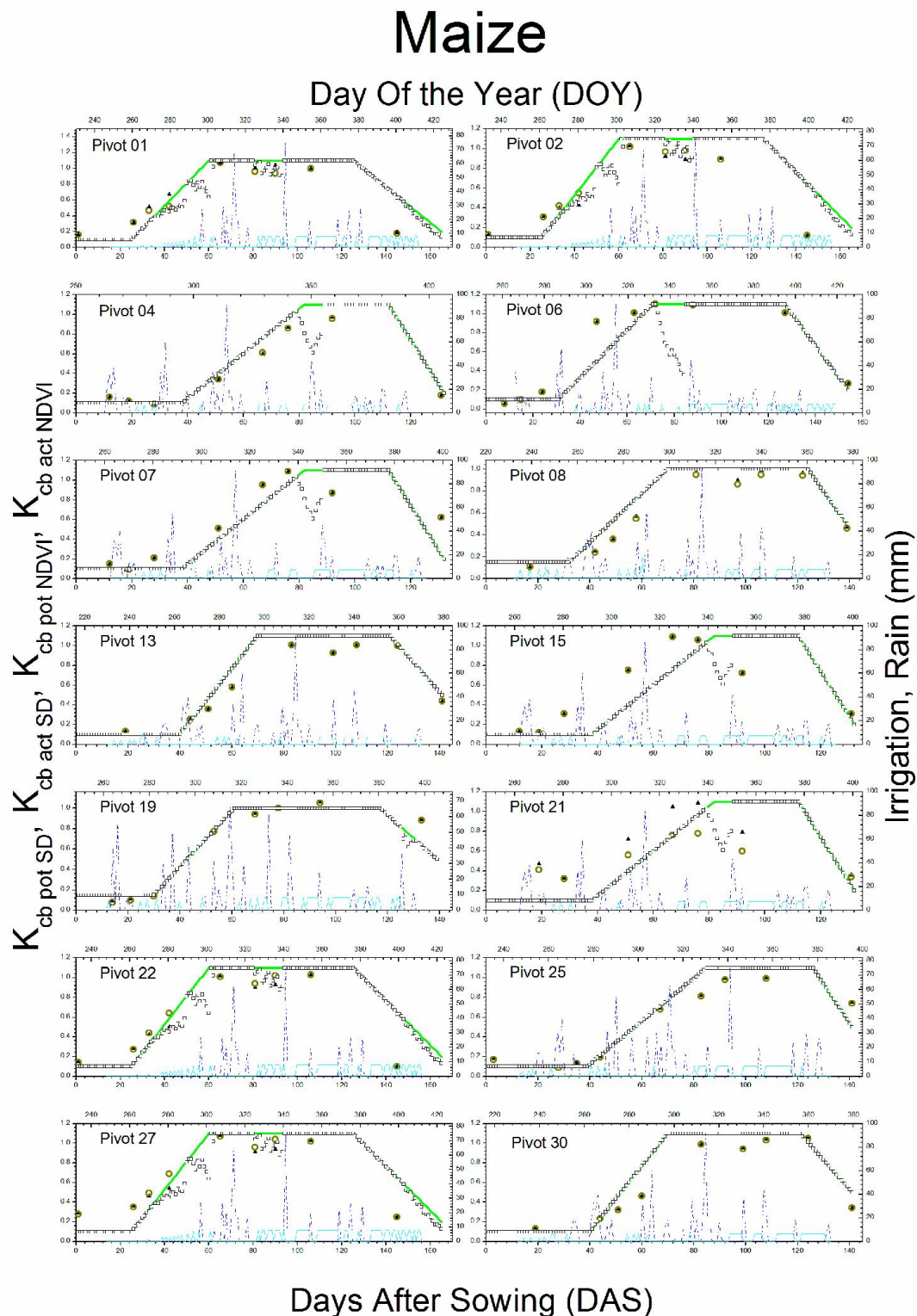


Fig. 4. Seasonal variation of daily basal crop coefficients obtained from SIMDualKc model for both potential ( $K_{cb\ pot\ SIMDual}$ ) and actual ( $K_{cb\ act\ SIMDual}$ ) conditions and those obtained from the NDVI ( $K_{cb\ pot\ NDVI}$ ) as well as the precipitation and irrigation during the maize crop cycle (September to February).

## CONCLUSIONS

The overall results obtained from the 28 pivots grown to maize and soybeans irrigated showed good performance for the assimilation of NDVI to the potential  $K_{cb}$  from SIMDualKc model, implemented using the recommendations of the FAO 56 guidelines. The stress coefficient ( $K_s$ ) obtained from the model can be used as a multiplier to obtain the actual values of assimilated  $K_{cb \text{ act NDVI}}$  in cases when water stress is present. It is observed that the assimilated crop coefficients differed from those obtained using FAO based models, although the difference was less than 30%. Part of the fitting differences perceived is associated to the considerable number of pivots analyzed, and the existence of various crop cultivars and differences in management systems, especially for maize. These imbalances may be improved simply with more specific correlations of each pivot and each crop cultivar.

But some of the differences observed between the  $K_{cb \text{ act NDVI}}$  and  $K_{cb \text{ act SIMDual}}$  is attributed to the introduction of more accurate information about the status of the crop during the cycle, given by the assimilation of NDVI. This information allows better fitting of  $K_{cb}$  under water stress conditions as it is difficult to know to what extent the stress indicated by soil water balance will actually affect the plants. The need for adjusting the FAO values for tropical climates has been recommended by researchers, and is also a corollary of this study.

The use of a large number of pivots and the availability of satellite images covering the entire crop cycle gives a good robustness to the results.

From these results, the estimation of  $K_{cb}$  through NDVI could be a useful option for determining the water needs of several other crops in irrigation pivots in the region, with a view to supporting the planning and management of irrigation. It could also serve as a tool for the evaluation of adequacy of irrigation management for farmers and companies that require this kind of service.

## REFERENCES

- Allen, R. G., Pereira, L., Raes, D., Smith, M. 1998. "FAO Irrigation and drainage paper No. 56." In: *FAO Food and Agriculture Organization of the United Nations*.
- Allen, R. G.; Pereira, L. S.; Smith, M.; Raes, D.; Wright, J. L. 2005a. "FAO-56 Dual crop coefficient method for estimating evaporation from soil and application extensions." **Journal of Irrigation and Drainage Engineering** 131: 2-13. DOI: 10.1061/(ASCE)0733-9437(2005)131:1(2)
- Allen, R. G., Clemmens, A. J., Burt, C. M., Solomon, K., O'Kalloran, T. 2005b. "Prediction accuracy for project wide evapotranspiration using crop coefficients and reference



evapotranspiration.” **Journal of Irrigation and Drainage Engineering, American Society of Civil Engineers** 131: 24-36. doi.org/10.1061/(ASCE)0733-9437(2005)131:1(24).

Allen, R. G., Tasumi, M., Morse, A., Trezza, R., Wright, J. L., Bastiaanssen, W., Kramber, W., Lorite, I., Robison, C. W. 2007. “Satellite-based energy balance for mapping evapotranspiration with internalized calibration (METRIC)—Applications.” **Journal of Irrigation and Drainage Engineering** 133: 395-406. doi.org/10.1061/(ASCE)0733-9437(2007)133:4(395).

Allen R. G., Pereira, L. S. 2009. “Estimating crop coefficients from fraction of ground cover and height.” **Irrigation Science** 28: 17-34. doi: 10.1007/s00271-009-0182-z.

Allen, R. G., Pereira, L. S., Howell, T. A., Jensen, M. E. 2011. “Evapotranspiration information reporting: I. Factors governing measurement accuracy.” **Agricultural Water Management** 98: 899-920. doi:10.1016/j.agwat.2010.12.015.

ANA. Agência Nacional de Águas. 2014. *Relatório de Conjuntura dos Recursos Hídricos*. <http://www2.ana.gov.br/Paginas/default.aspx>

Bastiaanssen, W. G. M., Pelgrum, H., Wabg, J. 1998. “A remote sensing surface energy balance algorithm for land (SEBAL): 2. Validation.” **Journal of Hydrology**, 212: 213-229. doi:10.1016/S0022-1694(98)00254-6.

BRASIL. Ministério da Integração Nacional, Secretaria Nacional de Irrigação. *Plano Plurianual 2012-2016*. Brasília, 2013.

[http://mi.gov.br/c/document\\_library/get\\_file?uuid=e1c70db2-f7c4-40f9-b8aa-33fadec76a1f&groupId=10157](http://mi.gov.br/c/document_library/get_file?uuid=e1c70db2-f7c4-40f9-b8aa-33fadec76a1f&groupId=10157)

Câmara, G., Souza, R. C. M., Freitas, U. M., Garrido, J. C. P. 1996. "Integrating remote sensing and GIS by object-oriented data modeling." **Computers & Graphics** 20: 395-403. doi:10.1016/0097-8493(96)00008-8.

Campos, I., Neale, C. M. U., Calera, A., Balbontin, C., González-Piqueras, J. 2010. "Assessing satellite-based basal crop coefficients for irrigated grapes (*Vitis vinifera* L.)." **Agricultural Water Management** 98: 45-54. doi:10.1016/j.agwat.2010.07.011

Campos, I., Boteta, L., Balbontín, C., Fabião, M., Maia, J., Calera, A. 2012. “Remote sensing based water balance to estimate evapotranspiration and irrigation water requirements. Case study: Grape vineyards.” **Options Méditerranéennes B** 67: 85-94.

Chander, G., Markham, B. L., Barsi, J. A. 2007. "Revised Landsat-5 Thematic Mapper Radiometric Calibration". **IEEE Geoscience and Remote Sensing Letters** 4, n. 3: 490-494.

Chander, G., Markham, B.L. & Helder, D.L. 2009."Summary of current radiometric calibration coefficients for Landsat MSS, TM, ETM+, and EO-1 ALI sensors". **Remote sensing of environment** 113: 893-903.

Duchemin, B., Hadria, R., Erraki, S., Boulet, G., Maisongrande, P., Chehbouni, A., Escadafal, R., Ezzahar, J., Hoedjes, J. C. B., Kharrou, M. H. 2006. “Monitoring wheat phenology and irrigation in Central Morocco: On the use of relationships between evapotranspiration, crops coefficients, leaf area index and remotely-sensed vegetation indices.” **Agricultural Water Management** 79: 1-27. doi:10.1016/j.agwat.2005.02.013.

El Nahry, A. H., Ali, R. R., El Baroudy A. A. 2010. “An approach for precision farming under pivot irrigation system using remote sensing and GIS techniques” **Agricultural Water Management** 98, n. 4, p. 517–531.

Embrapa. 2006. Centro Nacional de Pesquisa de Solos. *Sistema Brasileiro de Classificação de Solos*. 2.ed. Rio de Janeiro: Embrapa Solos.

- Er-Raki, S., Chehbouni, A., Guemouria, N., Duchemin, B., Ezzahar, J., Hadria, R. 2007. "Combining FAO-56 model and ground-based remote sensing to estimate water consumptions of wheat crops in a semi-arid region." **Agricultural Water Management** 87: 41-54. doi:10.1016/j.agwat.2006.02.004.
- Er-Raki, S., Rodriguez, J. C., Garatuza-Payan, J., Watts, C. J., Chehbouni, A. 2013. "Determination of crop evapotranspiration of table grapes in a semi-arid region of Northwest Mexico using multispectral vegetation index." **Agricultural Water Management** 122: 12-19. doi:10.1016/j.agwat.2013.02.007.
- FAO. (Food and Agriculture Organization of the United Nations). 2012. "Coping with water scarcity. An action framework for agriculture and food security." *FAO water reports* 38. Rome.
- Glen, E. P., Huete, A. R., Negler, P. L., Nelson, S. G. 2008. "Relationship between remotely-sensed vegetation indices, canopy attributes and plant physiological processes: what vegetation indices can and cannot tell us about the landscape." **Sensor** 8: 2136-2160. doi: 10.3390/s8042136.
- Glen, E.P., Neale, C.M.U., Hunsaker, D.J., Nagler, P.L. 2011. "Vegetation index-based crop coefficients to estimate evapotranspiration by remote sensing in agricultural and natural ecosystems." **Hydrol Process** 25: 4050–4062.
- González-Dugo, M. P., Mateos, L. 2008. "Spectral vegetation indices for benchmarking water productivity of irrigated cotton and sugarbeet crops." **Agricultural Water Management** 95: 48-58. doi:10.1016/j.agwat.2007.09.001.
- Gonzalez-Piquera, J., Calera, A. Belmonte, Gilabert, M. A., Cuestas, A. García, De la Cruz, F. Tercero. 2003. "Estimation of crop coefficients by means of optimized vegetation indices for corn." *Proceedings of the SPIE Congress. Barcelona, Spain*: 110-118.
- Gürtler, S., Epiphanyo, J. C. N., Luiz, A. J. B., Formaggio, A. R. "Planilha Eletrônica Para o Cálculo da Reflectância em Imagens TM e ETM+ Landsat". **Revista Brasileira de Cartografia**, 57/02: 162-167. 2005.
- Huete, A. R. 1988. "A soil-adjusted vegetation index (SAVI)." **Remote Sensing of Environment** 25: 295-309.
- Hunsaker, D. J., Pinter, P. J., Barnes, E. M., Kimball, B. A. 2003. "Estimating cotton evapotranspiration crop coefficients with a multispectral vegetation index." **Irrigation Science** 22: 95-104. DOI: 10.1007/S00271-003-0074-6.
- Hunsaker, D., Pinter, P. J., Kimball, B. 2005. Wheat basal crop coefficients determined by normalized difference vegetation index. **Irrigation Science** 24: 1-14. doi: 10.1007/s00271-005-0001-0.
- Johnson, L. F., Trout, T. J. 2012. "Satellite NDVI assisted monitoring of vegetable crop evapotranspiration in California's San Joaquin valley." **Remote Sensing** 4: 439-455.
- Kottek, M., J. Grieser, C. Beck, B. Rudolf, and F. Rubel, 2006. "World Map of the Köppen-Geiger climate classification updated." **Meteorologische Zeitschrift** 15: 259-263. DOI: 10.1127/0941-2948/2006/0130.
- Moriasi, J. D. N., Arnold, M. G., Van Liew, R. W., Bingner, R., D. Harmel, T., Veith, L. L. 2007. "Model Evaluation Guidelines for Systematic Quantification of Accuracy in Watershed Simulations". **Transactions of the ASABE** 50: 885-900.
- Martins, Juliano Delcin, Rodrigues, C. Gonçalo, Paredes, Paula, Carlesso, Reimar, Oliveira, Zanandra, Knies, Alberto, Petry, Mirta, Pereira, Luis S. 2013. "Dual crop coefficients for

- maize in southern Brazil: Model testing for sprinkler and drip irrigation and mulched soil.” **Biosystems Engineering** 115: 291-310. doi:10.1016/j.biosystemseng. 2013.03.016.
- Mateos, L., González-Dugo, M. P., Testi, L., Villalobos, F. J. 2013. “Monitoring evapotranspiration of irrigated crops using crop coefficients derived from time series of satellite images.I. Method.” **Agricultural Water Management** 125: 81-91. doi:10.1016/j.agwat.2012.11.005.
- Padilha, F. L. M., González-Dugo, M. P., Gavilán, P., Domínguez, J. 2011. "Integration of vegetation indices into a water balance model to estimate evapotranspiration of wheat and corn." **Hydrology Earth System Sciences** 15: 1213-1225. doi:10.5194/hess-15-1213-2011.
- Paredes, P., Rodrigues, G.C., Alves, I., Pereira, L.S. "Partitioning evapotranspiration, yield prediction and economic returns of maize under various irrigation management strategies". **Agricultural Water Management** 135: 27-39, 2014.
- Pereira, Luis S., Allen, G. Richard, Smith, Martin, Raes, Dirk. 2015a. “Crop evapotranspiration estimation with FAO56: Past and future.” **Agricultural Water Management** 147: 4-20. doi:10.1016/j.agwat.2014.07.031.
- Pereira, L. S., Paredes, P., Rodrigues, G. C., Neves, M. 2015b. “Modeling malt barley water use and evapotranspiration partitioning in two contrasting rainfall years. Assessing AquaCrop and SIMDualKc models.” **Agricultural Water Management** 159: 239-254. doi:10.1016/j.agwat.2015.06.006.
- Pôças, Isabel, Paço, Tereza A., Paredes, Paula, Cunha, Mário, Pereira, Luís S. 2015. “Estimation of Actual Crop Coefficients Using Remotely Sensed Vegetation Indices and Soil Water Balance Modelled Data.” **Remote Sensing** 7(3): 1-29. doi:10.3390/rs70302373.
- Raziei, T., Pereira, L. S. 2013. “Spatial variability analysis of reference evapotranspiration in Iran utilizing fine resolution gridded datasets” **Agricultural Water Management** 126: 104–118.
- Rosa, R. D., Paredes, P., Rodrigues, G. C., Alves, I., Fernando, R. M., Pereira, L. S., Allen, R. G. 2012. “Implementing the dual crop coefficient approach in interactive software. 1. Background Comput.” **Strat** 103: 1204-1213. doi:10.1016/j.agwat.2011.10.013.
- Rouse, J. W., Haas, R. H., Schell, J. A., Deering, D. W. 1974. "Monitoring vegetation systems in Great Plains with ERST". *Proceeding of the Third ERTS Symposium, NASA*. Washington, DC: US Government printing office, 309-317.
- Shuttleworth, W. J., Wallace, J. S. 2009. "Calculating the water requirements of irrigated crops in Australia using the Matt-Shuttleworth approach." **American Society of Agricultural and Biological Engineers** 52: 1895-1906. doi: 10.13031/2013.29217
- Stagakis, S., González-Dugo, V., Cid, P., Guillén-Climent, M. L., Zarco-Tejada, P. J. 2012. "Monitoring water stress and fruit quality in an orange orchard under regulated deficit irrigation using narrowband structural and physiological remote sensing indices." **Photogrammetry and Remote Sensing** 71: 41-61.
- Todorovic, M., Steduto, P. 2003. “A GIS for irrigation management,” **Physics and Chemistry of the Earth, Parts A/B/C** 28: 163–174.
- UNESCO WWAP (United Nations World Water Assessment Programme). 2015. "*The United Nations World Water Development. Report 2015: Water for a Sustainable World*. Paris.

## DISCUSSÃO GERAL

Este trabalho analisou a aplicação de técnicas de sensoriamento remoto e sistema de informação geográfica visando o apoio ao monitoramento de áreas irrigadas por pivô central com ênfase principalmente na incorporação de índices de vegetação na estimativa do coeficiente de cultura basal.

Inicialmente foi feita uma revisão bibliográfica acerca da utilização do sensoriamento remoto para a estimativa da evapotranspiração e coeficientes de cultura (Artigo I), abordando principalmente as metodologias que vem sendo utilizadas e aplicadas em caráter científico e operacional visando o apoio ao manejo da irrigação.

Foi possível perceber a existência de várias metodologias para se estimar a evapotranspiração que diferem principalmente nas variáveis de entrada escolhidas para a medição e nos modelos de cálculo. Esta diversidade de opções é justificada pela grande variedade de situações climáticas e disponibilidades de dados encontradas na prática. Sua importância é devida principalmente ao planejamento da irrigação em áreas agrícolas, gestão dos recursos hídricos e possibilidade de se obter uma estimativa mais próxima da realidade em termos de consumo de água pelas culturas.

Além do universo existente de abordagens meteorológicas pode-se perceber que vêm avançando - principalmente nas últimas duas décadas - o uso de informações espectrais de sensores de moderada resolução espacial, como o TM/Landsat. Essas informações implementadas em modelos de balanço de energia à superfície como SEBAL e METRIC, ou assimiladas e correlacionadas com modelos de balanço de água no solo como SIMDualKc podem prover estimativas de coeficientes de cultura e a evapotranspiração mais condizentes com as condições locais, de uma forma espacializada, visto que as imagens de satélite possuem informações específica em cada pixel.

A principal vantagem do uso do sensoriamento remoto na estimativa dos coeficientes de cultura e da evapotranspiração é a visão espacializada que se obtém. Esse fato possibilita a percepção dos padrões de variabilidade no espaço das variáveis estimadas, sendo isso fundamental especialmente quando a região sob avaliação é heterogênea. Pode-se ainda mencionar que as metodologias que lançam mão do sensoriamento remoto não substituem os demais métodos que levam em consideração as medidas feitas em campo, ou seja, os métodos tradicionais de estimativa dos fluxos de energia e balanço de água no solo, mas funcionam como uma alternativa metodológica e em caráter de complementaridade.

A tendência em desenvolvimento é o monitoramento de áreas agrícolas por meio de veículo aéreo não tripulado, os VANTS ou DRONES, onde as informações como coeficientes de cultura e evapotranspiração poderão ser estimadas, ajustadas, calibradas e assimiladas em modelos de balanço de água no solo e/ou modelos de balanço de energia à superfície. Os dados provenientes de sensoriamento remoto poderão apoiar o manejo da irrigação e ser agrupados e organizados em banco de dados geográficos que permitirão uma visualização eficiente da dinâmica agrícola de forma mais condizente com a realidade de cada lavoura.

O banco de dados geográfico foi analisado e discutido no Artigo II. Este artigo teve como objetivo elaborar e discutir a organização de um sistema de informação geográfica com dados de 30 pivôs localizados no município de Cruz Alta, RS, Brasil com vistas a apoiar o manejo da irrigação. Foi apresentado dentro do SIG um histórico da área sob estudo com informações referentes ao: i) relevo: declividade e hipsometria; ii) uso do solo: tipo de cultura, época de plantio, estágio fenológico; iii) clima: precipitação, velocidade dos ventos, temperatura, umidade do ar e do solo e evapotranspiração; iv) análises estatísticas dos valores de NDVI dos pixels dentro de cada pivô, tais como: variância, desvio padrão, coeficiente de variação, assimetria, curtose, valor mínimo e máximo, quartil inferior e superior e mediana.

As informações integradas ao SIG possibilitaram o acesso e a visualização de informações cruzadas capazes de permitir o entendimento da dinâmica da vegetação, do solo, da precipitação e da demanda de água pelas culturas. O SIG criado foi capaz de identificar:

- i) a distribuição espacial das chuvas, em qualquer data, para cada pivô monitorado, por meio de imagens de satélite ou mapas da região cruzados com informações climáticas obtidas de estações meteorológica instaladas nas proximidades da área de estudo;
- ii) culturas e estágios fenológicos distintos dentro dos pivôs, bem como sua distribuição espacial, por meio de valores de NDVI;
- iii) classes de uso dos solos por meio da classificação supervisionada por regiões das imagens de satélites; e
- iv) áreas de risco a erosão, bem como a aptidão agrícola da região através de modelos, cálculos e cruzamento das informações obtidas por meio de sensores remotos.

Há evidências que o banco de dados geo-relacional criado pode ser uma ferramenta que potencialize o gerenciamento, monitoramento e apoio a irrigação, facilitando a tomada de decisão devido à possibilidade de obter um monitoramento de forma espacializada.

O monitoramento da soja e do milho irrigados por pivô central por meio do sensoriamento remoto foi discutido no Artigo III. Que teve como objetivo avaliar a

sensibilidade do NDVI para identificar estádios fenológicos e sua variabilidade dentro dos pivôs de irrigação, bem como os intervalos de duração de cada estágio de desenvolvimento da cultura do milho e da soja com intuito de apoiar o manejo da irrigação.

A sensibilidade do NDVI em função dos dias após a semeadura foi de 0,02 unidades de NDVI para o reconhecimento da fenologia. Essa sensibilidade foi suficientemente precisa para fins de monitoramento da fenologia com objetivo de determinar os principais estádios de desenvolvimento da cultura de acordo com FAO56 e desta forma apoiar o calendário de irrigação.

Os resultados dos períodos para a soja e milho foram respectivamente: 0,0-0,3 e 0,0-0,4 inicial; 0,3-0,85 e 0,4-0,75 desenvolvimento rápido; 0,85-1,0 e 0,75-1,0 desenvolvimento médio; 0,85-0,3 e 0,75-0,3 estação final. O erro médio (ARE) ficou em torno de 7%. As curvas de NDVI também mostraram uma espécie de impressão digital das variedades de culturas locais e práticas de manejo agrícola.

A uniformidade do pivô central ( $\sigma < 0,1$ ), e o grande número de plantas por pixel reduziu o erro aleatório do NDVI em um fator entre 840-890 para o milho e entre 1610-1840 para a soja, desempenhando um papel importante na precisão de 0,02 obtido em média nas medições de NDVI nos pivôs.

Os resultados mostraram-se apropriados para a sua utilização em ambiente SIG, onde mapas temáticos das diferentes fases fenológicas podem ser adequadamente preparados.

Por outro lado, estes resultados mostram-se promissores para o apoio ao manejo da irrigação com a utilização de dados provindos de VANTS e DRONES, que podem fornecer imagens do local além das informações obtidas de satélites, e cujos dados mais frequentes podem ser assimilados em modelos.

Por fim o Artigo IV propõe-se assimilar dados de NDVI obtidos por sensoriamento remoto aos  $K_{cb}$  das culturas de milho e soja irrigadas por pivô central, obtidos localmente a partir de modelo de balanço de água no solo. O modelo utilizado, SIMDualKc, forneceu dados de saída de  $K_{cb}$  potencial que foram correlacionados com o NDVI, obtendo assim um melhor ajuste dos  $K_{cb}$  ao comportamento da cultura descrito no NDVI. O coeficiente de estresse,  $K_s$ , produzido pelo modelo SIMDualKc foi também utilizado para calcular o  $K_{cb\ act} = K_{cb\ pot} * K_s$ .

Os resultados globais obtidos mostraram um bom desempenho para a aproximação do  $K_{cb}$  a partir do NDVI em 28 parcelas irrigadas de milho e soja. O erro relativo médio (ARE) estimado entre o modelo geral de  $K_{cb\ NDVI}$  e os modelos individuais de cada pivô, foram menores que 30%, indicando a possibilidade de usar as equações obtidas para o planejamento

da irrigação na região. Os dados de  $K_{cb}$  obtidos tem potencial para estarem melhor ajustados com a real demanda das plantas, devido ao ajuste à curva de NDVI realizado.

Desta forma, propõe-se uma metodologia para obter estimativas de  $K_c$  e ET mais próximas à realidade do solo e clima para culturas estabelecidas na região subtropical úmida do sul do Brasil.

A utilização de uma grande diversidade de parcelas de estudo, com diferentes especificidades e cobrindo todo o ciclo cultural de cada uma das culturas, confere uma boa robustez aos resultados.

Considerando os resultados obtidos, a estimativa de  $K_{cbs}$  por meio de NDVI pode representar uma ferramenta útil para determinação das necessidades hídricas das duas culturas em estudo, em pivôs de irrigação no sul do Brasil, visando apoiar o planejamento e gerenciamento da irrigação. Também pode servir de avaliação e adequação do manejo da irrigação para empresas que prestam este serviço na região.

## CONCLUSÃO GERAL

Com a conclusão da presente pesquisa faz-se necessário revisar os objetivos propostos inicialmente. O objetivo geral consistiu em *"Monitorar e mapear as variáveis importantes para o manejo da irrigação, como a fenologia, ET, K<sub>c</sub> e K<sub>cb</sub> das culturas de milho e soja em 30 pivôs centrais, por meio da combinação de dados de sensoriamento remoto e modelos de balanço de água no solo, organizando as informações em um sistema de informação geográfica (SIG)".* Este objetivo foi atingido, pois as variáveis importantes para o planejamento, gerenciamento e manejo da irrigação por pivô central no Sul do Brasil, puderam ser estimadas e mapeadas com o apoio de técnicas de sensoriamento remoto assimiladas a modelos de balanço de água no solo e associadas a informações de campo.

Na sequência são retomados os objetivos específicos, bem como os principais resultados e comentários relativos a cada um deles, juntamente com as sugestões e recomendações identificadas.

- 1º Objetivo específico: *"Propor uma estrutura baseada em bancos de dados geográfico dentro de um SIG que seja adequada para o gerenciamento da irrigação por pivô central".*

O banco de dados integrado ao SIG permitiu o acesso e a visualização de informações cruzadas e possibilitou o entendimento da dinâmica da vegetação referente ao seu crescimento e estágio fenológico dentro de cada pivô central; distribuição espacial dos diferentes tipos e usos do solo; distribuição das precipitações; além de possibilidade de se visualizar os K<sub>obs</sub>, ET<sub>o</sub> e ET<sub>c</sub> em cada pixel dentro das áreas irrigadas e desta forma, possibilitar a estimativa da demanda de água pelas culturas de milho e soja de forma espacializada. O 1º objetivo específico deixa em evidências que o banco de dados geo-relacional criado pode ser uma ferramenta que potencialize o gerenciamento, monitoramento e apoio a irrigação, facilitando a tomada de decisão devido à possibilidade de obter um monitoramento de forma espacializada.

- 2º Objetivo específico: *"Analisar a sensibilidade do NDVI para a descrição do ciclo das culturas de soja e milho irrigados com pivô central e para a detecção de estádios fenológicos no Sul do Brasil".*

Os estádios fenológicos das culturas de milho e soja foram precisamente identificados por meio dos valores de NDVI que apresentou uma sensibilidade de 0,02 unidades, sendo suficiente para fins de determinação dos períodos de desenvolvimento das culturas de acordo com FAO56 e adequados para as condições locais da região sob estudo.



- 3º Objetivo específico: *"Determinar os intervalos de valores de NDVI correspondentes aos períodos de desenvolvimento descritos pelo boletim FAO56 (inicial, crescimento rápido, intermediário e final)".*

Os valores de NDVI para período inicial da cultura da soja foi de [0,0-0,3], período de crescimento rápido foi de [0,3-0,85], período intermediário [0,85-1,0] e período final [0,85-0,3]. Os valores de NDVI para período inicial da cultura do milho foi de [0,0-0,4], período de crescimento rápido foi de [0,4-0,75], período intermediário [0,75-1,0] e período final [0,75-0,3].

- 4º Objetivo específico: *"Desenvolver um procedimento de assimilação dos dados de NDVI com os dados provenientes do procedimento da FAO56 implementado em um modelo de balanço de água no solo, o SIMDualKc".*

A assimilação dos dados de NDVI obtidos por sensoriamento remoto aos  $K_{cb}$  das culturas de milho e soja irrigadas por pivô central, obtidos localmente a partir de modelo de balanço de água no solo, o modelo SIMDualKc, mostraram um bom desempenho para a aproximação do  $K_{cb}$  a partir do NDVI. Desta forma, propõe-se uma metodologia para obter estimativas de  $K_c$  e ET mais próximas à realidade do solo e clima para culturas estabelecidas na região subtropical úmida do Sul do Brasil.

- 5º Objetivo específico: *"Determinar a curva geral de valores do coeficiente de cultura basal atual para o ciclo da soja e o milho no Sul do Brasil, e compará-la com curvas específicas individuais de cada pivô para determinar o grau de ajuste esperado".*

Os resultados mostraram um bom desempenho na aproximação da curva geral de  $K_{cb}$  com as curvas individuais de  $K_{cb}$  em cada pivô central. As curvas de  $K_{cb}$  obtidas pela assimilação dos valores de NDVI, para as culturas de milho e soja no Sul do Brasil, mostram um bom ajuste quando não há a ocorrência de estresse hídrico, na ocorrência de estresse hídrico o ajuste é menor. O método de assimilação de valores de  $K_{cb}$  por NDVI e modelos de balanço de água no solo, como SIMDualKc, tem potencial para estarem melhor ajustados com a demanda hídrica atual das culturas de soja e milho sob irrigação por aspersão na região sob estudo. Este fato ocorre devido ao bom ajuste dos valores do NDVI durante o ciclo das culturas e os  $K_{cb}$  modelados pelo SIMDualKc, o que permite ao NDVI fornecer informações que complementem a modelagem.

- 6º Objetivo específico: *"Determinar os intervalos de valores de  $K_{cb}$  atuais assimilado ao NDVI para os períodos inicial, crescimento rápido, intermediário e final".*

Para o período inicial da soja os valores de  $K_{cb \text{ act NDVI}}$  foram de [0,10-0,20], no período de desenvolvimento rápido variaram entre [0,15-1,0], chegando no período intermédio ao valor de [0,95-1,1] e no período final variaram entre [0,5-0,3]. Para a cultura do milho, os valores de  $K_{cb \text{ act NDVI}}$  para o conjunto de pivôs foram de [0,10-0,25] no período inicial e de [0,95-1,2] no período intermédio, variando no período de desenvolvimento rápido entre [0,2-1,0] e no período final entre [0,5-0,2]. Estes resultados aproximam-se dos valores tabelados em Allen et al., (1998), bem como dos valores de  $K_{cb}$  aproximados a partir do SAVI apresentados por Padilla et al. (2011). Os valores finais do ciclo para o  $K_{cb}$  dependem muito das condições de manejo, tanto pelas condições de umidade dos grãos escolhidas para colheita, quanto pelas limitações de resolução temporal das imagens de satélite, que podem não coincidir em tempo com a colheita.

Portanto conclui-se que há evidências que as metodologias utilizadas são adequadas para a estimativa dos estádios fenológicos, períodos de crescimentos descritos por FAO56 e  $K_{cb}$  assimilados por NDVI, para as culturas de milho e soja no Sul do Brasil. A utilização de SIG com informações integradas (informações de campo, meteorológicas, do SIMDualKc e sensoriamento remoto) são importantes para um melhor planejamento, gerenciamento, manejo e monitoramento da irrigação por aspersão.

## REFERÊNCIAS BIBLIOGRÁFICAS GERAIS

- Allen, R. G., Pereira, L., Raes, D., Smith, M. 1998. "FAO Irrigation and drainage paper No. 56." In: *FAO Food and Agriculture Organization of the United Nations*.
- Allen, R. G., Bastiaanssen, W., Tasumi, M., Morse, A. 2001. Evapotranspiration on the watershed scale using the SEBAL model and Landsat images. **ASAE Meeting Presentation**. doi: 10.13031/2013.4047.
- Allen, R. G., Tasumi, M., Morse, M., Trezza, R. 2005. "A Landsat-based energy balance and evapotranspiration model in Western US water rights regulation and planning." **Irrigation and Drainage Systems** 19: 251-268. doi: 10.1007/s10795-005-5187-z.
- Allen, R. G., Tasumi, M., Morse, A., Trezza, R., Wright, J. L., Bastiaanssen, W., Kramber, W., Lorite, I., Robison, C. W. 2007a. "Satellite-based energy balance for mapping evapotranspiration with internalized calibration (METRIC)—Applications." **Journal of Irrigation and Drainage Engineering** 133: 395-406. doi.org/10.1061/(ASCE)0733-9437(2007)133:4(395).
- Allen, R. G., Wright, J. L., Pruitt, W. O., Pereira, L. S., Jensen, M. E. *Water requirements*. 2007b. In: Design and Operation of Farm Irrigation Systems. Edited by Hoffman, G. J., Evans, R. G., Jensen, M. E., Martin, D. L., Elliot, R. L. ASABE: 208-288.
- Allen, R. G., Tasumi, M., Trezza, R. 2007c. "Satellite-based energy balance for mapping evapotranspiration with internalized calibration (METRIC)—Model." **Journal of irrigation and drainage engineering** 133: 380-394. doi.org/10.1061/(ASCE)0733-9437(2007)133:4(380).
- Allen, R. G., Pereira, L. S., Howell, T. A., Jensen, M. E. 2011. "Evapotranspiration information reporting: I. Factors governing measurement accuracy." **Agricultural Water Management** 98: 899-920. doi:10.1016/j.agwat.2010.12.015.
- Allen R. G., Pereira, L. S. 2009. "Estimating crop coefficients from fraction of ground cover and height." **Irrigation Science** 28: 17-34. doi: 10.1007/s00271-009-0182-z.
- Anderson, M. C., Allen, R. G., Morse, A., Kustas, W. P. 2012a. "Use of Landsat thermal imagery in monitoring evapotranspiration and managing water resources." 2012a. **Remote Sensing of Environment** 122: 50-65. doi:10.1016/j.rse.2011.08.025.
- Anderson, M. C., Kustas, W. P., Alfieri, J. G., Gao, F., Hain, C., Prueger, J. H., Evett, S., Colaizzi, P., Howell, T., Chávez, J. L. 2012b. "Mapping daily evapotranspiration at Landsat spatial scales during the BEAREX'08." **Advances in Water Resources** 50: 162-177, 2012b. doi: 10.1016/j.advwatres.2012.06.005.
- ASCE-EWRI. 2005. "The ASCE standardized reference evapotranspiration equation". In: *Report 0-7844-0805-X* edited by Allen, R. G., Walter, I. A., Elliot, R. L., Howell, T. A., Itenfisu, D., Jensen, M. E., Snyder, R. L. Environ. Water Resources Institute.
- Bastiaanssen, W. G. M. 1995. "Regionalization of surface flux densities and moisture indicators in composite terrain : a remote sensing approach under clear skies in Mediterranean climates." Wageningen, Netherlands: *Ph.D. Thesis*, 273.

- Bastiaanssen, W., Menenti, M., Feddes, R., Holtslag, A. 1998a "A remote sensing surface energy balance algorithm for land (SEBAL). 1. Formulation." **Journal of hydrology** 212: 198-212. doi:10.1016/S0022-1694(98)00253-4.
- Bastiaanssen, W. G. M., Pelgrum, H., Wabg, J. 1998b. "A remote sensing surface energy balance algorithm for land (SEBAL): 2. Validation." **Journal of Hydrology**, 212: 213-229. doi:10.1016/S0022-1694(98)00254-6.
- Bois, B., Pieri, P., Van Leeuwen, C., Wald, L., Huard, F., Gaudillere, J. P., Saur, E. 2008. "Using remotely sensed solar radiation data for reference evapotranspiration estimation at a daily time step." **Agricultural and Forest Meteorology** 148: 619-630.
- Calera, A. B., Jochum, A. M., Cuesta, G. A, Montoro, A. L. 2005. "Irrigation management from space: towards user-friendly products." **Irrigation Draining Systems** 19: 337-353.
- Cruz-Blanco, M., Lorite, I. J., Santos, C. 2014. An innovative remote sensing based reference evapotranspiration method to support irrigation water management under semi-arid conditions. **Agricultural Water Management** 131: 135-145.
- De Bruin, H. A. R., Trigo, I. F., Gavalán, P., Martínez-Cob, A., González-Dugo, M. P. 2010. "Reference crop evapotranspiration derived from geo-stationary satellite imagery: a case study for the Fogera flood plain, NW-Ethiopia and the Jordan Valley." **Journal Hydrology and Earth System Sciences** 14: 2219-2228.
- De Bruin, H. A. R., Trigo, I. F., Gavalán, P., Martínez-Cob, A., González-Dugo, M. P. 2012. "Reference crop evapotranspiration estimated from geostationary satellite imagery." In: NEALE, C. M., COSH, M. H. **Remote Sensing and Hydrology**. Wallingford: IAHS Publication: 111-114.
- Droogers, P., Immerzeel, W. W., Lorite, I. J. 2010. "Estimating actual irrigation application by remotely sensed evapotranspiration." **Agricultural Water Management** 97: 1351-1359.
- Duchemin, B., Hadria, R., Erraki, S., Boulet, G., Maisongrande, P., Chehbouni, A., Escadafal, R., Ezzahar, J., Hoedjes, J. C. B., Kharrou, M. H. 2006. "Monitoring wheat phenology and irrigation in Central Morocco: On the use of relationships between evapotranspiration, crops coefficients, leaf area index and remotely-sensed vegetation indices." **Agricultural Water Management** 79: 1-27. doi:10.1016/j.agwat.2005.02.013.
- D'Urso, G., Richter, K., Calera, A., Osann, M. A., Tapia, J. B., Vuolo, F. 2010. "Earth Observation products for operational irrigation management in the context of the PLEIADeS project." **Agricultural Water Management** 98: 271-282.
- Er-Raki, S., Chehbouni, A., Guemouria, N., Duchemin, B., Ezzahar, J., Hadria, R. 2007. "Combining FAO-56 model and ground-based remote sensing to estimate water consumptions of wheat crops in a semi-arid region." **Agricultural Water Management** 87: 41-54. doi:10.1016/j.agwat.2006.02.004.
- Er-Raki, Salah, Chehbouni, Abdelghani, Duchemin, Benoit. 2010. "Combining Satellite Remote Sensing Data with the FAO-56 Dual Approach for Water Use Mapping In Irrigated Wheat Fields of a Semi-Arid Region." **Remote Sensing** 2: 375-387. doi:10.3390/rs2010375.
- Er-Raki, S., Rodriguez, J. C., Garatuza-Payan, J., Watts, C. J., Chehbouni, A. 2013. "Determination of crop evapotranspiration of table grapes in a semi-arid region of Northwest

- Mexico using multispectral vegetation index.” **Agricultural Water Management** 122: 12-19. doi:10.1016/j.agwat.2013.02.007.
- Fassnacht, K. S., Gower, S. T., Mackenzie, M. D., Nordheim, E. V., Lillesand, T. M. 1997. “Estimating the leaf area index of north central Wisconsin forests using the Landsat Thematic Mapper.” **Remote sensing of environment**.61: 229-245. doi:10.1016/S0034-4257(97)00005-9.
- FEALQ. Fundação de Estudos Agrários Luiz de Queiroz. 2014. *Análise territorial para o desenvolvimento da agricultura irrigada no Brasil*. Piracicaba: 1-217.
- Folhes, M. T. 2007 “Modelagem da evapotranspiração para a gestão hídrica de perímetros irrigados com base em sensores remotos.” *Tese de D.Sc*, São José dos Campos
- Glenn, E. P., Huete, A. R., Nagler, P. L., Hirschboeck, K. K., Brown, P. 2007. "Integrating remote sensing and ground methods to estimate evapotranspiration." **Critical Reviews in Plant Sciences Journal** 26: 139-168.
- González-Dugo, M. P., Mateos, L. 2008. “Spectral vegetation indices for benchmarking water productivity of irrigated cotton and sugarbeet crops.” **Agricultural Water Management** 95: 48-58. doi:10.1016/j.agwat.2007.09.001.
- González-Dugo, M. P., Escuin, E., Cano, F., Cifuentes, V., Padilla, F. L. M., Tirado, J. L., Oyonarte, N., Fernández, P., Mateos, L. 2013. “Monitoring evapotranspiration of irrigated crops using crop coefficients derived from time series of satellite images. II. Application on basin scale.” **Agricultural Water Management** 125: 92-104. doi: org/10.1016/j.agwat.2013.03.024.
- Gonzalez-Piquera, J., Calera, A. Belmonte, Gllabert, M. A., Cuestas, A. García, De la Cruz, F. Tercero. 2003. “Estimation of crop coefficients by means of optimized vegetation indices for corn.” *Proceedings of the SPIE Congress. Barcelona, Spain*: 110-118.
- Heilman, J., Kanemasu, E., Bagley, J., Rasmussen, V. 1977. “Evaluating soil moisture and yield of winter wheat in the Great Plains using Landsat data.” **Remote Sensing of Environment** 6: 315-326. doi:10.1016/0034-4257(77)90051-7.
- Hong, S. 2009. "Up-scaling of SEBAL derived evapotranspiration maps from LANDSAT (30 m) to MODIS (250 m) scale." **Journal of Hydrology** 370: 122-138.
- Huffaker, R., Whittleson, N., Michelsen, A., Taylor, R., McGuckin, T. 1998. "Evaluating the effectiveness of conservation water-pricing programs." **Journal of Agricultural and Resources Economics**, 23: 12-19.
- Hunsaker, D. J., Pinter, P. J., Barnes, E. M., Kimball, B. A. 2003. “Estimating cotton evapotranspiration crop coefficients with a multispectral vegetation index.” **Irrigation Science** 22: 95-104. DOI: 10.1007/S00271-003-0074-6.
- Hunsaker, D., Pinter, P. J., Kimball, B. 2005. Wheat basal crop coefficients determined by normalized difference vegetation index. **Irrigation Science** 24: 1-14. doi: 10.1007/s00271-005-0001-0.

- Jhorar, R. K., Bastiaanssen, W. G. M., Feddes, R. A., Van Dam, J. C. 2002. "Inversely estimating soil hydraulic functions using evapotranspiration fluxes." **Journal of Hydrology** 258: 198-213.
- Kalman, J. D., Mcvicar, T., McCabe, M. F. 2008. "Estimating land surface evaporation: a review of methods using remotely sensed surface temperature data." **Surveys in Geophysics** 29: 421-469.
- Kanamasu, E., Hellman, J., Bagley, J., Powers, W. 1977. "Using Landsat data to estimate evapotranspiration of winter wheat." **Environmental Management** 1: 515-520. doi: 10.1007/BF01866686.
- Karnieli, A., Agam, N., Pinker, R. T., Anderson, M., Anderson, M. L., Anderson, G. G., Anderson, N., Anderson, A. 2010. "Use of NDVI and land surface temperature for drought assessment: Merits and limitations." **Journal of Climate** 23: 618-633. doi: 10.1175/2009JCLI2900.1.
- Irmak, A., Ratcliffe, I., Ranade, P., Hubbard, K., Singh, R. K., Kamble, B., Kjarsgaard, J. 2012. "Operational Remote Sensing of ET and Challenges." In: IRMAK, A. **Evapotranspiration—Remote Sensing and Modeling**. [S.l.]: DOI 10.5772/25174, ISBN ISBN 978-953-307-808-3.
- Mateos, L., González-Dugo, M. P., Testi, L., Villalobos, F. J. 2013. "Monitoring evapotranspiration of irrigated crops using crop coefficients derived from time series of satellite images.I. Method." **Agricultural Water Management** 125: 81-91. doi:10.1016/j.agwat.2012.11.005.
- Moran, M. S., Jackson, R. D., Raymond, L. H., Gay, L. W., Slater, P. N. 1989. "Mapping surface energy balance components by combining Landsat Thematic Mapper and ground-based meteorological data." **Remote Sensing of Environment** 30: 77-87. doi:10.1016/0034-4257(89)90049-7.
- Padilha, F. L. M., González-Dugo, M. P., Gavilán, P., Domínguez, J. 2011. "Integration of vegetation indices into a water balance model to estimate evapotranspiration of wheat and corn." **Hydrology Earth System Sciences** 15: 1213-1225. doi:10.5194/hess-15-1213-2011.
- Pereira, L. S., Perrier, A., Allen, R. G., Alves, I. 1999. "Evapotranspiration: concepts and future trends." **Journal of Irrigation and Drainage Engineering, American Society of Civil Engineers**: 45-51. doi.org/10.1061/(ASCE)0733-9437(1999)125:2(45).
- Pereira, Luis S., Allen, G. Richard, Smith, Martin, Raes, Dirk. 2015a. "Crop evapotranspiration estimation with FAO56: Past and future." **Agricultural Water Management** 147: 4-20. doi:10.1016/j.agwat.2014.07.031.
- Reisig, D., Godfre, L. 2006. "Remote sensing for detection of cotton aphid–(homoptera: aphididae) and spider mite–(acari: tetranychidae) infested cotton in the San Joaquin Valley." **Environmental Entomology Pest Management** 1 1635-1675. doi: http://dx.doi.org/10.1093/ee/35.6.1635 1635-1646.

Scherer-Warren, M., Rodrigues, L. N. 2013. "Estimativa da Evapotranspiração Real por Sensoriamento Remoto: Procedimentos e aplicações em pivô central." *Embrapa*. Planaltina, p. 35. (ISSN 1676-918X).

Szilagyi, J., Rundquist, D., Gosselin, D., Parlange, M. 1998. "NDVI relationship to monthly evaporation." **Geophysical Research Letters** 25: 1753-1756.

Teixeira, A. H. C. 2010. "Determining regional actual evapotranspiration of irrigated crops and natural vegetation in the São Francisco river basin (Brazil) using remote sensing and Penman–Monteith equation." **Remote Sensing** 2: 1287-1319.

Yang, Z., Rao, M. N., Elliot, N. C., Kindler, S. D., Popham, T. W. 2005. "Using ground-based multispectral radiometry to detect stress in wheat caused by greenbug (Homoptera: Aphididae) infestation". **Computers and Electronics in Agriculture** 47: 121–135. doi:10.1016/j.compag.2004.11.018.